

HUMBOLDT-UNIVERSITÄT ZU BERLIN

MATHEMATISCH-NATURWISSENSCHAFTLICHE FAKULTÄT I

Institut für Physik

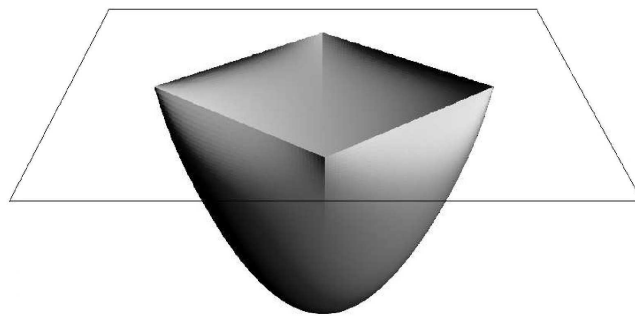
AG Quantenfeldtheorie und Stringtheorie



Diplomarbeit
zur Erlangung des akademischen Grades der
Diplom-Physikerin (Dipl.-Phys.)

Wilson Loops and Gluon Scattering Amplitudes in the AdS/CFT Correspondence

eingereicht von Charlotte Grosse Wiesmann,
geboren am 23.09.1984 in Henstedt-Ulzburg



Gutachter: PD Dr. Harald Dorn
Prof. Dr. Jan Plefka

Berlin, den 1. Dezember 2008

Abstract

This thesis deals with different aspects of the Wilson loop operator in the AdS/CFT correspondence.

In the context of the recently proposed duality between light-like polygonal Wilson loops and planar MHV gluon scattering amplitudes in $\mathcal{N} = 4$ super Yang-Mills theory, we propose a regularisation of the Wilson loop in order to match off-shell scattering amplitudes. The thus regularised Wilson loop is explicitly shown to match the dual off-shell 4-gluon amplitude to 1-loop order in Feynman gauge. The leading divergent terms, related to the cusp anomalous dimension, are shown to be gauge invariant.

In a second part, the properties of Wilson loops along several specific contours in Minkowski space are examined. Light-like tangents along the contour can lead to divergences. We show that while smooth curves remain finite, curves with a discontinuity in the second derivative in a point with light-like tangent are divergent. We compute these divergences and define a corresponding anomalous dimension, in analogy to the cusp anomalous dimension. Furthermore, we point out that Wilson loops with straight extended light-like segments are divergent and construct a coupling of the locally supersymmetric Wilson loop to the scalars, that makes it finite. Finally, we compute the Minkowskian rectangular Wilson loop and compare it to the Euclidean one.

Zusammenfassung

Diese Arbeit setzt sich mit verschiedenen Aspekten des Wilson-Schleifen-Operators in der AdS/CFT-Korrespondenz auseinander.

Im Kontext der kürzlich vorgeschlagenen Dualität zwischen Wilson-Schleifen und MHV Gluonstreuamplituden in der $\mathcal{N} = 4$ Super-Yang-Mills-Theorie, schlagen wir eine Regularisierung der Wilson Schleifen vor, die dual zu den nicht auf der Massenschale liegenden Streuamplituden ist. Diese wird explizit für den Fall der 4-Gluonstreuamplitude zu 1. Ordnung und in Feynman-Eichung geprüft. Die Eichinvarianz des führenden divergenten Terms, der mit der *cusp* anomalen Dimension zusammenhängt, wird gezeigt.

In einem zweiten Teil werden Eigenschaften von Wilson-Schleifen entlang unterschiedlicher spezifischer Kurven im Minkowski-Raum untersucht. Lichtartige Tangenten an der Kurve können zu Divergenzen führen. Während glatte Kurven endlich bleiben, zeigen wir, dass Kurven mit Unstetigkeiten in der 2. Ableitung in Punkten mit lichtartiger Tangente divergent sind. Wir berechnen diese Divergenzen und definieren eine zugehörige anomale Dimension, in Analogie zu der *cusp* anomalen Dimension. Des Weiteren, halten wir die Divergenz von Wilson-Schleifen mit geraden ausgedehnten lichtartigen Stücken fest und konstruieren eine Kopplung der lokal supersymmetrischen Wilson-Schleife an die Skalare, so dass diese endlich wird. Schließlich berechnen wir die rechteckige Wilson Schleife im Minkowski-Raum und vergleichen das Ergebnis mit dem euklidischen.

Acknowledgments

First of all, I would like to thank my parents for their constant love and support throughout my studies. I would especially like to thank my father, Paul, for introducing me to the passionating problems and open questions of physics and for all the stimulating and critical discussions on physical topics in general and on my subject of specialisation. I would like to thank my mother, Roswitha, for her moral support and her patience with my concerns.

I would like to thank my supervisor, Dr. Harald Dorn, for his intensive support, for all the helpful advice and the guidance, he gave me throughout the past year and for always being available for questions. I am deeply indebted to him for the great amount of time he dedicated to my assistance, which was, I believe, far more than one could expect from any supervisor.

Furthermore, I am very grateful to Prof. Jan Plefka for willing to be the second reviewer of my thesis and for his competent guidance of the group, enabling an open and fruitful scientific atmosphere.

In the same context, let me thank the former and present members of the Quantum Field Theory and String Theory group at the Humboldt University Berlin for contributing to this open and friendly atmosphere: Dr. Nadav Drukker, Prof. Dietmar Ebert, Dr. Valentina Forini, Dr. Johannes Henn, Dr. George Jorjadze, Dr. Hans-Jörg Otto, Dr. Subodh Patil, Per Sundin, Dr. Donovan Young, especially thanking my office colleagues and fellow graduands Nikolai Beck, Volker Branding, Hai Than Ngo, Andreas Rodigast, Ralf Sattler, Theodor Schuster and Konstantin Wiegandt for all the stimulating discussions on physical and non-physical topics, for computer support and most of all for creating a very personal atmosphere, which made every day work a great pleasure. Cordial thanks also to Sylvia Richter for her administrative assistance.

I am especially indebted to Andreas Rodigast for intensive computer support and to Johannes Henn and Theodor Schuster for various helpful discussions on matters of my thesis and technical advice. In particular, I would like to thank Konstantin Wiegandt for all his support regarding the contents and for his moral support and encouragement during the past year and throughout the time of my studies.

I am very obliged to Johannes Henn, Andreas Rodigast, Theodor Schuster and Konstantin Wiegandt for comments on the manuscript.

Contents

Introduction	1
1 The AdS/CFT Correspondence	5
1.1 Symmetries of Minkowski and AdS Space	5
1.1.1 Conformal Group of Minkowski Space	5
1.1.2 Isometries of AdS Space	7
1.2 Geometry of AdS and Minkowski Space	7
1.2.1 Conformal Compactification of Minkowski Space	7
1.2.2 Conformal Boundary of AdS Space	10
1.2.3 Poincaré Coordinates	12
1.3 Aspects of $\mathcal{N} = 4$ Super Yang-Mills Theory	12
1.3.1 Correlation Functions of Conformal Primary Operators	13
1.4 The AdS/CFT Correspondence	13
1.4.1 The 't Hooft and the Large λ Limit	14
1.4.2 Mapping String Theory Fields and CFT Operators	15
2 Wilson Loops in the AdS/CFT Correspondence	17
2.1 The Wilson Loop Operator	17
2.1.1 The Wilson Loop and the Quark-Antiquark Potential	18
2.2 The Wilson Loop in the AdS/CFT Correspondence	19
2.2.1 The Supersymmetric Wilson Loop and its Coupling to the Scalars	20
2.3 Wilson Loops and Gluon Scattering Amplitudes Duality	22
2.3.1 Motivation for the Duality at Strong Coupling	22
2.3.2 The Cusp Anomalous Dimension of the Wilson Loop	23
2.3.3 The BDS Conjecture for MHV Scattering Amplitudes	25
2.3.4 Dual Conformal Symmetry of Wilson Loops and Scattering Amplitudes	26
3 Regularisation of Amplitudes and Wilson Loops	29
3.1 Duality at Weak Coupling in Dimensional Regularisation	29
3.2 Amplitudes and Wilson Loops in Off-Shell Regularisation	31
3.2.1 Dimensional Regularisation of the Cusp Divergences	35
3.2.2 Regularisation of the Cusp Divergences by Cutoff	39
4 Special Properties of Wilson Loops in Minkowski Space	45
4.1 Minkowskian Circle with Light-Like Tangents	45
4.2 Wilson Loops with Discontinuities in Higher Derivatives	50
4.3 Wilson Loops with Straight Finite Light-Like Segments	56
4.4 Rectangular Wilson Loop in Minkowskian Space	61
5 Conclusion and Outlook	71

A Aspects of SU(N) Gauge Theory	75
A.1 Generators of SU(N)	75
A.2 Propagators	75
A.3 Propagators in Dimensional Regularisation	76
B Integrals	77
B.1 Wilson Loops and Amplitudes in Off-Shell Regularisation	77
B.2 Circular Wilson Loop	79
C Wilson Loop with Straight Light-Like Segment	81
Bibliography	85

Introduction

The *standard model* of elementary particle physics offers a very successful description of nature on the microscopic level and has been verified to high precision. However, despite its predictive power, it suffers from several deficits. Depending on a large number of parameters, it in particular lacks a deep explanation of the mass spectrum of the fundamental particles. Furthermore, the construction of a consistent quantum theory of gravity remains one of the main problems of fundamental physics. String theory is a promising candidate for this concern. It gives up the notion of point-like particles as the fundamental objects of nature, replacing them by one-dimensional *strings*. Consistent string theories cannot live in an arbitrary number of dimensions. While pure bosonic string theory is constrained to 26 dimensions, additionally admitting fermionic excitations gives rise to 10-dimensional superstring theories. At currently accessible energy scales, the different vibrational modes of a string would look like different point-like particle states. All string theories automatically include a massless spin two particle as oscillation mode of a closed string. The only consistent interaction of such an oscillation mode describes gravity.

Originally though, string theory was not developed as a theory of quantum gravity, but as a theory of strong interactions, in the 1960s. It is only later, that quantum chromodynamics (QCD) was discovered. QCD is a non-Abelian gauge theory with gauge group $SU(3)$, expressing the fact that it has three colours. The running of the coupling constant leads to the asymptotic freedom of QCD at high energies, whereas at low energies, particles are confined. In the weakly coupled high energy regime, perturbation theory can be applied, whereas the strongly coupled regime is hard to access. The best tool to perform calculations in this regime so far, are numerical simulations on the lattice. It was proposed by 't Hooft in the 1970s, that one should consider $SU(N)$ gauge theory for large number of colours N [1], in the hope that the theory may simplify and that an expansion in orders of $\frac{1}{N}$ may lead to a better understanding of QCD. This expansion resembles a topological expansion in string theory, in which for $N \rightarrow \infty$, only planar diagrams contribute. In this sense, in the limit of large N , gauge theories are connected with string theories. However, even in the limit of large N , QCD is far from being solved and it thus seems natural to consider simpler supersymmetric Yang-Mills gauge theories. The maximally supersymmetric $\mathcal{N} = 4$ super Yang-Mills (SYM) theory, in particular, has vanishing β -function and its superconformal invariance therefore extends to the quantum theory.

It is from these considerations that the Anti-de Sitter/conformal field theory (AdS/CFT) correspondence arose. Originally proposed by Maldacena in 1997 [2], the correspondence states an equivalence between superconformal $\mathcal{N} = 4$ SYM theory in four-dimensional Minkowski space on one side, and type IIB

superstring theory in ten-dimensional curved $AdS_5 \times S^5$ background on the other side. As we will explain in more detail below, the four-dimensional theory is said to live on the conformal boundary of the string theory background. The fact that all ten-dimensional degrees of freedom of the string theory are in a sense contained in the four-dimensional gauge theory on the boundary, is often expressed by referring to the AdS/CFT correspondence as *holographic*. Thus relating a theory that contains gravity, namely string theory, with a four-dimensional field theory with no gravity at all, the AdS/CFT correspondence is very remarkable.

In its strongest version, the AdS/CFT correspondence holds for all values of the rank N of the gauge group, and for all values of the coupling. It then is a correspondence between full interacting superstring theory and gauge theory in all regimes of the coupling. In weaker versions, taking $N \rightarrow \infty$, the conjecture only holds for free superstring theory, or even weaker only for its low energy limit, supergravity. In this limit, low energy dynamics of string theory are mapped onto strongly coupled SYM theory. On the other side, considering the perturbatively accessible regime of finite effective coupling in the gauge theory, implies having free superstring theory or even full interacting superstring theory in $AdS_5 \times S^5$, which has not been solved, as yet. In case the correspondence is true, it would thus be a powerful tool in order to perform strong coupling calculations of both theories through the respective weakly coupled dual theory. On the other hand, the fact that in either of the regimes, one of the partners remains unsolved, makes it very hard to be proved.

Yet, in its weakest form, concerning supergravity, the problem offers a reasonable chance of solution and the connection between a strongly coupled gauge theory in four-dimensional Minkowski space and a weakly coupled string theory seems very appealing. One might hope to learn more about strongly coupled QCD from it some time. However, as mentioned above, $\mathcal{N} = 4$ SYM has many special properties, which QCD has not, first of all, being a superconformal quantum field theory. Furthermore, this limit of the correspondence concerns $N \rightarrow \infty$, while for QCD $N = 3$.

Nevertheless, being the first concrete realisation of a correspondence between a large N gauge theory and a string theory as proposed by 't Hooft, the AdS/CFT correspondence remains of outstanding interest.

A true duality of the two theories implies that all observable objects, including gauge invariant operators, states and correlation functions of both theories be equivalent. An important non-local gauge invariant operator in gauge theories is the Wilson loop operator, whose significance was pointed out by Wilson in the 1970s [3]. Therein, the Wilson loop in QCD was shown to be related to the potential of confined quarks.

Right from the beginnings of the correspondence, it was suggested that the Wilson loop operator in the gauge theory be related to open strings in the AdS space, ending on the contour of the Wilson loop on the boundary of AdS [4]. The validity of this duality would signify that one could perform strong coupling calculations of gauge theory quantities described by the Wilson loop, such as the quark-antiquark potential, through the weakly coupled string theory dual.

Next to the long known significance of a rectangular Wilson loop as being related to the quark-antiquark potential, another striking duality within the gauge theory was recently found, motivated through the AdS/CFT correspondence at strong coupling [5, 6]. It suggests that gluon scattering amplitudes in $\mathcal{N} = 4$ SYM be associated with polygonal Wilson loops, whose sides are determined by the gluon momenta. Though motivated at strong coupling, the duality also seems to hold at weak coupling [7, 8].

Already in the 1980s an intimate relationship between the infrared (IR) divergences of the scattering of massless particles and the ultraviolet (UV) divergences of a Wilson loop with cusps was found in QCD [9, 10, 11]. The leading IR divergent term of the scattering amplitudes was shown to be governed by the *cusplike anomalous dimension* resulting from the UV divergences of the Wilson loop with cusps. This relationship led to the applicability of renormalisation group methods for the IR divergences of the scattering amplitudes.

Another interesting aspect in the context of the duality between Wilson loops and scattering amplitudes concerns their finite part. The two objects seem to possess a broken dual conformal symmetry. It was found in [12] that in certain *dual coordinates* four-gluon scattering amplitudes unveil a *dual conformal invariance*, broken by their IR divergences. On the other side, for light-like polygonal Wilson loops, a conformal Ward identity was found [13], which severely restricts the form of its finite part. If the duality is valid at all orders in the coupling, the dual conformal symmetry of the scattering amplitudes would be a direct consequence of this conformal Ward identity for the Wilson loop. The coupling dependence of the amplitudes' finite part would then fully be determined by the cusp anomalous dimension of the Wilson loop.

Although scattering amplitudes in $\mathcal{N} = 4$ SYM theory are much simpler than in QCD, one might hope that these new insights could shed some light on the all-order form of QCD amplitudes. However, an important ingredient for the duality between Wilson loops and scattering amplitudes and for their dual conformal symmetries, is the conformal invariance of $\mathcal{N} = 4$ SYM. In this light, a direct transfer of such a duality to the non-conformal QCD seems out of reach. Nevertheless, with an explicit formula for all tree-level amplitudes in $\mathcal{N} = 4$ SYM found in [14], the tree-level gluon amplitudes, which are valid for any gauge theory, could already be computed.

As mentioned above, the two objects of the scattering amplitude/Wilson loop duality in $\mathcal{N} = 4$ SYM are divergent. Therefore, for a full comparison of the two objects, including their infinite parts, a regularisation needs to be specified on both sides. This has usually been done in dimensional regularisation [7, 8]. It seems interesting to ask, though, how robust the duality is regarding the choice of regularisation. Another natural regularisation of the gluon scattering amplitudes is to take their momenta off-shell. The question then arises, how the Wilson loop needs to be regularised in order to match the off-shell amplitudes. A proposal for such a regularisation of the Wilson loop will be presented in this thesis.

The significance of the Wilson loop and its renormalisation properties in

gauge theory motivate an investigation of its divergences for different contours. In Minkowski space, Wilson loops have many special features, specific to their embedding in space-time, that do not find an equivalent in Euclidean space. We will examine some of these features in the present thesis, focusing on the locally supersymmetric Wilson loop considered in the AdS/CFT correspondence. We have mentioned above, that the fact that $\mathcal{N} = 4$ SYM is supersymmetric leads to important simplifications. For certain quantities the supersymmetry constraints are so strong that all quantum corrections cancel and that they do not need to be renormalised. This is for instance the case for the expectation value of a straight Wilson line. The construction of Wilson loops, that preserve a certain amount of global supersymmetry, has been discussed in [15, 16, 17, 18] with view to such non-renormalisation theorems. In this context, we will construct a form of the locally supersymmetric Wilson loop, such that it becomes finite for certain contours, that otherwise give rise to divergences in Minkowskian background.

Outline

We will review the basics and main statements of the AdS/CFT-correspondence in chapter 1 and focus on the role of the Wilson loop in the correspondence in chapter 2. There, we further review the recently proposed duality between scattering amplitudes in $\mathcal{N} = 4$ SYM and Wilson loops. A full comparison of the two objects including the infinite parts, requires a regularisation on both sides of the duality. This comparison is usually performed in dimensional regularisation, as will be summarised in section 3.1.

In section 3.2, we then propose a regularisation of the Wilson loop in order to match off-shell scattering amplitudes, as an alternative to the matching of Wilson loops and on-shell amplitudes in dimensional regularisation. In chapter 4, the properties of Wilson loops along different specific contours in Minkowski space are examined. Special embedding in space-time, such as light-like tangents and extended light-like segments along the contour of the Wilson loop can lead to divergences. We will examine these properties of Wilson loops in Minkowski space, also treating the aspect of the coupling of the locally supersymmetric Wilson loop to the scalars.

A short discussion of the results and an outlook will be given in the last chapter.

I

The AdS/CFT Correspondence

The Anti-de Sitter/ Conformal Field Theory (AdS/CFT) correspondence, as originally conjectured by Maldacena, relates type IIB superstring theory in 10-dimensional $AdS_5 \times S^5$ background with the 4-dimensional conformal $\mathcal{N} = 4$ super Yang-Mills (SYM) theory. An essential feature of the correspondence is that the symmetries of the background space-time, in which the string theory lives, are reflected by the symmetries of the superconformal gauge theory. The isometries of AdS_5 correspond to the conformal symmetries of the gauge theory, as will be explained in more detail in section 1.1. As mentioned in the introduction, the 4-dimensional conformal gauge theory is often referred to as living on the conformal boundary of the 10-dimensional string theory. In section 1.2, we will explain how this statement can be understood from the point of view of the background geometries. We will then briefly resume a few basics of $\mathcal{N} = 4$ SYM theory and conclude this chapter by presenting the main statements of the correspondence and making it more explicit by indicating some objects of the two theories, which are matched.

An extensive introduction to the AdS/CFT correspondence can be found in [19]. For a more detailed introduction the reader is referred to [20] or as a first approach, the more pedagogical introduction [21] can be recommended.

1.1 Symmetries of Minkowski and AdS Space

1.1.1 Conformal Group of Minkowski Space

Yang-Mills theories in 4 dimensions classically are conformal field theories. Conformal invariance is a generalisation of Poincaré invariance, adding to it scale invariance and invariance under special conformal transformations. In general, this conformal invariance does not extend to the quantum theory, since renormalisation requires introducing a scale, which explicitly breaks scale invariance. This is for instance the reason why QCD is not conformal. However, in the case of $\mathcal{N} = 4$ super Yang-Mills theory (SYM) in 4 dimensions, scale invariance does extend to the quantum theory. In the AdS/CFT correspondence, we are thus dealing with a conformal quantum field theory.

The theory thus is invariant under conformal transformations, i.e. transformations $x \rightarrow x'$ that keep the metric invariant up to a scale factor, which depends on the coordinates:

$$\frac{\partial x'^{\mu}}{\partial x^{\alpha}} \frac{\partial x'^{\nu}}{\partial x^{\beta}} g_{\mu\nu}(x') = \lambda(x) g_{\alpha\beta}(x) \quad (1.1)$$

These are precisely the transformations that preserve angles.

Solving the conformal Killing equation for infinitesimal conformal transformations, we find that for d-dimensional flat Minkowski space the continuous conformal group contains the Poincaré transformations, including the Lorentz transformations generated by $M_{\mu\nu}$ and the translations generated by P_μ . Additionally, there is a rigid scale transformation with generator D:

$$x^\mu \rightarrow x'^\mu = \lambda x^\mu \quad (1.2)$$

and furthermore, there are the special conformal transformations, consisting of the composition of an inversion with respect to the unit hyperboloid ($x^\mu \rightarrow x'^\mu = \frac{x^\mu}{x^2}$), a translation and again an inversion. The special conformal transformations are generated by K_μ :

$$x^\mu \rightarrow x'^\mu = \frac{x^\mu + c^\mu x^2}{1 + 2c \cdot x + c^2 x^2} \quad (1.3)$$

From their infinitesimal forms, we find that the generators suffice the following conformal algebra: the usual Poincaré algebra

$$[M_{\mu\nu}, M_{\rho\sigma}] = i(\eta_{\mu\sigma}M_{\nu\rho} + \eta_{\nu\rho}M_{\mu\sigma} - \eta_{\mu\rho}M_{\nu\sigma} - \eta_{\nu\sigma}M_{\mu\rho}), \quad (1.4)$$

$$[M_{\mu\nu}, P_\rho] = i(\eta_{\mu\rho}P_\nu - \eta_{\nu\rho}P_\mu), \quad [P_\mu, P_\nu] = 0 \quad (1.5)$$

and additionally

$$[D, P_\mu] = -iP_\mu, \quad [D, K_\mu] = iK_\mu, \quad [D, M_{\mu\nu}] = 0, \quad [K_\mu, K_\nu] = 0, \quad (1.6)$$

$$[K_\mu, P_\nu] = 2i(\eta_{\mu\nu}D - M_{\mu\nu}), \quad [K_\rho, M_{\mu\nu}] = i(\eta_{\rho\nu}K_\mu - \eta_{\rho\mu}K_\nu).$$

Defining the antisymmetric operator J_{ab} (with $a, b = 0, \dots, d+1$) by

$$\begin{aligned} J_{\mu\nu} &:= M_{\mu\nu}, & J_{(d+1)d} &:= D, \\ J_{\mu d} &:= \frac{1}{2}(K_\mu - P_\mu), & J_{\mu(d+1)} &:= \frac{1}{2}(K_\mu + P_\mu), \end{aligned} \quad (1.7)$$

the conformal algebra takes the form

$$[J_{ab}, J_{cd}] = i(g_{ad}J_{bc} + g_{bc}J_{ad} - g_{ac}J_{bd} - g_{bd}J_{ac}) \quad (1.8)$$

with the metric

$$g_{ab} = \begin{pmatrix} + & & & & \\ & - & & & \\ & & \dots & & \\ & & & - & \\ & & & & + \end{pmatrix}.$$

This is the standard form of the $SO(2,d)$ algebra, as one can easily recall by comparing with the Lorentz algebra $SO(1,d-1)$ in (1.4).

We thus see that the conformal group of d-dimensional Minkowski space is $SO(2,d)$.

1.1.2 Isometries of AdS Space

$(d + 1)$ -dimensional Anti-de Sitter space (AdS_{d+1}) with radius R can be represented as a hyperboloid

$$-X_0^2 - X_{d+1}^2 + \sum_{i=1}^d X_i^2 = R^2 \quad (1.9)$$

in $(d + 2)$ -dimensional flat space $\mathbb{R}^{2,d}$ with metric

$$ds^2 = dX_0^2 + dX_{d+1}^2 - \sum_{i=1}^d dX_i^2. \quad (1.10)$$

By construction this submanifold of $\mathbb{R}^{2,d}$ preserves the symmetry-group $SO(2,d)$ of the embedding space, just as the sphere preserves the rotation invariance of Euclidean space. The isometry-group of AdS_{d+1} thus is $SO(2,d)$.

The conformal group of d -dimensional Minkowski space therefore equals the symmetry group of AdS_{d+1} . This is an important feature of the AdS/CFT correspondence, relating the symmetries of the string theory background, AdS_5 with the conformal symmetries of $\mathbb{R}^{1,3}$.

We will see below, that the symmetry group of the S^5 , $SO(6)$, is reflected by the R-symmetry group of $\mathcal{N} = 4$ SYM, $SU(4)_R \cong SO(6)_R$.

1.2 Geometry of AdS and Minkowski Space

In the AdS/CFT correspondence, it is often stated that the 4-dimensional gauge theory lives on the boundary of the string theory. To see this, it is essential to understand why the boundary of the AdS_5 can conformally be mapped onto 4-dimensional Minkowski space. In this section we will explain how this statement is to be understood. A detailed description of AdS geometry can be found in [20].

1.2.1 Conformal Compactification of Minkowski Space

Let us first have a look at 2-dimensional Minkowski space, $\mathbb{R}^{1,1}$, with metric

$$ds^2 = dt^2 - dx^2. \quad (1.11)$$

With a series of coordinate transformations

$$\begin{aligned} \tan u_{\pm} &:= t \pm x, & -\frac{\pi}{2} < u_{\pm} < \frac{\pi}{2} \\ u_{\pm} &:= \frac{\tau \pm \Theta}{2} \end{aligned} \quad (1.12)$$

the metric becomes

$$ds^2 = \frac{1}{4 \cos^2 u_+ \cos^2 u_-} (d\tau^2 - d\Theta^2). \quad (1.13)$$

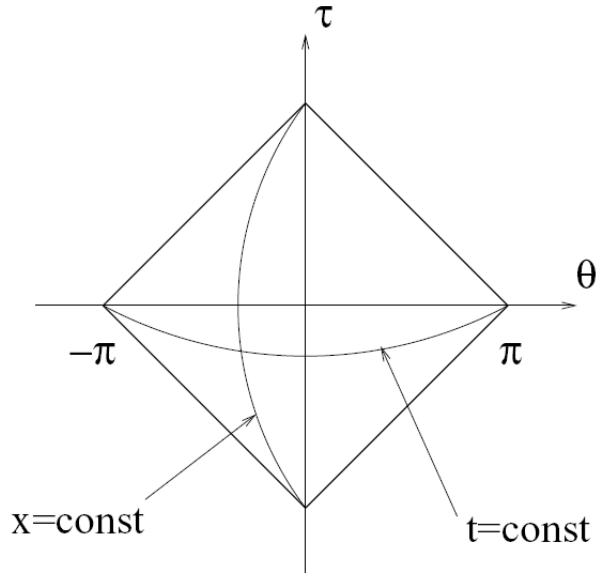


Figure 1.1: 2-dimensional Minkowski space can conformally be mapped into the interior of this compact rectangle. In the diagram, lines of constant time and lines of constant x are denoted. Light ray trajectories are invariant under conformal rescaling and thus stay the lines of slope 1 and -1, parallel to the boundaries.¹

This metric can conformally be rescaled to

$$ds'^2 = d\tau^2 - d\Theta^2 \quad (1.14)$$

and taking into account the area to which u_{\pm} is restricted, we see that Minkowski space is conformally mapped into the compact rectangle shown in fig. 1.1. By identifying the two corners of the rectangle at $(\tau, \Theta) = (0, \pm\pi)$, corresponding to the spatial infinities $x = \pm\infty$, it can be embedded in the cylinder, which is the 2-dimensional Einstein static universe (*ESU*), as shown in fig. 1.2. Mack and Lüscher have shown in [22] that correlation functions of conformal field theories can analytically be continued to the whole Einstein static universe.

The situation for general dimensions d is analogous. the metric then is

$$ds^2 = dt^2 - dr^2 - r^2 d\Omega_{d-1}^2 \quad (1.15)$$

where $d\Omega_{d-1}$ is the line element on the S^{d-1} unit sphere. We can define the same coordinate transformations as in (1.12), taking into account that now $r \geq 0$, and by conformal rescaling we find

$$ds'^2 = d\tau^2 - d\Theta^2 - \sin^2 \Theta d\Omega_{d-1}^2. \quad (1.16)$$

The (t, r) -half-plane now is conformally mapped into the triangular region shown in figure 1.3.

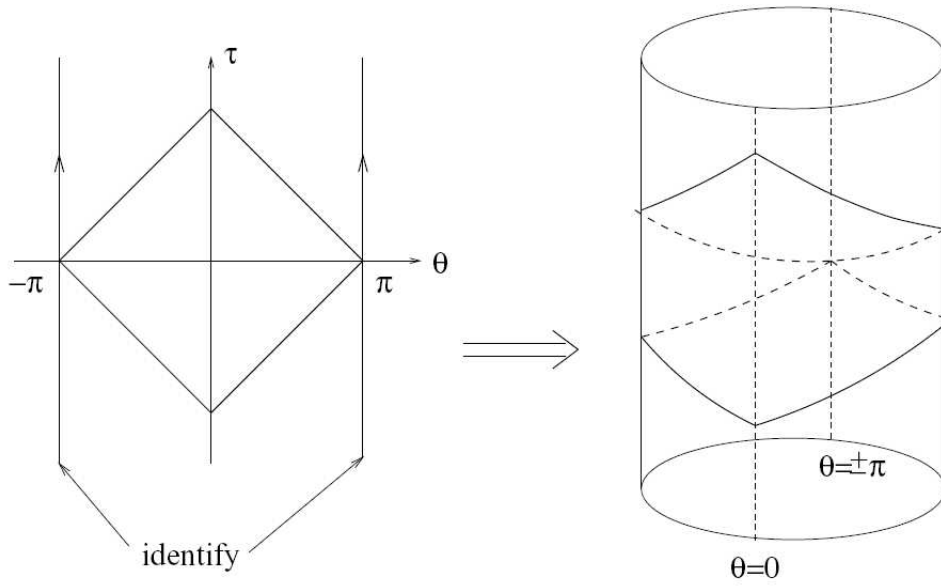


Figure 1.2: The conformal compactification of 2D Minkowski space can be embedded in the cylindrical 2D ESU by identifying two points at spatial infinity.¹

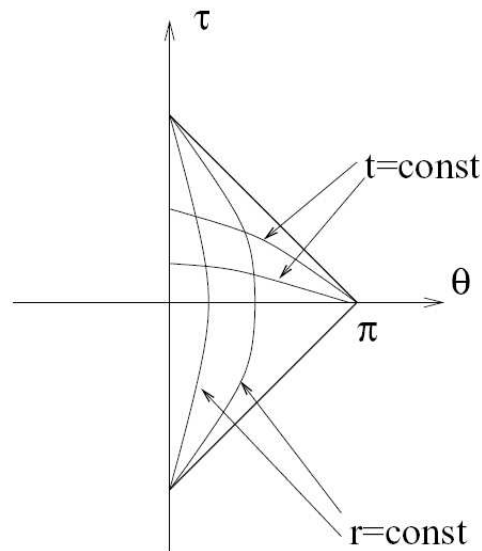


Figure 1.3: d-dim. Minkowski space can conformally be mapped into this compact triangular region.¹

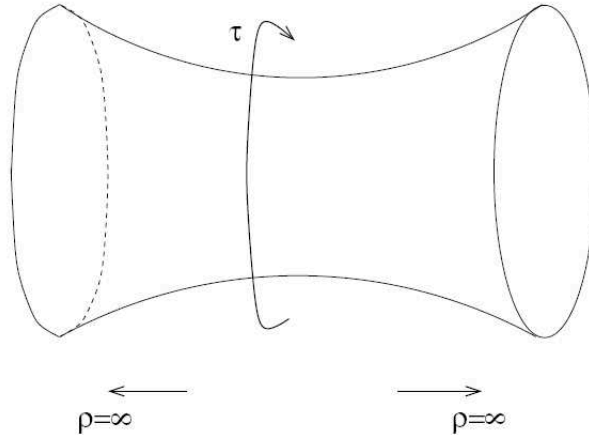


Figure 1.4: Global coordinates of AdS_{d+1} , realized as a hyperboloid in $\mathbb{R}^{2,d}$. For the case of AdS_2 the unit sphere described by the additional coordinates Ω_i becomes a S^0 , consisting of only two points, attributed to the two halves of the hyperboloid. The hyperboloid has closed timelike curves along the τ -direction: $0 \leq \tau < 2\pi$.¹

Taking

$$0 \leq \Theta \leq \pi, \quad -\infty < \tau < \infty \quad (1.17)$$

this triangle can again be embedded into the Einstein static universe.

1.2.2 Conformal Boundary of AdS Space

The defining equation for $(d+1)$ -dimensional AdS space (1.9) can be solved by the following choice of coordinates:

$$\begin{aligned} X_0 &= R \cosh \rho \cos \tau \\ X_{d+1} &= R \cosh \rho \sin \tau \\ X_i &= R \sinh \rho \Omega_i \quad i = 1, \dots, d \end{aligned} \quad (1.18)$$

where $\sum \Omega_i^2 = 1$ describes a S^{d-1} unit sphere. With $0 \leq \tau < 2\pi$ and $\rho \geq 0$, these coordinates cover the entire hyperboloid and are therefore called *global coordinates* of AdS (see fig. 1.4). Inserting these into the metric of the embedding space (1.10), we obtain the metric of AdS_{d+1} :

$$ds^2 = R^2(\cosh^2 \rho d\tau^2 - d\rho^2 - \sinh^2 \rho d\Omega_{d-1}^2) \quad (1.19)$$

with $d\Omega_{d-1}^2 = \sum d\Omega_i^2$.

In τ -direction, the hyperboloid has closed timelike curves. For causal spacetime, we therefore need to unwrap the τ -direction, i.e. take $-\infty < \tau < \infty$ without

¹The pictures were taken from [20].

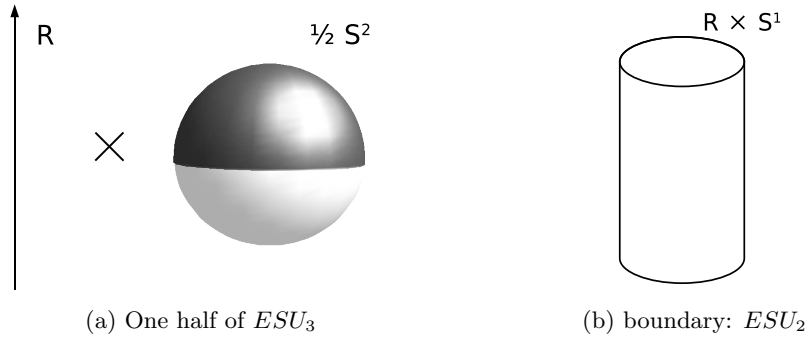


Figure 1.5: Half of the $(d + 1)$ -dimensional Einstein static universe $R \times S^d$ (ESU_{d+1}). The boundary of half of S^d is the whole sphere in one dimension less, S^{d-1} . Thus the boundary of half of ESU_{d+1} is the whole ESU_d . In the case of $d = 2$, this is the cylinder represented in (b).

identifications, and thus get the *universal covering* of AdS.

Introducing the coordinate

$$\tan \Theta := \sinh \rho \quad \text{with } \rho \geq 0 \quad \Rightarrow \quad 0 \leq \Theta < \frac{\pi}{2} \quad (1.20)$$

the metric takes the form

$$ds^2 = \frac{R^2}{\cos^2 \Theta} (d\tau^2 - d\Theta^2 - \sin^2 \Theta d\Omega_{d-1}^2). \quad (1.21)$$

We can now conformally rescale the metric to

$$ds'^2 = d\tau^2 - d\Theta^2 - \sin^2 \Theta d\Omega_{d-1}^2. \quad (1.22)$$

This is the metric of the $(d + 1)$ -dimensional Einstein static universe, $\mathbb{R} \times S^d$. Here however, the coordinate Θ only takes values $0 \leq \Theta < \frac{\pi}{2}$, i.e. only covers half of the S^d ; the metric therefore only covers half of the ESU . AdS_{d+1} can thus conformally be mapped onto half of ESU_{d+1} .

The boundary of half of the ESU in $(d + 1)$ dimensions is the entire ESU_d in one dimension less (see fig. 1.5). This means that the boundary of AdS_{d+1} is conformally mapped to the d -dimensional Einstein static universe.

We can finally conclude that the conformal boundary of AdS_{d+1} has the same structure as the conformally compactified $\mathbb{R}^{1,d-1}$. This is what is meant by the statement that the conformal boundary of AdS_{d+1} is d -dimensional Minkowski space.

1.2.3 Poincaré Coordinates

Another frequently used set of coordinates on AdS_{d+1} are the Poincaré coordinates (u, x) , defined by

$$\begin{aligned} X_0 &= \frac{1}{2u}(1 + u^2(R^2 + x_0^2 - \vec{x}^2)) \\ X_d &= \frac{1}{2u}(1 - u^2(R^2 - x_0^2 + \vec{x}^2)) \\ X_i &= R u x_i \quad i = 1, \dots, d-1 \\ X_{d+1} &= R u x_0 \end{aligned} \quad (1.23)$$

where $\vec{x}^2 = \sum_{i=1}^{d-1} x_i^2$. With $u > 0$, these coordinates cover half of AdS_{d+1} and the metric becomes

$$ds^2 = R^2 \left(\frac{du^2}{u^2} + u^2 dx^2 \right) \quad (1.24)$$

where $dx^2 = dx_0^2 - d\vec{x}^2$. Performing another substitution $u = \frac{1}{z}$, the metric becomes

$$ds^2 = R^2 \frac{dz^2 + dx^2}{z^2}. \quad (1.25)$$

The metric is singular for $z \rightarrow 0$, reflecting the fact that this is the boundary of AdS and that z plays the role of a radial coordinate.

1.3 Aspects of $\mathcal{N} = 4$ Super Yang-Mills Theory

Super Yang-Mills theory with maximal number of supersymmetries $\mathcal{N} = 4$ contains a gauge field A_μ , four Weyl spinors and six scalars ϕ^I ($I = 1, \dots, 6$), all in the adjoint representation of the gauge algebra. It is convenient to put the fermions into a single 10-dimensional 16-component Weyl spinor χ_α . The form of the Lagrangian then is uniquely determined by supersymmetry:

$$\begin{aligned} \mathcal{L} = \frac{2}{g_{\text{YM}}^2} \text{Tr} \left(\frac{1}{4} F_{\mu\nu} F^{\mu\nu} + \frac{1}{2} \sum_I D_\mu \phi^I D^\mu \phi^I - \frac{1}{4} ([\phi^I, \phi^J])^2 + \right. \\ \left. + \frac{1}{2} \bar{\chi}^\alpha \Gamma^\mu D_\mu \chi_\alpha - \frac{i}{2} \sum_I \bar{\chi}^\alpha \Gamma_I [\phi_I, \chi_\alpha] \right) \end{aligned} \quad (1.26)$$

where g_{YM} is the Yang-Mills coupling constant, $F_{\mu\nu}$ is the field strength to the gauge field A_μ and D_μ the covariant derivative. (Γ_μ, Γ_I) are 10-dimensional Dirac matrices, entering in the Lagrangian through its construction by dimensional reduction of $\mathcal{N} = 1$ SYM in 10 dimensions [23].

It can be seen by consideration of the mass dimensions of the terms in the Lagrangian, that the theory is scale invariant, which together with the usual Poincaré invariance gives the conformal symmetry group $SO(2, 4) \simeq SU(2, 2)$. Additionally, the Lagrangian is invariant under $\mathcal{N} = 4$ Poincaré supersymmetry

by construction. The supercharges may be rotated into one another under the R-symmetry group $SU(\mathcal{N})_R$. The combination of conformal invariance with the $\mathcal{N} = 4$ Poincaré supersymmetry then produces an even larger superconformal symmetry, forming the supergroup $SU(2, 2|\mathcal{N})$. Its maximal bosonic subgroup $SU(2, 2) \times SU(4)_R \simeq SO(2, 4) \times SO(6)$ exactly reflects the isometries of the $AdS_5 \times S^5$ background of the dual string theory.

A special property of $\mathcal{N} = 4$ SYM is that its conformal invariance is not broken by quantum corrections, since its coupling constant does not depend on any renormalisation scale. Its β -function was shown to vanish to three loop order and is believed to vanish identically [24], which implies that superconformal symmetry survives quantisation.

1.3.1 Correlation Functions of Conformal Primary Operators

Conformal invariance is remarkably restrictive on the form of the correlation functions of conformal operators. Under conformal transformation $x \rightarrow x'$, scalar operators $\mathcal{O}(x)$ transform as

$$\mathcal{O}'(x') = \left| \det \frac{\partial x'^\beta}{\partial x^\alpha} \right|^{-\frac{\Delta}{d}} \mathcal{O}(x), \quad (1.27)$$

where d is the space-time dimension of the CFT. Then Δ defines the scaling dimension of the operator \mathcal{O} , which we denote by \mathcal{O}_Δ . Such operators are conformal primary operators and the dilation operator introduced in (1.2) acts on them as follows:

$$[D, \mathcal{O}_\Delta(x)] = (x^\mu \partial_\mu + \Delta) \mathcal{O}_\Delta. \quad (1.28)$$

Conformal symmetry severely restricts the form of the n-point-functions of primary operators. The 2-point-function, for example, is constrained to the form

$$\langle \mathcal{O}_{\Delta_1}(x_1) \mathcal{O}_{\Delta_2}(x_2) \rangle = c \frac{\delta_{\Delta_1, \Delta_2}}{|x_1 - x_2|^{2\Delta_1}}. \quad (1.29)$$

It is thus fixed except for the normalisation factor c and the dynamically determined scaling dimensions Δ_1 and Δ_2 .

Classically, the scaling dimension simply is the sum of the dimensions of the fields the operator is composed of. Upon quantisation, however, the scaling dimension receives corrections and the operator acquires an anomalous dimension.

1.4 The AdS/CFT Correspondence

The AdS/CFT correspondence conjectures a duality between the following two theories:

- Type IIB superstring theory in 10-dimensional $AdS_5 \times S^5$ with string coupling g_s and where both, AdS and the sphere, have radius R .

- Maximally supersymmetric conformal $\mathcal{N} = 4$ super Yang-Mills theory in 4 dimensions with coupling constant g_{YM} and gauge group $\text{SU}(N)$.

The above parameters of the two theories are matched as follows

$$g_s = g_{\text{YM}}^2 \quad R^4 = 4\pi g_{\text{YM}}^2 N \alpha'^2 \quad (1.30)$$

where α' is the inverse string tension.

A duality of the above theories implies, that they are equivalent to one another, including all observable operators, states and correlation functions. Besides the identification of the parameters, we therefore need a precise map between the observable objects on both sides of the correspondence, i.e. between states and fields on the string theory side and gauge invariant operators on the gauge theory side, as well as between the correlators of both theories. In section 1.4.2, we will specify this identification for some important objects of the two theories.

The validity of this duality for all values of the above parameters would yield the strongest form of the AdS/CFT conjecture, which, however, is highly non-trivial. We will thus present certain limits of the theories, that offer a better chance of solution below.

1.4.1 The 't Hooft and the Large λ Limit

The 't Hooft limit consists in letting N go to infinity, while keeping the 't Hooft coupling, $\lambda \equiv g_{\text{YM}}^2 N$ fixed. In Yang-Mills theory, this limit corresponds to a topological expansion of the field theories Feynman diagrams [25]. On the string theory side, the string coupling constant can be expressed by the 't Hooft coupling: $g_s = \frac{\lambda}{N}$ and, as λ is kept fixed, here the 't Hooft limit corresponds to weakly coupled perturbative string theory. The validity of the AdS/CFT conjecture in the 't Hooft limit, would thus be a correspondence between free string theory (no loops) and the large N limit of $\mathcal{N} = 4$ SYM theory.

After having taken the 't Hooft limit, a further limit $\lambda \rightarrow \infty$ can be taken. While small λ would correspond to weak coupled gauge theory, large λ corresponds to small inverse string tensions α' , on the string theory side and the above limit reduces classical string theory to classical supergravity with action

$$S_{\text{SUGRA}} = \frac{1}{16\pi G_{10}} \int d^{10}x \sqrt{-g} e^{-2\phi_D} (\mathcal{R} + 4\partial^\mu \phi_D \partial_\mu \phi_D + \dots) \quad (1.31)$$

where G_{10} is the 10-dimensional Newton constant, \mathcal{R} is the Ricci-scalar and ϕ_D is the dilaton field. The dots denote contributions from other fields.

Thus, if the correspondence is valid in the large λ limit, strongly coupled SYM theory is mapped onto classical low energy supergravity, which offers a reasonable chance for solution. The correspondence would therefore be a powerful tool for the calculation of gauge theory results at strong coupling.

1.4.2 Mapping String Theory Fields and CFT Operators

As mentioned above, the duality should imply a precise map between the observable objects on both sides of the correspondence. On the string theory side, the dynamics depends on fields ϕ in AdS_5 , while in the conformal field theory the observable objects are gauge invariant operators \mathcal{O}_Δ characterised by their scaling dimension Δ , as described in section 1.3.1.

The generating functional of such an operator \mathcal{O} in terms of the source fields ϕ_0 is

$$Z_{\mathcal{O},CFT}[\phi_0] = \left\langle e^{\int d^4x \phi_0(x) \mathcal{O}(x)} \right\rangle_{CFT} . \quad (1.32)$$

From this we get the correlation functions by differentiating with respect to the sources $\phi_0(x)$.

On the other side, the dynamics of the string theory is described by the string partition function

$$\begin{aligned} Z_{\text{string}}[\phi(z, x)] &= \int \mathcal{D}X(\sigma, \tau) e^{-S[X(\sigma, \tau), \phi(z, x)]} \\ &= e^{-S_{\text{eff}}[\phi(z, x)]} \end{aligned} \quad (1.33)$$

where the integration over the space-time embedding $X(\tau, \sigma)$ of the string has been performed, leading to an effective action depending on the fields $\phi(z, x)$ of the string excitations. (z, x) denote the Poincaré coordinates defined in section 1.2.3, i.e. z is the radial direction of AdS and the boundary is characterised by $z = 0$. In the limit of supergravity, the effective action becomes the supergravity action of (1.31). In free supergravity, a field of mass m then satisfies $(\square + m^2)\phi(z, x) = 0$. On the boundary of AdS, for $z \rightarrow 0$, the field then behaves as

$$\phi(z, x) \xrightarrow{z \rightarrow 0} \begin{cases} z^\Delta \phi_0(x) \\ z^{4-\Delta} \phi_0(x) \end{cases} \quad (1.34)$$

where

$$\Delta := 2 + \sqrt{4 + m^2} \quad (1.35)$$

defines the dimension of the field, we denote by ϕ_Δ . The solutions of the interacting theory will have the same boundary behaviour as in the free case. Δ being ≥ 4 , the first boundary solution is normalisable and is interpreted to determine the vacuum expectation value of operators of associated dimension, whereas the second one is non-normalisable and defines an associated field on the boundary:

$$\phi_0(x) = \lim_{z \rightarrow 0} z^{\Delta-4} \phi_\Delta(z, x) \quad (1.36)$$

Assuming that these boundary fields are in a one-to-one correspondence with the bulk fields, i.e. uniquely define a solution $\phi_\Delta(z, x)$ of the string theory, the mapping prescription, proposed by Witten in [26], is to identify the generating functional of an operator $\mathcal{O}_\Delta(x)$ with scaling dimension Δ and source field $\phi_0(x)$ in the conformal boundary theory with the string partition function of the field

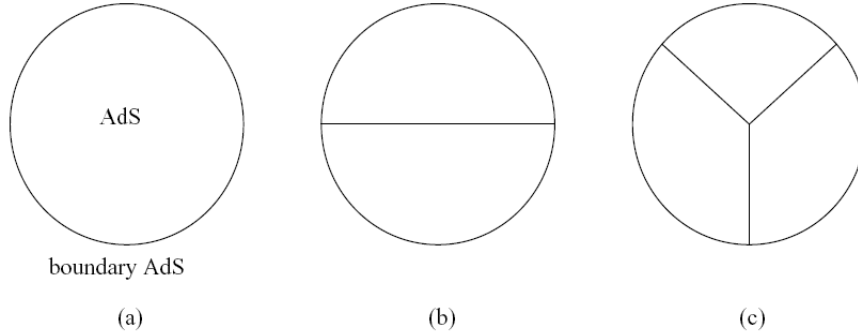


Figure 1.6: Witten diagrams for the 2-point function in (b) and the 3-point functions in (c). A perturbative expansion of supergravity leads to Feynman-like rules for the computation of these diagrams.

$\phi_\Delta(z, x)$ of equal dimension Δ , uniquely determined by the source fields $\phi_0(x)$ as the corresponding boundary field:

$$Z_{\mathcal{O}_\Delta, \text{CFT}}[\phi_0(x)] = Z_{\text{string}} \left[\phi_\Delta(z, x) \Big|_{\phi_0(x)} \right] \quad (1.37)$$

Thus, identifying the dimension of the string field ϕ_Δ , defined by its mass through (1.35) in the limit of supergravity, with the scaling dimension of the associated conformal operator \mathcal{O}_Δ , (1.37) also defines a map between masses of fields in supergravity and scaling dimensions of conformal operators.

As mentioned above, correlation functions of the gauge theory can be computed by differentiating the generating function (1.32) with respect to the sources ϕ_0 . In the large λ limit, the string theory action can be approximated by the supergravity action (1.31) and one can perform a perturbative expansion, leading to Feynman-like rules. In the supergravity limit only tree-level diagrams contribute, summarised as Witten diagrams [26], exemplarily shown for the 2- and 3-point function in fig. 1.6. The Witten-prescription thus allows computing correlation functions of gauge theory operators by calculating the corresponding tree level Witten diagrams.

From the identification of the correlators through (1.37) and their special form for conformal operators presented in section 1.3, the conjecture arises that the energy eigenvalues of string states equal the scaling dimensions of the dual conformal operators:

$$\mathcal{H}_{\text{string}}|\psi\rangle = E_{\text{string}}|\psi\rangle \quad \Leftrightarrow \quad E_{\text{string}} = \Delta \quad (1.38)$$

Finally, another interesting observable in gauge theory is the gauge invariant Wilson loop operator. As will be explained in more detail in chapter 2, the Wilson loop operator, as defined in the boundary theory, is going to be associated with string worldsheets in the AdS-bulk, ending on the loop contour on the 4-dimensional boundary of AdS.

II

Wilson Loops in the AdS/CFT Correspondence

In gauge theory, an important non-local gauge invariant object is the Wilson loop. As the Wilson loop is going to be the main object of this thesis, we dedicate the following chapter to it and its significance in the AdS/CFT correspondence. We will first motivate its origin in gauge theory in section 2.1. Then, in section 2.2, we will explain its role in the AdS/CFT correspondence and finally, we will present the recently proposed duality conjecture between Wilson loops and gluon scattering amplitudes in $\mathcal{N} = 4$ SYM, motivated through the AdS/CFT correspondence in section 2.3.

2.1 The Wilson Loop Operator

In gauge theory, the Wilson loop can be constructed as a parallel transporter along a closed curve in the fibre bundle.

The parallel transport of some field $\phi(z)$ in the fibre bundle along a curve γ from z to y in the basis of the bundle is

$$U_\gamma[y, z] \phi(z) = \phi(y). \quad (2.1)$$

Constructing this parallel transport by a horizontal lift in the fibre bundle leads to a differential equation, which can be solved by

$$U_\gamma[y, z] = \mathcal{P} \exp \left(ig \int_\gamma A_\mu(x) dx^\mu \right) \quad (2.2)$$

where \mathcal{P} is the path-ordering, g is the coupling constant of the gauge theory and A_μ the gauge field. Under gauge transformations $\sigma'(z) = h(z)\sigma(z)$, where σ and σ' are local sections of the fibre bundle, it transforms as

$$U_\gamma[y, z] = h^{-1}(y) U_\gamma[y, z] h(z). \quad (2.3)$$

From this transformation behaviour and from the cyclic invariance of the trace, it follows that the trace of the parallel transporter along a closed curve \mathcal{C} is gauge invariant. This gauge invariant operator defines the Wilson loop:

$$\begin{aligned} W(\mathcal{C}) &:= \frac{1}{N} \text{Tr} U[\mathcal{C}] \\ &= \frac{1}{N} \text{Tr} \mathcal{P} \exp \left(ig \oint_{\mathcal{C}} A_\mu(x(t)) \dot{x}^\mu(t) dt \right) \end{aligned} \quad (2.4)$$

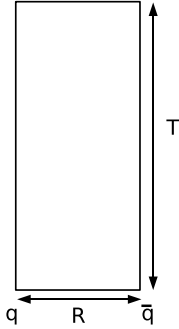


Figure 2.1: The static quark-antiquark potential corresponds to a rectangular Wilson loop with infinite time-like edges $T \rightarrow \infty$ and space-like edges corresponding to the distance of the quarks R .

where the factor of $\frac{1}{N}$ is introduced for convenience.¹ Since it depends on the path \mathcal{C} , the Wilson loop is a non-local operator.

Its significance lies in the fact, that all gauge invariant functions of the gauge field A_μ can be constructed from combinations of Wilson loops along different contours \mathcal{C} and that they thus form a complete basis of gauge invariant operators in Yang-Mills theory [27].

2.1.1 The Wilson Loop and the Quark-Antiquark Potential

The most prominent physical significance of the Wilson loop was found by Wilson [3]. He showed that the static quark-antiquark potential $V_{q\bar{q}}(R)$ in QCD equals the expectation value of a rectangular Wilson loop, as shown in fig. 2.1, with infinite timelike edges, and space-like edges corresponding to the distance of the quarks R (see also [28]):

$$V_{q\bar{q}}(R) = - \lim_{T \rightarrow \infty} \frac{1}{T} \ln W(\mathcal{C}_{R,T}) \quad (2.5)$$

If the QCD string tension

$$\alpha := \lim_{R \rightarrow \infty} \frac{1}{R} V_{q\bar{q}}(R) \quad (2.6)$$

is small, the potential rises linearly with the distance

$$V_{q\bar{q}}(R) \sim \alpha R \quad (2.7)$$

which leads to confinement [3]. It then follows from (2.5) that the Wilson loop obeys the area law

$$\lim_{R,T \rightarrow \infty} W(\mathcal{C}_{R,T}) = c e^{-\alpha RT} = c e^{-\alpha A}, \quad (2.8)$$

¹The conventional factor of $\frac{1}{N}$ makes sure that the zeroth order term of the Wilson loop in an expansion in the coupling constant gives one.

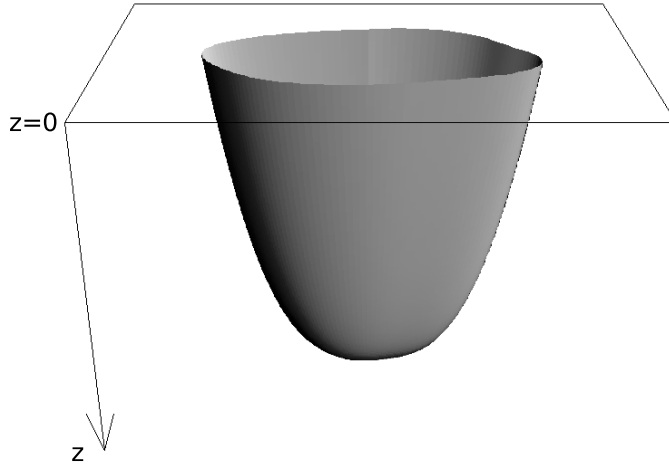


Figure 2.2: In the AdS/CFT correspondence, the Wilson loop operator in gauge theory is identified with string worldsheets, ending on the contour of the loop on the boundary of AdS.

where A is the area covered by the rectangle.

Another important application of the Wilson loop was the relation between the IR divergences of on-shell scattering amplitudes and the UV divergences of a Wilson loop with cusps found in [9, 10, 11], which led to the applicability of renormalisation group methods for the IR divergences of the scattering amplitudes. We will come back to this in section 2.3.2.

Lately, another interpretation of a certain type of Wilson loops was proposed: polygonal Wilson loops with light-like sides are conjectured to equal gluon scattering amplitudes in $\mathcal{N} = 4$ SYM, whose gluon momenta correspond to the sides of the Wilson loop. The argument for this correspondence comes from the AdS/CFT correspondence [5] and will be presented in more detail in section 2.3.

2.2 The Wilson Loop in the AdS/CFT Correspondence

It was proposed in [4] that in the AdS/CFT correspondence, the Wilson loop on the gauge theory side be identified with open strings in AdS, ending on the contour of the Wilson loop on the boundary. In the classical limit of string theory, the strings are described by minimal surfaces. Due to the curvature of the background space, these minimal surfaces do not lie on the boundary, but extend deeply into the bulk of AdS, as visualised in fig. 2.2. $\mathcal{N} = 4$ SYM being a supersymmetric gauge theory, we would want the Wilson loop to be a supersymmetric object. Suppressing the fermion fields, the appropriate Wilson

loop to consider has the form:

$$W = \frac{1}{N} \text{Tr } \mathcal{P} \exp \left(ig \int dt \left(\dot{x}^\mu(t) A_\mu(x(t)) + \dot{y}^I(t) \phi_I(x(t)) \right) \right), \quad (2.9)$$

where the ϕ_I are the six scalars in the adjoint representation of the gauge group, $x^\mu(t)$ are the actual contour coordinates in 4 dimensions as for the pure gauge theory Wilson loop and $y^I(t)$ can be understood as six extra coordinates, coming from the dimensional reduction of 10-dimensional $\mathcal{N} = 1$ SYM to 4-dimensional $\mathcal{N} = 4$ SYM. Usually, in a gauge theory containing a matter field in the fundamental representation, the coupling of the Wilson loop to the gauge field, can be found by consideration of the phase factor in the path integral over the trajectories of the corresponding particle. However, $\mathcal{N} = 4$ SYM does not contain such a field. It was therefore argued by Maldacena in [4], that one can introduce a massive W-boson by breaking of the gauge group $SU(N+1) \rightarrow SU(N) \times U(1)$ through the Higgs mechanism which determines the coupling of the Wilson loop to the gauge field and to the scalars:

$$W = \frac{1}{N} \text{Tr } \mathcal{P} \exp \left(ig \int dt \left(\dot{x}^\mu(t) A_\mu(x(t)) + \sqrt{\dot{x}^2(t)} \Theta^I \phi_I(x(t)) \right) \right) \quad (2.10)$$

where Θ^I is a constant unit vector: $(\Theta^I)^2 = 1$. It can depend on the contour parameter t , though, and can be interpreted as position on the S^5 , in the dual string theory. For further details of the derivation of the coupling see [29].

Another interpretation of the above coupling results from supersymmetry and will be discussed below, as well as special choices of the coupling $\Theta^I(t)$ to the scalars.

2.2.1 The Supersymmetric Wilson Loop and its Coupling to the Scalars

It was argued above, that the appropriate Wilson loop to be considered in the AdS/CFT correspondence should have the form (2.10), where the coupling to the scalars obeys the constraint $\dot{x}^2 = \dot{y}^2$. There is another interpretation of this constraint resulting from supersymmetry [29]. Above, we have only considered the coupling to the gauge field A_μ and the scalars ϕ_I . For the full supersymmetric Wilson loop, one would also have to allow coupling to the fermionic fields χ^α . Under bosonic supersymmetry variation

$$\begin{aligned} \delta_\zeta A_\mu &= \bar{\chi}^\alpha \Gamma_\mu \zeta_\alpha \\ \delta_\zeta \phi_I &= \bar{\chi}^\alpha \Gamma_I \zeta_\alpha \end{aligned} \quad (2.11)$$

with the fermionic loop variables $\zeta_\alpha(t)$ and the 10-dimensional Dirac matrices (Γ_μ, Γ_I) , the Wilson loop picks a fermionic term:

$$\begin{aligned} \delta_\zeta W &= \frac{1}{N} \text{Tr } \mathcal{P} \int dt \bar{\chi}^\alpha(t) \left(\Gamma_\mu \dot{x}^\mu(t) + \Gamma_I \dot{y}^I(t) \right) \zeta_\alpha(t) \\ &\quad \exp \left(ig \int \left(\dot{x}^\mu(t') A_\mu(x(t')) + \sqrt{\dot{x}^2(t')} \Theta^I \phi_I(x(t')) \right) dt' \right). \end{aligned} \quad (2.12)$$

The variation will vanish and the supersymmetry will be preserved, if

$$\left(\Gamma_\mu \dot{x}^\mu(t) + \Gamma_I \dot{y}^I(t) \right) \zeta_\alpha(t) = 0. \quad (2.13)$$

With the constraint $\dot{x}^2 = \dot{y}^2$ this becomes

$$\left(\Gamma_\mu \dot{x}^\mu(t) + \Gamma_I \Theta^I(t) |\dot{x}(t)| \right) \zeta_\alpha(t) = 0. \quad (2.14)$$

This combination of the gamma matrices squares to zero and consequently, (2.14) has 8 independent solutions for the fermionic loop coordinates $\zeta_\alpha(t)$ for a given t . A Wilson loop, coupling to the scalars as in (2.10), thus is locally supersymmetric.

However, local supersymmetry is not a symmetry of the action. Global supersymmetry would require that ζ be t -independent. The number of linearly independent solutions then determines the amount of supersymmetry preserved. For constant Θ^I , one finds $\ddot{x}^\mu = 0$. So there is no solution, except for a straight line. We have mentioned above, though, that generally $\Theta^I(t)$ can depend on t .

An interesting ansatz for the coupling was proposed by Zarembo in [15]. There, the t -dependence of the coupling is exclusively put into the constraint, that it follow the direction of the tangent vector \dot{x}^μ of the space-time contour:

$$\Theta^I(t) = M_\mu^I \frac{\dot{x}^\mu(t)}{|\dot{x}(t)|} \quad (2.15)$$

Due to the unit-vector condition of $\Theta^I(t)$ for equal t , the matrices M_μ^I have to satisfy

$$M_\mu^I M_\nu^I = \eta_{\mu\nu}. \quad (2.16)$$

Inserting this choice into (2.14), the t -dependence factors out and one obtains

$$(\Gamma_\mu - M_\mu^I \Gamma^I) \zeta = 0. \quad (2.17)$$

There is only one Weyl spinor that satisfies this equation (see [15]) and hence, one of the sixteen supercharges is preserved.

An operator that commutes with all supercharges is called BPS². A Wilson loop operator that couples to the scalars as in (2.15):

$$W = \frac{1}{N} \text{Tr } \mathcal{P} \exp \left(ig \int \left(A_\mu(x(t)) + M_\mu^I \phi_I(x(t)) \right) \dot{x}^\mu(t) dt \right) \quad (2.18)$$

thus is 1/16 BPS. The amount of supersymmetry can be augmented by choosing Wilson loops for certain contour types. A Wilson loop restricted to 3 dimensions conserves 1/8 of the total supersymmetry, if the contour is restricted to a 2-dimensional plane, the loop is 1/4 BPS and the one-dimensional Wilson line with constant Θ^I is 1/2 BPS [15].

In a similar way, in [17] and [18] it was shown, that for Wilson loops, whose contours lie on certain submanifolds, such as the S^3 , one can choose special couplings to the scalars, such that it preserves at least 1/8 of the total supersymmetry.

²BPS stands for Bogomolnyi-Prasad-Sommerfield.

2.3 Wilson Loops and Gluon Scattering Amplitudes Duality

Recently, a duality between planar maximally helicity violating (MHV) scattering amplitudes in $\mathcal{N} = 4$ SYM and light-like polygonal Wilson loops, whose sides correspond to the gluon momenta, was proposed. The argument for this duality presented by Alday and Maldacena [5, 6] comes from the AdS/CFT correspondence at strong coupling and will be reviewed in section 2.3.1. Later, the duality was also shown to hold at weak coupling [7, 8], as will be explained in more detail in chapter 3. An important feature of the duality is that the leading IR divergent part of the scattering amplitudes were long known to be governed by the cusp anomalous dimension, originally defined for the UV singularities of a Wilson loop with cusps [9, 10, 11], as will briefly be explained in section 2.3.2. Another motivation for the duality proposal was a conjecture for the all-loop order form of n-gluon MHV scattering amplitudes by Bern, Dixon and Smirnov (BDS) [30], which is going to be summarised in section 2.3.3. Furthermore, it was discussed in [7, 8, 13] that the duality between scattering amplitudes and Wilson loops may be a reflection of an underlying dual conformal symmetry of the two objects. This will be commented in section 2.3.4.

2.3.1 Motivation for the Duality at Strong Coupling

The duality between planar MHV gluon scattering amplitudes and light-like polygonal Wilson loops spanned by the momenta of the gluons, was proposed at strong coupling by Alday and Maldacena in [5] (see also [6, 31]). Their argument for this duality of two objects in $\mathcal{N} = 4$ SYM comes from the AdS/CFT correspondence.

On the string theory side of the correspondence, at leading order, planar amplitudes at strong coupling correspond to scattering amplitudes of open strings ending on the boundary of AdS at radial coordinate $z = 0$. These are IR-divergent and hence, a D-brane at small $z = z_{\text{IR}}$ is introduced as an IR-cutoff. On the boundary of AdS, their momenta are fixed by the gluon momenta, but from the point of view of the deep interior of AdS, the ‘proper momenta’ [5] of the strings scale with a factor, depending on the metric and blow up as we take $z_{\text{IR}} \rightarrow 0$. It was shown in [32], that in flat space, for large string momenta, one can consider classical string theory. Now, in the limit of classical string theory, the string scattering amplitudes may be considered as worldsheets with the topology of a disc with vertex operator insertions corresponding to the external gluon states (see fig. 2.3). Each colour ordering of the amplitude corresponds to a fixed order of vertex operators on the disc.

The momenta of the gluons p^μ fix the boundary conditions at the corresponding vertex operator. *T-dual coordinates*, y^μ ($\mu = 0, \dots, 3$), on the boundary are introduced:

$$\partial_\alpha y^\mu = iw^2(z)\epsilon_{\alpha\beta}\partial_\beta x^\mu \tag{2.19}$$

where $\partial_\alpha \equiv \frac{\partial}{\partial\sigma^\alpha}$ with $(\alpha, \beta) = (0, 1)$, i.e. the role of the worldsheet coordinates $(\sigma^0, \sigma^1) \equiv (\sigma, \tau)$ is exchanged. $w(z)$ is a factor that determines the metric on

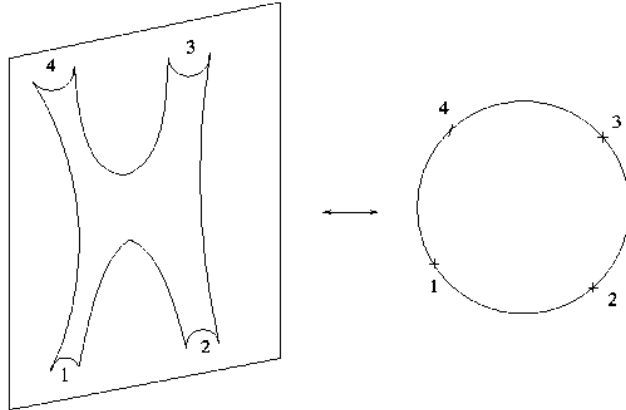


Figure 2.3: In the limit of classical string theory, the scattering of 4 open strings corresponds to a string worldsheet with the topology of a disc with vertex insertions corresponding to the external states.²

the brane at some ‘depth’ z of AdS:

$$ds^2 = w^2(z) dx^\mu dx_\mu. \quad (2.20)$$

In these coordinates, the boundary conditions on the brane translate into:

$$\Delta y^\mu = 2\pi p^\mu \quad (2.21)$$

i.e. the distances between the coordinates of the vertex operator insertions Δy^μ , interpreted as ‘winding’, are associated with the gluon momenta. This is what is meant by calling the coordinates *T-dual*.

On the boundary, at $z = z_{\text{IR}}$, we thus have segments of length $2\pi p^\mu$, which we can concatenate to a light-like polygon, according to the colour ordering of the scattering amplitude. The contour will be closed due to momentum conservation of the scattering process. A string worldsheet in AdS, ending on such a closed contour on the boundary, according to Maldacena’s string-Wilson loop duality presented in section 2.2, now corresponds to the Wilson loop along the said contour (see fig. 2.4).

Hence, through the AdS/CFT correspondence, at strong coupling, a duality between gluon scattering amplitudes and light-like polygonal Wilson loops spanned by the gluon momenta, both on the $\mathcal{N} = 4$ SYM theory side of the correspondence, has been established.

This duality has also been observed at weak coupling, as will be explained in more detail in chapter 3. If it is valid, it would yield a very helpful tool for the calculation of planar MHV scattering amplitudes in $\mathcal{N} = 4$ SYM.

2.3.2 The Cusp Anomalous Dimension of the Wilson Loop

From the cusps of a polygonal Wilson loop as in the duality presented above, UV-divergences arise. Hence, such a Wilson loop satisfies an evolution equation

²The picture was taken from [31].

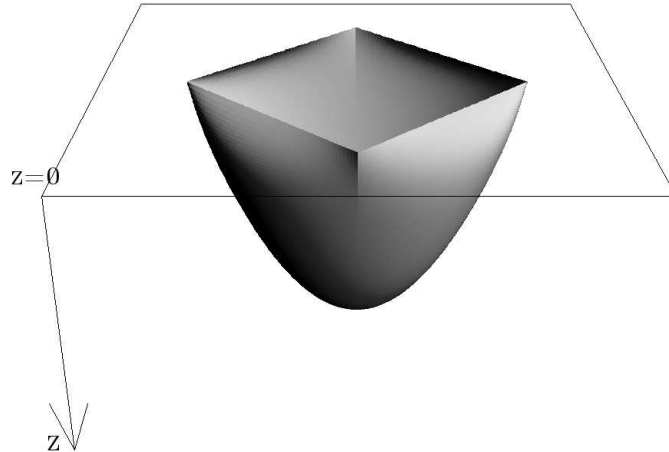


Figure 2.4: In ‘T-dual’ coordinates defined in (2.19), the string worldsheet for the scattering of open strings, dual to a gluon scattering amplitude of certain colour ordering, ends on a light-like polygon, whose sides are determined by the gluon momenta. Following the duality prescription of AdS/CFT for the Wilson loop, this exactly corresponds to the string dual of a Wilson loop along the polygon on the boundary.

with an anomalous dimension Γ_{cusp} , depending on the angle Θ_i formed by the respective cusp [9]:

$$\left(\mu \frac{\partial}{\partial \mu} + \beta(g) \frac{\partial}{\partial g} + \sum_i \Gamma_{\text{cusp}}(\Theta_i, g) \right) W = 0, \quad (2.22)$$

where μ is the renormalisation group parameter, $\beta(g)$ is the β -function and g the coupling constant. The cusp anomalous dimension was first calculated to one-loop order in [9]:

$$\Gamma_{\text{cusp}}(\Theta, g) = \frac{g^2 N}{8\pi^2} (\Theta \cot \Theta - 1). \quad (2.23)$$

It was shown in [10], that the IR asymptotics of scattering processes in perturbative QCD can be factorised into vacuum averages of path ordered exponentials of the form of the Wilson loop, whose contour specific UV divergences are in a one-to-one correspondence with the IR divergences of the original amplitude. This led to understanding that the leading IR divergent terms of the gluon scattering amplitudes are determined by the cusp anomalous dimension of a Wilson loop, whose integration contour is uniquely determined by the particle momenta.

Defining the angle Θ_{p_1, p_2} between two momenta in Minkowski space as

$$\cosh \Theta_{p_1, p_2} := \frac{p_1 p_2}{\sqrt{p_1^2 p_2^2}}, \quad (2.24)$$

in the case where the momenta become light-like, $p^2 \rightarrow 0$, the angle gets very

large: $\Theta \rightarrow \infty$. It was shown in [11], that in this limit, the cusp anomalous dimension scales linearly with the cusp angle to all orders in perturbation theory:

$$\Gamma_{\text{cusp}}(\Theta, g) =: \Theta \Gamma_{\text{cusp}}(g) + \mathcal{O}(\Theta^0). \quad (2.25)$$

In the following, the term ‘cusp anomalous dimension’ will be used in the sense of this definition, referring to $\Gamma_{\text{cusp}}(g)$.

Similar to QCD, the dependence of scattering amplitudes in $\mathcal{N} = 4$ SYM on the IR cutoff is determined by the cusp anomalous dimension. Due to the fact, that the β -function of $\mathcal{N} = 4$ SYM vanishes, the structure of their divergent part is much simpler, though.

This relationship between the singularities of both objects is an important feature in the correspondence between Wilson loops and gluon scattering amplitudes, presented above.

Another reason, why the cusp anomalous dimension has gained attention in the AdS/CFT correspondence in the past years is, that its value was predicted from conjectured integrable models, which describe the spectrum of anomalous dimensions in $\mathcal{N} = 4$ SYM [33]. Its computation could thus serve to test these models.

2.3.3 The BDS Conjecture for MHV Scattering Amplitudes

Some inspiration for the duality between scattering amplitudes and Wilson loops came from a conjecture for the form of the finite part of n-gluon MHV scattering amplitudes proposed in [34] and generalised to all-loop order by Bern, Dixon and Smirnov (BDS) in [30]. Scattering amplitudes are IR-divergent and can be split into a finite part F_n and an IR-divergent part D_n . For a colour ordered n-gluon MHV amplitude A_n , we then obtain:

$$\ln \frac{A_n}{A_n^{\text{tree}}} := \ln \mathcal{M}_n = D_n(a, p_i) + F_n(a, p_i) \quad (2.26)$$

where p_i are the gluon momenta and

$$a := \frac{g_{\text{YM}}^2 N}{8\pi^2} \quad (2.27)$$

is the coupling. The structure of the divergent part is well-understood in gauge theory and, as we have seen in the previous section, is related to the cusp anomalous dimension. The BDS conjecture is a conjecture about the form of the finite part of the amplitude:

$$F_n^{\text{BDS}}(a, p_i p_j) = \frac{1}{2} \Gamma_{\text{cusp}}(a) F_n^{(1)}(p_i p_j) \quad (2.28)$$

where $F_n^{(1)}$ is the one-loop contribution to the finite part and $p_i p_j$ are the generalised Mandelstam variables of the n-particle scattering process. This means that the only coupling dependence enters through the cusp anomalous

dimension, $\Gamma_{\text{cusp}}(a)$. Following the BDS ansatz, the functional dependence of the finite part on the momenta is independent of the coupling and could hence be determined through a one-loop calculation. As an example, the one-loop finite part of the 4-gluon scattering amplitude takes the form:

$$F_4^{(1)} = \frac{1}{2} \ln^2 \frac{s}{t} + \text{const.} \quad (2.29)$$

where s and t are the usual Mandelstam variables of the 4-particle scattering problem. For $n = 4$ gluons, the conjecture has been confirmed up to 3 loops, for $n = 5$ gluons, up to 2 loops. It seems very surprising that the loop corrections to the finite term should take such a simple form and the validity of the conjecture would thus be a hint for a hidden symmetry.

Indeed, in the past years, such a new ‘dual’ symmetry of the scattering amplitudes has been discussed and the arguments will be presented in brief in the next section.

2.3.4 Dual Conformal Symmetry of Wilson Loops and Scattering Amplitudes

At one and two loops, planar 4-gluon scattering amplitudes are expressed in terms of so-called *scalar box integrals* [34], which, expressed in *dual coordinates*

$$p_i = x_i - x_{i+1} \equiv x_{i,i+1}, \quad (2.30)$$

unveil a *dual* conformal symmetry [12]. In 4 dimensions, this symmetry is broken by the fact that the integrals are IR divergent and their regularisation requires introducing a scale. The conformal invariance of the integrals determining the 4-gluon scattering amplitude in dual coordinates, was shown to hold at least up to 4 loops [35].

Remarkably, the dual coordinates that unveil these conformal properties of the gluon scattering amplitudes correspond to the dual coordinates introduced by Alday and Maldacena in order to set up the duality between scattering amplitudes and Wilson loops, explained in section 2.3.1. There the x_i describe the position of the Wilson loop’s cusps. In order to get a better understanding of the amplitudes’ dual conformal symmetry, we will have a look at the dual Wilson loop, which naturally has a dual conformal symmetry, also broken by its UV divergence.

Since conformal transformations map a straight light-like segment into another straight light-like segment, an n -sided light-like polygonal Wilson loop contour is mapped onto another n -sided light-like polygon. Since, furthermore, A_μ has conformal weight one, it follows that such a Wilson loop is conformally invariant but for the change of the contour. From this, a conformal Ward identity can be derived. However, such a polygonal Wilson loop with cusps is UV divergent and thus a regularisation scale needs to be introduced, which breaks conformal invariance. As a consequence, the conformal Ward identity will receive an anomalous contribution [13]. If we split the Wilson loop into a UV

divergent part D_n^{WL} and a finite part F_n^{WL} , the conformal Ward identity takes the form:

$$\sum_{i=1}^n \left(2x_i^\mu (x_i \cdot \frac{\partial}{\partial x^i}) - x_i^2 \frac{\partial}{\partial x_{i\mu}} \right) F_n^{\text{WL}} = \frac{1}{2} \Gamma_{\text{cusp}}(a) \sum_{i=1}^n x_{i,i+1}^\mu \ln \frac{x_{i,i+2}^2}{x_{i-1,i+1}^2}. \quad (2.31)$$

The only coupling dependence of the anomalous term enters through the cusp anomalous dimension. For the case of $n = 4$ and 5 gluons this implies, that the finite part only depends on the coupling through $\Gamma_{\text{cusp}}(a)$ and is uniquely fixed to the form predicted by the BDS conjecture for the gluon scattering amplitudes. The anomalous conformal Ward identity further leads to a prediction of the finite term's form for arbitrary number of gluons. For $n > 6$ gluons, the form thus predicted, contains some freedom, which can be captured by a non-trivial function of conformal invariants, which can only be built for $n > 6$.

The computation of the 6-gluon scattering amplitude, numerically performed to 2 loops in [36], and its comparison to the BDS ansatz on the one hand, and to the hexagonal Wilson loop on the other hand, therefore yielded a non-trivial test of the two conjectures. The comparison shows, that for 6 gluons at 2 loops the BDS ansatz needs to be modified, whereas a computation of the hexagonal Wilson loop at 2 loops performed in [37, 38] shows, that the duality with the Wilson loops holds. The fact that the Wilson loop calculation yields the same non-trivial function of conformal invariants as the scattering amplitude, seems to indicate, that there is more to the duality than dual conformal symmetry and gives further evidence, that it should hold at all orders in the coupling.

If indeed the duality between Wilson loops and scattering amplitudes is valid in general, the dual conformal symmetry of the amplitudes would simply follow from the ordinary conformal symmetry of the light-like Wilson loop. This, however, would not explain the origin of the duality itself. A validity of the duality to all orders would suggest an even larger symmetry of the two objects. Very recently, the dual conformal symmetry was extended to a dual superconformal symmetry [39] and its relation to the AdS/CFT correspondence and the scattering amplitude/Wilson loop duality was discussed in [40].

A good summary of the discussion on the subject of dual conformal symmetry can be found in [41], for a detailed account see [42].

III

Regularisation of Scattering Amplitudes and Wilson Loops

In section 2.3, we have presented the recently proposed duality between gluon scattering amplitudes and Wilson Loops spanned by the gluon momenta in $\mathcal{N} = 4$ SYM and have explained its motivation at strong coupling through the AdS/CFT correspondence. In this chapter, we will now see that the duality also seems to be valid at weak coupling. The quantities to be compared are divergent. While gluon scattering amplitudes are known to be IR divergent, a Wilson loop with cusps is UV divergent, as we have seen in section 2.3.2. For a full comparison of the two objects, including the infinite parts, we therefore need to regularise both objects and define a matching of the regularisation parameters on both sides. The comparison has been done for dimensional regularisation in [7], which will be summarised briefly in section 3.1. Another regularisation for the gluon scattering amplitudes, for instance discussed in [7], is to take their external momenta being slightly off-shell: $p^2 = -m^2$. In section 3.2, we will thus propose a regularisation of the corresponding polygonal Wilson Loop, whose sides equal the off-shell gluon momenta, in order to match the off-shell gluon scattering amplitudes, as also presented in [43].

3.1 Duality at Weak Coupling in Dimensional Regularisation

The dimensionally regularised 4-gluon scattering amplitude, divided by the tree-level amplitude, has been calculated at one-loop order in [30]:

$$\mathcal{M}_4 = 1 + a\mathcal{M}^{(1)} + \mathcal{O}(a^2) \quad (3.1)$$

where the coupling is given by

$$a := \frac{g^2 N}{8\pi^2}. \quad (3.2)$$

As mentioned before, gluon scattering amplitudes in $\mathcal{N} = 4$ SYM are IR divergent and regularising dimensionally, one thus needs to increase the dimensions to $D = 4 - 2\epsilon_{\text{IR}}$, where ϵ_{IR} is negative. The change of dimensionality leads to a change of the dimension of the coupling constant $g^{(D)}$. One therefore customarily introduces a scale μ_{IR} in order to recover a dimensionless coupling constant g :

$$g^{(D)} = (\mu_{\text{IR}})^{\epsilon_{\text{IR}}} g \quad (3.3)$$

Redefining

$$\mu^2 := 4\pi e^{-\gamma} \mu_{\text{IR}}^2 \quad (3.4)$$

with the Euler constant γ , the colour ordered one-loop gluon scattering amplitude takes the form:

$$\mathcal{M}_{onshell}^{(1)} = -\frac{1}{\epsilon_{\text{IR}}^2} \left(\left(\frac{\mu^2}{-s} \right)^{\epsilon_{\text{IR}}} + \left(\frac{\mu^2}{-t} \right)^{\epsilon_{\text{IR}}} \right) + \frac{1}{2} \ln^2 \frac{s}{t} + \frac{2\pi^2}{3} \quad (3.5)$$

$$\begin{aligned} &= -\frac{2}{\epsilon_{\text{IR}}^2} - \frac{1}{\epsilon_{\text{IR}}} \left(\ln \frac{\mu^2}{-s} + \ln \frac{\mu^2}{-t} \right) - \frac{1}{2} \left(\ln^2 \frac{\mu^2}{-s} + \ln^2 \frac{\mu^2}{-t} \right) + \\ &\quad + \frac{1}{2} \ln^2 \frac{s}{t} + \frac{2\pi^2}{3} \quad (3.6) \end{aligned}$$

where s and t are the usual Mandelstam variables of the 4-particle scattering problem.¹

The dependence of the scattering amplitude on the IR regularisation scale μ is governed by an evolution equation related to the cusp anomalous dimension of the Wilson loop, as explained in section 2.3.2 [44]:

$$\left(\frac{\partial}{\partial \ln \mu^2} \right)^2 \ln \mathcal{M}_4 = -\Gamma_{\text{cusp}}(a) + \mathcal{O}(\epsilon_{\text{IR}}) \quad (3.7)$$

Substituting the upper one-loop result (3.5) into this equation, we obtain

$$\Gamma_{\text{cusp}}(a) = 2a + \mathcal{O}(a^2) \quad (3.8)$$

for the cusp anomalous dimension, defined in the sense of (2.25).

The Wilson loop dual to the 4-gluon scattering amplitude is a tetragon spanned by the external gluon momenta. Such a light-like Wilson loop with cusps is UV-divergent in 4 dimensions. The origin of these divergences can be visualised by expanding the Wilson loop to one-loop order:

$$\langle W \rangle = \frac{1}{N} \left\langle \text{Tr} \mathcal{P} \exp \left(ig \int A_\mu \dot{x}^\mu dt \right) \right\rangle \quad (3.9)$$

$$\begin{aligned} &= 1 + \frac{(ig)^2}{2N} \text{Tr} T^a T^b \int dt_1 dt_2 \dot{x}^\mu(t_1) \dot{x}^\nu(t_2) \left\langle A_\mu^a(x(t_1)) A_\nu^b(x(t_2)) \right\rangle + \mathcal{O}(g^4) \\ &= 1 - \frac{a}{2} \int dt_1 dt_2 \frac{\dot{x}(t_1) \dot{x}(t_2)}{(x(t_1) - x(t_2))^2} + \mathcal{O}(a^2), \quad (3.10) \end{aligned}$$

where a is the coupling as in (3.2), T^a are the generators of $SU(N)$ in the fundamental representation for large N (see appendix A.1) and the propagator in Feynman gauge has been inserted (see appendix A.2). If the distance between the propagator endpoints becomes light-like or if the endpoints come together, $(x(t_1) - x(t_2))^2 = 0$ and the integrand in (3.10) becomes singular. Hence, from this situation, UV-divergences can arise.

For a full comparison with the gluon scattering amplitude, including the infinite parts, the Wilson loop thus also needs to be regularised and the regularisation parameters of both sides of the duality have to be identified. This has

¹It is convenient to choose s and t negative, which corresponds to the kinematical u -channel, to avoid an imaginary part of the considered colour ordered part of the scattering amplitude.

been done at one loop for dimensional regularisation in [7]. With the propagator in $D = 4 - 2\epsilon_{\text{UV}}$ dimensions (see appendix A.3), where this time ϵ_{UV} needs to be positive, since the Wilson loop is UV-divergent, and with

$$\mu^2 := \frac{1}{\pi e^\gamma \mu_{\text{UV}}^2} \quad (3.11)$$

where μ_{UV} is the regularisation scale, in analogy to the IR-case in (3.3), the Wilson loop to one-loop order becomes:

$$\langle W \rangle = 1 + a W^{(1)} + \mathcal{O}(a^2) \quad (3.12)$$

with

$$W^{(1)} = -\frac{1}{\epsilon_{\text{UV}}^2} \left(\left(\frac{\mu^2}{-s} \right)^{-\epsilon_{\text{UV}}} + \left(\frac{\mu^2}{-t} \right)^{-\epsilon_{\text{UV}}} \right) + \frac{1}{2} \ln^2 \frac{s}{t} + \frac{\pi^2}{3} \quad (3.13)$$

Comparing this result to the dimensionally regularised one-loop gluon scattering amplitude (3.5), we see that the divergent parts of the two expressions coincide if we formally identify

$$\epsilon_{\text{UV}} = -\epsilon_{\text{IR}} \quad (3.14)$$

where the minus sign is due to the fact that ϵ_{IR} is negative, while ϵ_{UV} is positive as explained above, and if we identify the regularisation scales μ as defined in (3.4) for the scattering amplitude and in (3.11) for the Wilson loop. The finite parts of the two expressions match up to a constant additive term independent of the kinematics.

This result was a first indication that the duality of section 2.3 proposed by [5] at strong coupling, is also valid at weak coupling. Further checks of this statement were performed by explicitly calculating the two objects in dimensional regularisation for 4 and 5 gluons up to 2-loops [8, 13] and for n gluons to one-loop [45]. For $n = 4$ and 5 gluons the functional form of the finite part indeed reduces to the BDS prediction, which is a consequence of the dual conformal symmetry, as discussed in section 2.3.4. As we have mentioned therein, for the case of $n = 6$ gluons, however, the BDS ansatz needs to be modified, whereas a computation of the hexagonal Wilson loop at 2-loops [37, 38] shows that the Wilson loop scattering amplitude duality holds. This gives evidence, that the duality might be valid at all orders in perturbation theory.

In the references mentioned above, the comparison of the divergent parts has always been performed in dimensional regularisation as described above. It thus seems interesting to examine, whether the duality is regularisation scheme dependent or not and to check whether it holds for an alternative regularisation of the two objects.

3.2 Amplitudes and Wilson Loops in Off-Shell Regularisation

An alternative regularisation of the gluon scattering amplitudes can be achieved by keeping the integrals in 4 dimensions, but instead introducing a small virtuality to the external legs as an IR cutoff:

$$p_i^2 = -m^2$$

where we have taken all the momenta off-shell in the same way and have chosen them to be negative ($m^2 > 0$) as in [7] for simplicity.² The resulting off-shell gluon scattering amplitudes in $\mathcal{N} = 4$ SYM have been calculated in [46]:

$$\mathcal{M}_{\text{off-shell}}^{(1)} = - \left(\ln^2 \left(\frac{m^2}{-s} \right) + \ln^2 \left(\frac{m^2}{-t} \right) \right) + \frac{1}{2} \ln^2 \left(\frac{s}{t} \right) - \frac{\pi^2}{6} \quad (3.15)$$

where the first two terms diverge as we take $m^2 \rightarrow 0$ and the last two terms constitute the finite part. Comparing this to (3.5), we see that the double pole singularity of the dimensionally regularised amplitude has been replaced by a double logarithmic singularity in the cutoff m . If for comparison, in (3.6), we in a natural way identify the IR regularisation parameter μ of dimensional regularisation with the IR-cutoff m and suppress terms that diverge for $\epsilon \rightarrow 0$, we see that there is a difference of a factor of 2 in front of the squared logarithmic terms in m^2 in the off-shell case compared to the on-shell case. The finite part being independent of the regularisation parameters, remains the same, except for an additive scheme-dependent constant, independent of the kinematics.

The additional factor of 2 in front of the leading divergent \log^2 -term also appears in the evolution equation for the scattering amplitude, which, as we have mentioned before, is related to the cusp anomalous dimension of the Wilson loop. In the off-shell case, the evolution equation takes the form [44]:

$$\left(\frac{\partial}{\partial \ln m^2} \right)^2 \ln \mathcal{M}_4^{\text{off-shell}} = -2 \Gamma_{\text{cusp}}(a) + \mathcal{O}(m) \quad (3.16)$$

where we have an additional factor of 2 in front of the cusp anomalous dimension compared to (3.7). In order to get the same cusp anomalous dimension $\Gamma_{\text{cusp}} = 2a + \mathcal{O}(a^2)$, we therefore indeed need the additional factor of 2 in front of the \log^2 -term. The question therefore arises, whether we can define a regularisation for the Wilson loop corresponding to the off-shell gluon scattering amplitude that makes it finite and reproduces the said factor of 2. We have investigated this question in [43] and the details will be presented in the following.

For this, let us have a look at the Wilson Loop dual to the off-shell gluon scattering amplitude. Following the duality prescription of section 2.3.1, it is the Wilson loop along a polygon whose sides are determined by the off-shell gluon momenta $p_i^2 = -m^2$.

As long as the sides of the polygon were light-like, the scalar part of the Wilson loop, being proportional to $|\dot{x}|$, vanished. It therefore made no difference whether we took the Wilson loop for the gauge field A_μ only, as in (2.4), or the locally supersymmetric Wilson loop of (2.10). However, as soon as the sides are no longer light-like, the scalar part contributes and the question arises, which one has to be taken. Out of the formal construction of the duality according to

²The choice of negative p^2 leads to the finiteness of the integrals to be solved for the computation of the Wilson Loop in the kinematical u -channel, i.e. for negative s and t .

AdS/CFT in [5], which we described in section 2.3.1, the locally supersymmetric version seems to be the natural partner, being the Wilson loop identified with the string-worldsheets in [4], as explained in section 2.2. Further support arises from the treatment of divergences: Choosing the locally supersymmetric loop with constant coupling Θ^I to the scalars, the linear divergences, arising from the limit of coincident propagator endpoints on one and the same side of the polygon, cancel each other.

This can easily be seen by computing the Wilson loop to one loop order:

$$\langle W \rangle = \frac{1}{N} \left\langle \text{Tr } \mathcal{P} \exp \left(ig \int_C \left(A_\mu \dot{x}^\mu + \sqrt{\dot{x}^2} \theta^I \Phi_I \right) dt \right) \right\rangle \quad (3.17)$$

$$\begin{aligned} &= 1 + \frac{(ig)^2}{2N} \text{Tr } T^a T^b \int dt_1 dt_2 \left(\dot{x}^\mu(t_1) \dot{x}^\nu(t_2) \langle A_\mu^a(x(t_1)) A_\nu^b(x(t_2)) \rangle + \right. \\ &\quad \left. + \sqrt{\dot{x}^2(t_1)} \sqrt{\dot{x}^2(t_2)} \Theta^I \Theta^J \langle \phi_I^a(x(t_1)) \phi_J^b(x(t_2)) \rangle \right) + \mathcal{O}(g^4) \end{aligned} \quad (3.18)$$

$$= 1 - \frac{a}{2} \int dt_1 dt_2 \frac{\dot{x}(t_1) \dot{x}(t_2) - \sqrt{\dot{x}^2(t_1)} \sqrt{\dot{x}^2(t_2)}}{(x(t_1) - x(t_2))^2} + \mathcal{O}(a^2) \quad (3.19)$$

where a is the coupling as in (3.2) and the T^a are the generators of $SU(N)$ in the fundamental representation, where we have assumed N to be large to obtain

$$\text{Tr}(T^a T^a) = \frac{N^2}{2} \quad (3.20)$$

(see appendix A.1). Furthermore, in (3.19), we have inserted the gauge field and the scalar propagators in Feynman gauge

$$\langle A_\mu^a(x(t_1)) A_\nu^b(x(t_2)) \rangle = \frac{1}{4\pi^2} \frac{\delta^{ab} \eta_{\mu\nu}}{(x(t_1) - x(t_2))^2} \quad (3.21)$$

and

$$\langle \phi_I^a(x(t_1)) \phi_J^b(x(t_2)) \rangle = -\frac{1}{4\pi^2} \frac{\delta^{ab} \delta_{IJ}}{(x(t_1) - x(t_2))^2}. \quad (3.22)$$

One can directly see from (3.19), that there is a singularity for $x(t_1) = x(t_2)$, i.e. when both propagator endpoints come together.³

To one-loop order, we have to take into account the following contributions: The gauge field and the scalar contributions for the case, where both propagator endpoints lie on the same side of the polygon, have to be considered 4 times, once for every side of the tetragon (fig. 3.1). Since for this case $\dot{x}(t_1) = \dot{x}(t_2) \equiv \dot{x}_0$,

³For the case where both propagator ends lie on the same side of the tetragon the distance now does not become light-like anymore and possible divergences from light-like distances between other points can be shown to cancel.

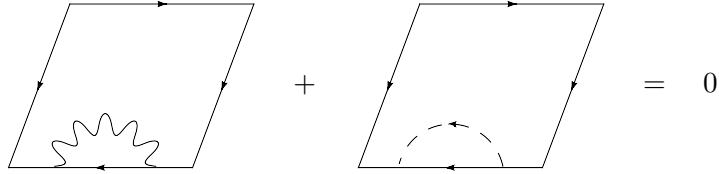


Figure 3.1: The vector and the scalar contribution with both propagator endpoints on the same edge of the tetragon cancel each other.

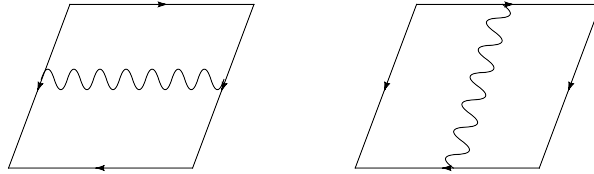


Figure 3.2: The one-loop vector contributions, where the propagator connects opposite sides of the tetragon, are finite. The corresponding scalar contributions are of order m^2 and can thus be neglected for small off-shellness m .

the vector and the scalar part indeed cancel and the integral in (3.19) vanishes:

$$W_{\text{one side}}^{(1)} = -\frac{1}{2} \int dt_1 dt_2 \frac{\dot{x}_0^2 - |\dot{x}_0|^2}{(x(t_1) - x(t_2))^2} = 0 \quad (3.23)$$

Then, there are the contributions from propagator ends on opposite sides of the tetragon, shown in fig. 3.2. Here, the scalar contributions, being proportional to \dot{x}^2 , are of order m^2 and can be neglected for small off-shellness. In this case, the propagator endpoints do not come together and the integrals thus remain finite.⁴ These contributions have for instance been calculated to one-loop order in [7]. Their sum is:

$$W_{\text{opposite}}^{(1)} = \frac{1}{2} \ln^2 \frac{s}{t} + \frac{\pi^2}{2} \quad (3.24)$$

Finally, the contributions coming from propagator endpoints on adjacent sides remain (see fig. 3.3). There are two types of such cusp contributions, respectively characterised by the Mandelstam variable describing the kinematics of the corner in question

$$\begin{aligned} s &= (p_1 + p_2)^2 = (p_3 + p_4)^2 & \text{and} \\ t &= (p_2 + p_3)^2 = (p_1 + p_4)^2. \end{aligned} \quad (3.25)$$

We have to consider twice each, once for every corner of the tetragon (fig. 3.3). Here again, the scalar contributions are of order m^2 and can be neglected for small off-shellness, as will be seen explicitly below. The remaining gauge

⁴The divergent contributions coming from potential crossing points or points with light-like distance in the case of polygons with $n > 4$ sides cancel.

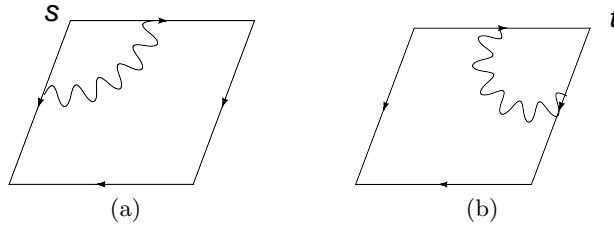


Figure 3.3: Cusp contributions to the one-loop tetragonal Wilson loop. Two corners of the tetragon are characterised by the Mandelstam variable s , fig. (a), and two corners by the Mandelstam variable t , fig. (b).

field cusp integral has a UV-divergence stemming from coincident propagator endpoints, which exactly happens at the cusp formed by the adjacent sides.

This *cusp divergence* exists, even though our sides are no longer light-like and the off-shell polygonal Wilson loop thus still is UV-divergent. We therefore need an additional regularisation in order to make the off-shell Wilson loop finite.

3.2.1 Dimensional Regularisation of the Cusp Divergences

Our first attempt is to regularise the cusp divergences by going to $D = 4 - 2\epsilon$ dimensions. In (3.18), we then have to insert the $(4 - 2\epsilon)$ -dimensional propagators. In Feynman gauge, the gauge field propagator takes the form:

$$\langle A_\mu^a(x(t_1))A_\nu^b(x(t_2)) \rangle = -\frac{\pi^\epsilon}{4\pi^2}\Gamma(1-\epsilon)\frac{\delta^{ab}\eta_{\mu\nu}}{(-(x(t_1)-x(t_2))^2)^{1-\epsilon}} \quad (3.26)$$

and the scalar propagator becomes

$$\langle \phi_I^a(x(t_1))\phi_J^b(x(t_2)) \rangle = \frac{\pi^\epsilon}{4\pi^2}\Gamma(1-\epsilon)\frac{\delta^{ab}\delta_{IJ}}{(-(x(t_1)-x(t_2))^2)^{1-\epsilon}}, \quad (3.27)$$

where $\Gamma(z)$ is the Euler gamma function. Introducing a dimensionless coupling g and a UV regularisation scale μ_{UV} in analogy to (3.3), the expectation value of the Wilson loop to one-loop order becomes:

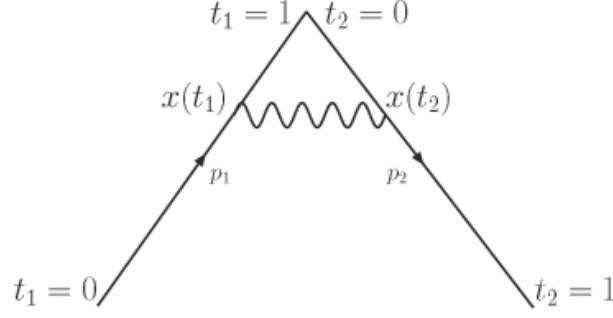
$$\langle W \rangle = 1 + (g\mu_{\text{UV}}^\epsilon)^2 N \frac{\pi^\epsilon}{16\pi^2}\Gamma(1-\epsilon) \int dt_1 dt_2 \frac{\dot{x}(t_1)\dot{x}(t_2) + m^2}{(-(x(t_1)-x(t_2))^2)^{1-\epsilon}} \quad (3.28)$$

The scalar part is of order m^2 and will be neglected in the following, assuming small off-shellness of the dual amplitude.

In order to compute the remaining gauge field cusp integrals, we choose the following parametrisation for the parameters t_1 along p_i and t_2 along p_j , as visualised in fig 3.4:

$$x(t_1) = -(1-t_1)p_i, \quad x(t_2) = t_2 p_j \quad \text{where} \quad t_1, t_2 \in [0, 1] \quad (3.29)$$

The one-loop contributions from the cusp diagrams then becomes


 Figure 3.4: Parametrisation, exemplarily for the cusp formed by p_1 and p_2 .

$$\begin{aligned}
 a W_{\text{cusp},(ij)}^{(1)} &= (g \mu_{\text{UV}}^\epsilon)^2 N \frac{\pi^\epsilon}{16\pi^2} \Gamma(1-\epsilon) \times \\
 &\times 2 \int_0^1 dt_1 \int_0^1 dt_2 \frac{p_i p_j}{(-((1-t_1)p_i + t_2 p_j)^2)^{1-\epsilon}} + \mathcal{O}(m^2)
 \end{aligned} \tag{3.30}$$

where the factor of 2 is due to the fact that we also have to take into account the situation where the parameters are exchanged, i.e. t_1 runs along p_j and t_2 along p_i . Inserting $p^2 = -m^2$ and substituting $(1-t_1) \rightarrow t_1$ we obtain

$$\begin{aligned}
 a W_{\text{cusp},(ij)}^{(1)} &= \frac{g^2 N}{8\pi^2} (\mu_{\text{UV}}^2 \pi m^2)^\epsilon \Gamma(1-\epsilon) \times \\
 &\times \underbrace{\frac{p_i p_j}{(m^2)} \int_0^1 dt_1 dt_2 \frac{1}{(t_1^2 + t_2^2 - 2\frac{p_i p_j}{m^2} t_1 t_2)^{1-\epsilon}}}_{=: I_{\text{cusp},(ij)}} + \mathcal{O}(m^2) \\
 &= a \left(1 + \epsilon \ln \frac{m^2}{\mu^2} \right) I_{\text{cusp},(ij)}
 \end{aligned} \tag{3.31}$$

where μ is defined in (3.11).⁵ Changing to polar coordinates:

$$t_1 = r \cos \phi \quad t_2 = r \sin \phi \tag{3.33}$$

and taking into account that the integrand is symmetric in t_1 and t_2 , the integral becomes

$$I_{\text{cusp},(ij)} = 2 B_{ij} \int_0^{\frac{\pi}{4}} d\phi \frac{1}{(1 - B_{ij} \sin(2\phi))^{1-\epsilon}} \int_0^{\frac{1}{\cos(\phi)}} dr r^{(2\epsilon-1)} \tag{3.34}$$

where we have defined

$$B_{ij} := \frac{p_i p_j}{m^2}. \tag{3.35}$$

⁵The expansion of the prefactor can be found in appendix A.3.

Solving the r -integral leads to a $\frac{1}{\epsilon}$ -pole:

$$I_{\text{cusp},(ij)} = B_{ij} \frac{1}{\epsilon} \int_0^{\frac{\pi}{4}} d\phi \frac{1}{(1 - B_{ij} \sin(2\phi))} \left(\frac{1 - B_{ij} \sin(2\phi)}{\cos^2(\phi)} \right)^\epsilon. \quad (3.36)$$

We can now expand in powers of ϵ ,⁶ and the one-loop contribution from the cusp formed by p_i and p_j becomes

$$\begin{aligned} W_{\text{cusp},(ij)}^{(1)} &= \left(1 + \epsilon \ln \frac{m^2}{\mu^2} \right) \frac{1}{\epsilon} \left(\frac{1}{4} \int_0^\pi d\phi \frac{1}{(1 - B_{ij} \sin \phi)} + \right. \\ &\quad \left. + \epsilon \frac{1}{4} \int_0^\pi d\phi \frac{\ln(1 - B_{ij} \sin \phi)}{(1 - B_{ij} \sin \phi)} - \epsilon \frac{1}{2} \int_0^{\frac{\pi}{2}} d\phi \frac{\ln(\cos^2 \frac{\phi}{2})}{(1 - B_{ij} \sin \phi)} \right) + \mathcal{O}(\epsilon) \\ &= \frac{B_{ij}}{4} \left(\frac{1}{\epsilon} I_{ij}^{(1)} + \ln \frac{m^2}{\mu^2} I_{ij}^{(1)} + I_{ij}^{(2)} \right) - \frac{1}{2} A_{ij} + \mathcal{O}(m^2) + \mathcal{O}(\epsilon) \end{aligned} \quad (3.37)$$

where we have defined the following integrals:

$$I_{ij}^{(1)} := \int_0^\pi d\phi \frac{1}{(1 - B_{ij} \sin \phi)} \quad (3.38)$$

$$= \frac{2}{\sqrt{B_{ij}^2 - 1}} \left(\ln(-B_{ij}) - \ln \left(\sqrt{1 - \frac{1}{B_{ij}^2}} + 1 \right) \right) \quad (3.39)$$

$$I_{ij}^{(2)} := \int_0^\pi d\phi \frac{\ln(1 - B_{ij} \sin \phi)}{1 - B_{ij} \sin \phi} \quad (3.40)$$

$$= -\frac{1}{B_{ij}} \left(\ln(-B_{ij}) + \ln(2) \right)^2 + \frac{1}{B_{ij}} \frac{\pi^2}{12} + \mathcal{O}\left(\frac{1}{B_{ij}^2}\right) \quad (3.41)$$

$$A_{ij} := B_{ij} \int_0^{\frac{\pi}{2}} d\phi \frac{\ln(\cos^2 \frac{\phi}{2})}{1 - B_{ij} \sin \phi} = \frac{\pi^2}{24} + \mathcal{O}\left(\frac{1}{B_{ij}}\right), \quad (3.42)$$

where, taking into account that $|B_{ij}|$ is large for $m^2 \rightarrow 0$, we have expanded (3.40) and (3.42) in orders of B_{ij}^{-1} (see appendix B.1). For later continuation to positive $p_i p_j$, we need to specify the issue of the phase in $\ln(-B_{ij})$ in (3.39) and (3.41). From the $i\epsilon$ -prescription of the propagator, we find that it has to be understood as $\ln(e^{i\pi} B_{ij})$.

For the cusps formed by p_1 and p_2 , resp. p_3 and p_4 , we have

$$B_{12} = B_{34} = \frac{s}{2m^2} + 1 \quad (3.43)$$

⁶thereby assuming though, that ϵ is small compared to m^2

and find the following one-loop contribution to the Wilson loop:

$$W_{\text{cusp},(s)}^{(1)} = \frac{1}{2} \left(\frac{1}{\epsilon} \ln \left(-\frac{m^2}{s} \right) + \ln \left(\frac{m^2}{\mu^2} \right) \ln \left(-\frac{m^2}{s} \right) - \frac{1}{2} \ln^2 \left(\frac{m^2}{-s} \right) \right) + \mathcal{O}(m^2 \ln m^2) + \mathcal{O}(\epsilon) \quad (3.44)$$

For the other two cusps, we have

$$B_{23} = B_{14} = \frac{t}{2m^2} + 1 \quad (3.45)$$

and receive the same contribution but substituting s by t :

$$W_{\text{cusp},(t)}^{(1)} = \frac{1}{2} \left(\frac{1}{\epsilon} \ln \left(-\frac{m^2}{t} \right) + \ln \left(\frac{m^2}{\mu^2} \right) \ln \left(-\frac{m^2}{t} \right) - \frac{1}{2} \ln^2 \left(\frac{m^2}{-t} \right) \right) + \mathcal{O}(m^2 \ln m^2) + \mathcal{O}(\epsilon) \quad (3.46)$$

To obtain the entire Wilson loop to one-loop order, we now have to add up all contributions (3.24), (3.44) and (3.46), remembering that the scalar and the vector contribution from diagram 3.1 cancel and obtain

$$\begin{aligned} \langle W \rangle &= 1 + a \left(2 W_{\text{cusp},(s)}^{(1)} + 2 W_{\text{cusp},(t)}^{(1)} + W_{\text{opposite}}^{(1)} \right) + \mathcal{O}(a^2) \quad (3.47) \\ &= 1 + a \left(\frac{1}{\epsilon} \left(\ln \left(-\frac{m^2}{t} \right) + \ln \left(-\frac{m^2}{s} \right) \right) + \ln^2 \left(\frac{m^2}{\mu^2} \right) - \right. \\ &\quad \left. - \frac{1}{2} \left(\ln^2 \left(\frac{\mu^2}{-s} \right) + \ln^2 \left(-\frac{\mu^2}{-t} \right) \right) + \frac{1}{2} \ln^2 \left(\frac{s}{t} \right) + \frac{\pi^2}{2} \right) \\ &\quad + \mathcal{O}(m^2 \ln m^2) + \mathcal{O}(\epsilon) + \mathcal{O}(a^2). \quad (3.48) \end{aligned}$$

Suppressing the pole term in ϵ yields the renormalised one-loop space-like Wilson Loop, which still depends on m^2 and μ^2 . Of course, μ^2 is no parameter of the off-shell gluon scattering amplitude. For our purpose, it thus seems natural to identify μ^2 with m^2 , which results in

$$W_{\text{ren}}^{(1)} = -\frac{1}{2} \left(\ln^2 \left(\frac{m^2}{-t} \right) + \ln^2 \left(\frac{m^2}{-s} \right) \right) + \frac{1}{2} \ln^2 \frac{s}{t} + \frac{\pi^2}{2} + \mathcal{O}(m^2 \ln m^2) \quad (3.49)$$

The fact that the renormalised expression diverges for $m^2 \rightarrow 0$ is a reflection of the divergence of the cusp anomalous dimension as soon as the sides approach the light-cone.

We can now compare our result to the expression for the off-shell amplitude (3.15).

The deviation of the finite part by an additive constant does not pose any problem and could even be removed by a purely numerical factor in the relation between μ^2 and m^2 .

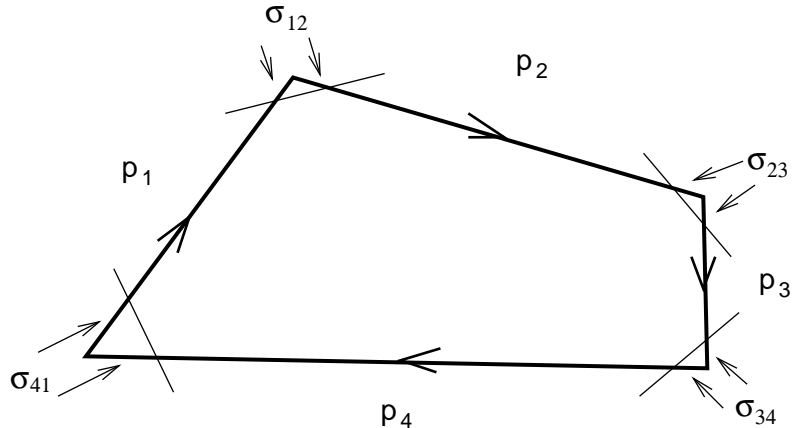


Figure 3.5: Cutoff at the cusps of the tetragonal Wilson loop.

Obviously though, the additional factor of 2 in front of the \log^2 -terms in the off-shell amplitude compared to the on-shell case, stressed in the opening of section 3.2 is not reproduced this way. This also remains true if one keeps μ^2 fixed and looks at the limit of $m^2 \rightarrow 0$. Then, the second term in (3.48) yields another $\ln^2(m^2)$ -term and in total, we still have a factor of $\frac{1}{2}$ in front of the \log^2 .

This discrepancy cannot be avoided either by, instead of considering the renormalised Wilson loop without ϵ -pole terms, mapping dimensional regularisation to a cutoff-regularisation with dimensionful parameter in the usual way: $\frac{1}{\epsilon} \sim -\log(\frac{m^2}{\mu^2})$.⁷

We are thus still in the need of an alternative regularisation of the non-light-like Wilson loop matching the dual off-shell gluon scattering amplitude.

3.2.2 Regularisation of the Cusp Divergences by Cutoff

After this first unsuccessful attempt, our second idea for the regularisation of the non-light-like Wilson loop dual to the off-shell amplitude is to introduce a cutoff σ on the contour parameter t at the cusps (fig. 3.5), since this is where the divergences come from.

Such a cutoff on the contour of the Wilson loop breaks its gauge invariance, since the integration path is no longer closed. This should be no obstacle though, since the dual off-shell scattering amplitudes are not gauge invariant either. We will thus compare the objects in Feynman gauge and add some comments on their gauge variance below.

As mentioned before, the contributions from the graphs, where the propagator endpoints are on opposite sides of the tetragonal Wilson loop (fig 3.2) are finite and thus do not need to be regularised. The sum of the vector and the

⁷which of course in our case is problematic anyway, since by expanding in ϵ , we have assumed $\epsilon \ln m^2$ to be small.

scalar graph with both propagator endpoints on the same side (fig. 3.1) vanishes. We therefore only need to regularise the cusp-contributions, as before.

With the parametrisation as in the last section, (3.29), the one-loop contribution to the Wilson loop (3.19) from the cusp formed by p_i and p_j , cut out with a cusp-dependent parameter σ_{ij} , becomes

$$I_{\text{cusp},\sigma_{ij}} := 2 \int_{\sigma_{ij}}^1 dt_2 \int_0^{1-\sigma_{ij}} dt_1 \frac{p_i p_j}{(t_2 p_j + (1-t_1) p_i)^2} \quad (3.50)$$

$$= 2 \int_{\sigma_{ij}}^1 dt_2 \int_{\sigma_{ij}}^1 dt_1 \frac{p_i p_j}{(t_1 p_i + t_2 p_j)^2} \quad (3.51)$$

Inserting our off-shell condition $p_i^2 = -m^2$ we obtain

$$I_{\text{cusp},\sigma_{ij}} = 2 \frac{p_i p_j}{-m^2} \int_{\sigma_{ij}}^1 dt_1 \int_{\sigma_{ij}}^1 dt_2 \frac{1}{(t_1^2 + t_2^2 - 2 \frac{p_i p_j}{m^2} t_1 t_2)}. \quad (3.52)$$

In polar coordinates as in (3.33) and with B_{ij} defined in (3.35) we get

$$I_{\text{cusp},\sigma_{ij}} = -4B_{ij} \int_0^{\frac{\pi}{4}} d\phi \frac{1}{(1 - B_{ij} \sin(2\phi))} \int_{\frac{\sigma_{ij}}{\cos \phi}}^{\frac{1}{\cos \phi}} \frac{dr}{r} \quad (3.53)$$

$$= B_{ij} \ln(\sigma_{ij}) \underbrace{\int_0^{\pi} d\phi \frac{1}{(1 - B_{ij} \sin \phi)}}_{=: I_{ij}^{(1)}}. \quad (3.54)$$

With $I_{ij}^{(1)}$ from (3.39) and expressing B_{ij} by the Mandelstam variables s , respectively t , as in (3.43) and (3.45) we obtain

$$I_{\text{cusp},\sigma_s} = 2 \ln(\sigma_s) \ln\left(\frac{m^2}{-s}\right) + \mathcal{O}(m^2 \ln(m^2)) \quad (3.55)$$

for the cusps characterised by s with cutoff $\sigma_{12} = \sigma_{34} \equiv \sigma_s$, and

$$I_{\text{cusp},\sigma_t} = 2 \ln(\sigma_t) \ln\left(\frac{m^2}{-t}\right) + \mathcal{O}(m^2 \ln(m^2)) \quad (3.56)$$

for the cusps characterised by t with cutoff $\sigma_{23} = \sigma_{14} \equiv \sigma_t$.

Adding up all contributions, taking the finite part from (3.24), the whole

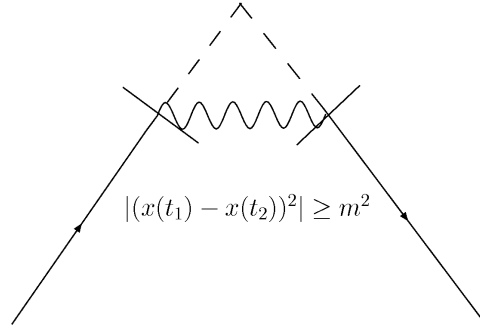


Figure 3.6: Relating the cutoff on the contour parameter to the IR regulator m^2 by claiming that the propagator be no shorter than m^2 .

Wilson Loop to one-loop order becomes

$$W = 1 - \frac{a}{2} \left(2 I_{\text{cusp}, \sigma_s} + 2 I_{\text{cusp}, \sigma_t} - 2 \cdot W_{\text{opposite}}^{(1)} \right) + \mathcal{O}(a^2) \quad (3.57)$$

$$= 1 - a \left(2 \left(\ln(\sigma_t) \ln\left(\frac{m^2}{-t}\right) + \ln(\sigma_s) \ln\left(\frac{m^2}{-s}\right) \right) - \frac{1}{2} \ln^2 \frac{s}{t} - \frac{\pi^2}{2} \right) + \mathcal{O}(m^2 \ln(m^2)) + \mathcal{O}(a^2) \quad (3.58)$$

Now, the cutoffs σ_s and σ_t remain to be specified. In order to compare our result to the gluon off-shell amplitude, we would like the cutoff to be related to the IR regulator m^2 . A first idea is to claim that the propagator length be no smaller than m^2 , as visualised in fig. 3.6:

$$|(x(t_1) - x(t_2))^2| \geq m^2 \quad (3.59)$$

For the above parametrisation (3.29), where here we have already taken $(1 - t_1) \rightarrow t_1$, this condition translates into

$$|(p_i t_1 + p_j t_2)^2| \geq m^2 \quad (3.60)$$

$$t_1^2 + t_2^2 - 2 \frac{p_i p_j}{m^2} t_1 t_2 \geq 1 \quad (3.61)$$

where we have made use of our off-shell condition $p^2 = -m^2$ and of the fact that, being space-like, the squared distance of the propagator is negative.

The inequality (3.61) describes the region cut out of the (t_1, t_2) -plane as visualised in fig. 3.7. Since divergences only arise when both propagator endpoints approach the cusp, i.e. when t_1 and t_2 are both small, condition (3.61) cuts out too much. Instead of cutting out the whole region delimited by the hyperbola that saturates (3.61), we therefore only cut out the squared region defined by the nearest point of the hyperbola to the origin at

$$t_1 = t_2 = \frac{1}{\sqrt{2 - 2 \frac{p_i p_j}{m^2}}} \quad (3.62)$$

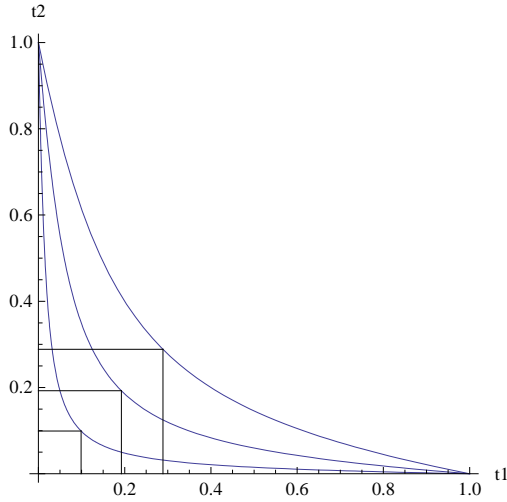


Figure 3.7: The curves visualise the region cut out of the (t_1, t_2) -plane by condition (3.61) for different values of s/m^2 , $t/m^2 = \{-10, -25, -100\}$. This condition cuts out too much; we therefore instead only cut out the squared region, which leads to (3.63).

as shown in fig. 3.7.

For the cusps formed by the respective pairs of momenta, we then get

$$\begin{aligned}\sigma_{12} = \sigma_{34} &= \sqrt{\frac{m^2}{-s}} \equiv \sigma_s \\ \sigma_{23} = \sigma_{14} &= \sqrt{\frac{m^2}{-t}} \equiv \sigma_t\end{aligned}\tag{3.63}$$

for our cutoff on the contour parameter.

This result seems to be a very plausible choice for the cutoff, motivated additionally by the following natural arguments: We wanted our parameter-cutoff to be related to the given IR regulator m^2 . A cutoff on the contour parameter needs to be dimensionless though. We are thus in the need of another dimensionful quantity in order to form a quotient with m^2 . For the cusp formed by the momenta p_i and p_j , the respective Mandelstam variable characterising the kinematics of the two momenta seems to be a natural choice to build the dimensionless quotients $\frac{m^2}{s}$, $\frac{m^2}{t}$. The cutoff being a cutoff on a momentum contour, it seems more natural though, to relate the cutoff with $\sqrt{m^2}$ instead of m^2 . Finally, taking into account that in the kinematical u-channel, the Mandelstam variables s and t are negative, we need to take $-s$ and $-t$ to build the quotient in order to avoid an imaginary cutoff.⁸ We thus arrive at our cutoff σ_s and σ_t found in (3.63).

Inserting our cutoff into equation (3.58), we obtain for the one-loop cut

⁸We later continue the cutoff to the other kinematical channels analytically.

Wilson loop:

$$\begin{aligned}
 W = 1 + a \left(- \left(\ln^2\left(\frac{m^2}{-t}\right) + \ln^2\left(\frac{m^2}{-s}\right) \right) + \frac{1}{2} \ln^2\left(\frac{s}{t}\right) + \frac{\pi^2}{2} \right) + \quad (3.64) \\
 + \mathcal{O}(m^2 \ln m^2) + \mathcal{O}(a^2).
 \end{aligned}$$

Up to a constant independent of the kinematics, this agrees with the result for the off-shell scattering amplitude (3.15). Note in particular, that we were able to reproduce the additional factor of 2 in front of the squared logarithmic terms related to the cusp anomalous dimension.

If one had alternatively used our first unmodified cutoff (3.61), we would again have had an unwanted factor of $\frac{1}{2}$ in front of the \log^2 -terms, reflecting the fact that we would have cut out a bigger region than necessary. It would be interesting to analyse, whether this is related to the exclusion of certain soft regions contributing to the off-shell amplitude as described in [7].

The result (3.64) can be continued to positive s and t . From the $i\epsilon$ -prescription in the integral $I_{(ij)}^{(1)}$ defined in (3.38), we found that in this case, the phase in $\ln(\frac{m^2}{-s})$ then has to be understood as $\ln(\frac{m^2}{s} e^{-i\pi})$ and in the same way for positive t .

Comments on Gauge Dependence

As mentioned before, the cut Wilson loop as well as the off-shell gluon scattering amplitudes are not gauge invariant and the above matching of the two objects concerns Feynman gauge. However, due to the relation of the factor in front of the leading divergent \log^2 -term to the cusp anomalous dimension, one should expect this term to be gauge invariant. We therefore check this explicitly by calculating the cut Wilson loop with the generally gauge dependent propagator

$$\left\langle A_\mu^a(x) A_\nu^b(y) \right\rangle_\alpha = \frac{\delta^{ab} \eta_{\mu\nu}}{4\pi^2((x-y)^2 - i\epsilon)} + \delta^{ab} \frac{\alpha - 1}{16\pi^2} \partial_\mu \partial_\nu \log(\Lambda^2(x-y)^2 - i\epsilon) \quad (3.65)$$

with gauge parameter α ($\alpha = 1$ in Feynman gauge) and an auxiliary scale parameter Λ^2 , which drops out after performing the differentiation. The scalar propagator remains independent of the gauge parameter. Thus calculating the gauge dependent one-loop contribution $W_\alpha^{(1)}$ to the cut Wilson loop, we can check whether the \log^2 -terms are independent of the gauge parameter α .

$$W = 1 + \underbrace{a W_{\alpha=1}^{(1)}}_{\text{as before}} + a (\alpha - 1) W_\alpha^{(1)} \quad (3.66)$$

with

$$W_\alpha^{(1)} = \frac{1}{16\pi^2} \int_{t_1 > t_2} dt_1 dt_2 \frac{d}{dt_1} \frac{d}{dt_2} \log(\Lambda^2(x(t_1) - x(t_2))^2 - i\epsilon) \quad (3.67)$$

For a Wilson loop with generic closed contour, the $i\epsilon$ -prescription of the propagator prevents the expression from diverging and in this case being the integral over a total derivative with the same starting- and endpoint of the integration, the term vanishes identically before ϵ is sent to zero.

This situation changes however, as soon as the integration path is no longer closed, as for our cut Wilson loop of fig. 3.5. We then again have to consider the different contributions from the diagrams 3.1 to 3.3, but this time of course, there are no scalar contributions. Therefore, now also the diagram of fig. 3.1, where both propagators lie on the same side, contributes. This diagram now has a divergence, when t_1 and t_2 coincide, as soon as we send ϵ to zero following the integration prescription. We therefore need to introduce an additional cutoff preventing such a coincidence of t_1 and t_2 on the same side of the tetragon. Equivalently to claiming that $x(t_1)$ and $x(t_2)$ should come no closer than some cutoff-parameter σ , we can simply add σ in the argument of the logarithm:

$$\log(\Lambda^2(x(t_1) - x(t_2))^2 - i\epsilon) \longrightarrow \log(\Lambda^2((x(t_1) - x(t_2))^2 - \sigma) - i\epsilon). \quad (3.68)$$

$|x(t_1) - x(t_2)|$ being expressed in dual coordinates (2.21), has the dimension of a momentum, i.e. positive mass dimension. In order to relate the cutoff σ to our former momentum cutoff, it therefore seems natural to choose $\sigma = m^2$. After taking $\epsilon \rightarrow 0$, we are thus left with an additional term: $\ln(\Lambda^2 m^2)$.

But in any case, due to the total derivative structure of (3.67), all other contributions will also have the form of single logarithms of functions of the cutoff σ_s and σ_t , which according to (3.63) are also proportional to m^2 . Thus, there will only be single logarithmic terms of m^2 and no α -dependent \log^2 -terms will come in. The leading divergent squared logarithmic term in our one-loop result (3.64) will thus remain gauge independent, as requested due to its relation to the gauge invariant cusp anomalous dimension.

IV

Special Properties of Wilson Loops in Minkowski Space

We have seen in the previous chapter that divergences arise from a Wilson loop with cusps, i.e. with discontinuities in the first derivative of the curve with respect to the curve-parameter. This is also true in the Euclidean case. A smooth Euclidean supersymmetric Wilson loop though, is finite. In the Minkowski case, the tangent to a curve can become light-like, i.e. $\dot{x}^2 = 0$, and we potentially have further divergences stemming from such points. As long as the curve is smooth in these points, however, the Wilson loop remains finite, as will be examined for the example of a circle in Minkowskian space in section 4.1 and as will be shown in a more general manner in section 4.2. If the second derivative of a curve in such a light-like point is discontinuous, however, divergences will arise depending on the saltus in \ddot{x} , as will be examined in section 4.2. In analogy to the cusp anomalous dimension as described in section 2.3.2, one can thus define an anomalous dimension for such a ‘higher order cusp’ in the second derivative.

In the same way, curves with straight finite light-like segments have divergences stemming from the transition between the light-like segments and the time- or space-like continuation of the curve. The question arises whether one can make these Wilson loops finite by choosing a special coupling to the scalars, in a similar but more general manner than Zarembo’s ansatz explained in section 2.2.1. This is going to be examined in section 4.3.

The Wilson loops for various simple geometrical objects, such as the circle and the rectangle, have been calculated in Euclidean space. Having seen how different the local properties of Wilson loops in Minkowskian background can be due to their embedding in space-time, it seems interesting to calculate the Wilson loop for such objects in Minkowski space and to compare the two results. With view to the Minkowskian circle, whose divergences due to points with light-like tangent are examined in section 4.1, we will, as a preliminary study, perform the calculation for the case of the rectangular Wilson loop in Minkowski space. We will explicitly show that in this case, the Minkowskian result simply arises from the Euclidean one by Wick rotation.

4.1 Minkowskian Circle with Light-Like Tangents

As mentioned above, Wilson loops in Minkowski space might have special properties depending on their embedding in space-time. Additional divergences might arise from some point x_0 with light-like tangent, i.e. $\dot{x}_0^2 = 0$, as can easily be seen by expanding around the concerned point. To one-loop order, the locally supersymmetric Wilson loop with constant coupling to the scalars

as in (2.10) takes the form:

$$\langle W \rangle = 1 - \frac{a}{2} I^{(1)} + \mathcal{O}(a^2) \quad (4.1)$$

$$\text{with} \quad I^{(1)} := \int dt_1 \int dt_2 \frac{\dot{x}(t_1)\dot{x}(t_2) - \sqrt{\dot{x}^2(t_1)}\sqrt{\dot{x}^2(t_2)}}{(x(t_1) - x(t_2))^2 - i\epsilon}, \quad (4.2)$$

where t_1 and t_2 run along the whole contour of the loop. In (4.2), we see that in Minkowski space, the coupling to the scalars picks a sign indeterminacy for space-like curves, i.e. $\dot{x}^2 < 0$, due to $\sqrt{-1} = \pm i$. We will specify this sign indeterminacy in the following by demanding that the Wilson loop along a smooth curve be finite.

For the one-loop contributions, stemming from the vicinity of the point with light-like tangent, say at $x(t=0) \equiv x_0$, we need to consider the case of having both propagator endpoints on the same side of x_0 , (+), and the case where the propagator connects the different sides of x_0 , (-). Throughout the chapter, we will maintain the convention, that on the side of negative contour parameters, we perform a shift $t \rightarrow -t$, i.e. the parameter is always positive. Expanding around x_0 , these two contributions become:

$$I_{\pm}^{(1)} = \int_0^{\dots} dt_1 \int_0^{\dots} dt_2 \frac{\dot{x}(t_1)\dot{x}(\pm t_2) - \sqrt{\dot{x}^2(t_1)}\sqrt{\dot{x}^2(\pm t_2)}}{(x(t_1) - x(\pm t_2))^2} \quad (4.3)$$

$$= \int_0^{\dots} dt_1 dt_2 \frac{\dot{x}_0^2 + (t_1 \pm t_2)\dot{x}_0\ddot{x}_0 - \sqrt{\dot{x}_0^2 + 2t_1\dot{x}_0\ddot{x}_0}\sqrt{\dot{x}_0^2 \pm 2t_2\dot{x}_0\ddot{x}_0}}{(t_1 \mp t_2)^2\dot{x}_0^2 + (t_1 \mp t_2)(t_1^2 - t_2^2)\dot{x}_0\ddot{x}_0} \quad (4.4)$$

$$= \int_0^{\dots} dt_1 dt_2 \frac{(t_1 \pm t_2)\dot{x}_0\ddot{x}_0 - 2|\dot{x}_0\ddot{x}_0|\sqrt{t_1}\sqrt{\pm t_2}}{(t_1 \mp t_2)(t_1^2 - t_2^2)\dot{x}_0\ddot{x}_0} \quad (4.5)$$

where we have dropped finite terms and have left the upper integration limit unspecified, since here, we are only interested in potential divergences at the point with light-like tangent at $t_1 = t_2 = 0$. In the Euclidean case, for potential divergences from this point, one only has to consider respectively the first term in the numerator and in the denominator of (4.4), since the next terms give finite contributions. For the supersymmetric Wilson loop, the vector and the scalar part then exactly cancel. Now, however, $\dot{x}_0^2 = 0$ and the contributions I_+ and I_- individually become divergent for $t_1 = t_2 = 0$. This disagrees with our expectations for a smooth curve, which we would expect to be finite, also in Minkowski space. Considering the example of the circle, we will show that the sign indeterminacy in the coupling to the scalars mentioned above, can be fixed such that the divergent contributions cancel each other and we recover a finite Wilson loop.

We will therefore have a closer look at these potential divergences for the case of a circle in the (x_0, x_1) -plane as represented in fig. 4.1. This circle has four points with light-like tangents. If we parametrise it by the angle Θ

$$x(\Theta) = R \begin{pmatrix} \cos \Theta \\ \sin \Theta \end{pmatrix} \quad \Rightarrow \quad \dot{x}(\Theta) = R \begin{pmatrix} -\sin \Theta \\ \cos \Theta \end{pmatrix} \quad (4.6)$$

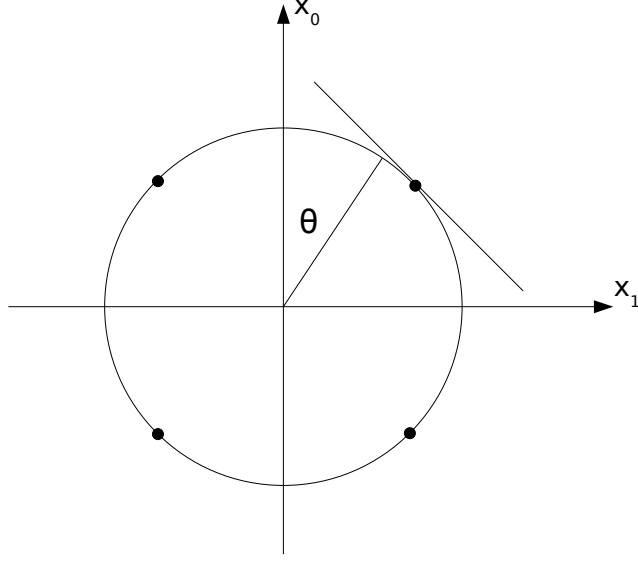


Figure 4.1: Circular Wilson loop in the (x_0, x_1) -plane. The points with $\Theta = \pm\frac{\pi}{4}, \pm\frac{3}{4}\pi$ have light-like tangents.

these points are at $\Theta = \pm\frac{\pi}{4}, \pm\frac{3}{4}\pi$ and the integral in the one-loop order Wilson loop becomes

$$I^{(1)} = \int_0^{2\pi} d\Theta_1 d\Theta_2 \frac{\dot{x}(\Theta_1)\dot{x}(\Theta_2) - \sqrt{\dot{x}^2(\Theta_1)}\sqrt{\dot{x}^2(\Theta_2)}}{(x(\Theta_1) - x(\Theta_2))^2 - i\epsilon} \quad (4.7)$$

$$= \int_0^{2\pi} d\Theta_1 d\Theta_2 \frac{\sin\Theta_1 \sin\Theta_2 - \cos\Theta_1 \cos\Theta_2}{(\cos\Theta_1 - \cos\Theta_2)^2 - (\sin\Theta_1 - \sin\Theta_2)^2 - i\epsilon} - \frac{\sqrt{\sin^2\Theta_1 - \cos^2\Theta_1}\sqrt{\sin^2\Theta_2 - \cos^2\Theta_2}}{(\cos\Theta_1 - \cos\Theta_2)^2 - (\sin\Theta_1 - \sin\Theta_2)^2 - i\epsilon} \quad (4.8)$$

$$= \int_0^{2\pi} d\Theta_1 d\Theta_2 \frac{-\cos(\Theta_1 + \Theta_2) + \sqrt{\cos 2\Theta_1}\sqrt{\cos 2\Theta_2}}{\cos 2\Theta_1 + \cos 2\Theta_2 - 2\cos(\Theta_1 + \Theta_2) - i\epsilon}. \quad (4.9)$$

Note, that the circular Wilson loop is independent of the radius R of the circle. Let us now examine the divergences coming from the point at $\Theta = \pi/4$. For this we need to consider the vector diagrams shown in figure 4.2 and the corresponding scalar diagrams.

Let us first compute the divergent terms of diagram 4.2b. For this purpose, we choose the following parameters

$$\Theta_1 = \frac{\pi}{4} - \psi_1 \quad \Theta_2 = \frac{\pi}{4} + \psi_2 \quad (4.10)$$

and expand around $\Theta = \pi/4$, i.e. for small ψ_1, ψ_2 . The divergent contribution

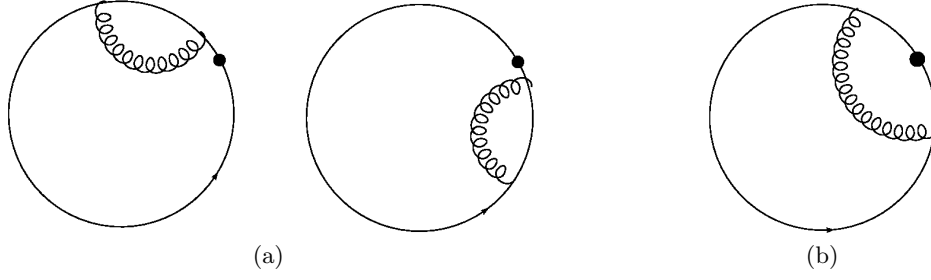


Figure 4.2: Divergent one-loop vector contributions to the circular Wilson loop from the point $\Theta = \pi/4$ with light-like tangent. Additionally, we have to consider the corresponding scalar contributions.

from the vicinity of the singular point then becomes

$$I_{(b)}^{(1)} = - \int_0^{\dots} d\psi_1 \int_0^{\dots} d\psi_2 \frac{\sin(\psi_1 - \psi_2) \mp i\sqrt{\sin 2\psi_1 \sin 2\psi_2}}{\sin 2\psi_1 - \sin 2\psi_2 - 2\sin(\psi_1 - \psi_2) - i\epsilon} \quad (4.11)$$

$$= - \int_0^{\dots} d\psi_1 \int_0^{\dots} d\psi_2 \frac{\psi_1 - \psi_2 \mp 2i\sqrt{\psi_1\psi_2} + \mathcal{O}(\psi^3)}{\psi_2^3 - \psi_1^3 - \psi_1^2\psi_2 + \psi_1\psi_2^2 + \mathcal{O}(\psi^4) - i\epsilon}, \quad (4.12)$$

where again, we have not written the upper integration limit explicitly, since, making only finite contributions, it is irrelevant to the discussion of the divergences. We will maintain this convention throughout the chapter. The \mp comes from the indeterminacy of $\sqrt{-1} = \pm i$ in the coupling to the scalars, mentioned above. The sign will be determined later, fixing the coupling in such a way that the divergences, coming from the coincidence of the propagator endpoints at some other point along the curve in diagram 4.2a, vanishes. Changing to polar coordinates as in (3.33) we obtain

$$I_{(b)}^{(1)} = - \int_0^{\frac{\pi}{2}} d\phi \frac{\cos \phi - \sin \phi \mp 2i\sqrt{\cos \phi \sin \phi}}{(\sin \phi + \cos \phi)^2(\sin \phi - \cos \phi) - i\epsilon} \int_0^1 \frac{dr}{r} + \text{finite} \quad (4.13)$$

and have thus split off the logarithmic divergence. The vector part of the remaining ϕ -integral obviously is finite and can easily be computed:

$$\int_0^{\frac{\pi}{2}} d\phi \frac{1}{(\sin \phi + \cos \phi)^2} = 1. \quad (4.14)$$

The scalar integrand has a singularity at $\phi = \frac{\pi}{4}$ which corresponds to $\psi_1 = \psi_2$, i.e the case when the distance between the propagator endpoints becomes light-like. By substituting $\phi = \frac{\pi}{4} + \alpha$, we see that the pole is a simple pole and we can compute the integral with the help of the $i\epsilon$ -prescription of the propagator

(see appendix B.2):

$$\mp 2i \int_0^{\frac{\pi}{2}} d\phi \frac{\sqrt{\cos \phi \sin \phi}}{(\sin \phi + \cos \phi)^2 (\sin \phi - \cos \phi) - i\epsilon} = \pm \frac{\pi}{2}. \quad (4.15)$$

The divergent contribution from diagram 4.2b thus is

$$I_{(b)}^{(1)} = -(1 \mp \frac{\pi}{2}) \ln(\delta) + \text{finite}, \quad (4.16)$$

where we have introduced a cutoff δ on r around the singular point.

Now, the divergent contributions from the diagrams in 4.2a still need to be computed. This time, we choose the substitution

$$\Theta_1 = \frac{\pi}{4} + \psi_1 \quad \Theta_2 = \frac{\pi}{4} + \psi_2 \quad (4.17)$$

in (4.8) and again expand for small ψ_1, ψ_2 :

$$I_{(a)}^{(1)} = \int_0^{\dots} d\psi_1 \int_0^{\dots} d\psi_2 \frac{\sin(\psi_1 + \psi_2) \pm \sqrt{\sin 2\psi_1 \sin 2\psi_2}}{-\sin 2\psi_1 - \sin 2\psi_2 + 2 \sin(\psi_1 + \psi_2) - i\epsilon} \quad (4.18)$$

$$= \int_0^{\dots} d\psi_1 \int_0^{\dots} d\psi_2 \frac{\psi_1 + \psi_2 \pm 2\sqrt{\psi_1 \psi_2} + \mathcal{O}(\psi^3)}{\psi_1^3 + \psi_2^3 - \psi_1^2 \psi_2 - \psi_1 \psi_2^2 + \mathcal{O}(\psi^4) - i\epsilon} \quad (4.19)$$

$$= \int_0^{\dots} d\psi_1 \int_0^{\dots} d\psi_2 \frac{(\sqrt{\psi_1} \pm \sqrt{\psi_2})^2 + \mathcal{O}(\psi^3)}{(\psi_1 - \psi_2)(\psi_1^2 - \psi_2^2) + \mathcal{O}(\psi^4) - i\epsilon}. \quad (4.20)$$

Performing another substitution $\sqrt{\psi_i} = \alpha_i$ this becomes

$$I_{(a)}^{(1)} = 4 \int_0^{\dots} d\alpha_1 d\alpha_2 \alpha_1 \alpha_2 \frac{(\alpha_1 \pm \alpha_2)^2 + \mathcal{O}(\alpha^6)}{(\alpha_1 - \alpha_2)^2 (\alpha_1 + \alpha_2)^2 (\alpha_1^2 + \alpha_2^2) + \mathcal{O}(\alpha^8) - i\epsilon}. \quad (4.21)$$

We are now able to determine the sign between the vector and the scalar part. In order to avoid a divergence for $\alpha_1 = \alpha_2$ all along the curve, we have to choose the minus-sign. Switching to polar coordinates in order to split off the remaining logarithmic divergence at $\alpha_1 = \alpha_2 = 0$, we obtain

$$I_{(a)}^{(1)} = \int_0^{\frac{\pi}{2}} d\phi \frac{\cos \phi \sin \phi}{(\sin \phi + \cos \phi)^2} \int_0^1 \frac{dr}{r} + \text{finite}. \quad (4.22)$$

The ϕ -integral can easily be solved to

$$\int_0^{\frac{\pi}{2}} d\phi \frac{\cos \phi \sin \phi}{(\sin \phi + \cos \phi)^2} = \frac{1}{2} \left(\frac{\pi}{2} - 1 \right). \quad (4.23)$$

If we again introduce a cutoff for small r , relating it to the cutoff in (4.16), while taking into account the performed substitution $\alpha = \sqrt{\psi}$, we will now have $\sqrt{\delta}$. We thus get

$$I_{(a)}^{(1)} = \left(1 - \frac{\pi}{2}\right) \ln(\delta) + \text{finite} \quad (4.24)$$

for the divergent contribution from each of the diagrams of fig. 4.2a.

The above fixing of the indeterminacy in the coupling to the scalars also determines the sign in (4.16) to be a minus. We also need to count this contribution twice, considering the case of exchanged parameters. Thus, summing up all divergent contributions coming from the singular point with light-like tangent at $\Theta = \frac{\pi}{4}$, gives zero. We can therefore conclude that, fixing the sign indeterminacy of the coupling to the scalars as proposed above, the Wilson loop of a Minkowskian circle with light-like tangents indeed remains finite, fulfilling our expectations for a smooth curve. Note, that with a different $i\epsilon$ -prescription, the sign would have been fixed the other way round.

4.2 Wilson Loops with Discontinuities in Higher Derivatives

As we have seen in section 4.1, Wilson loops with points with light-like tangent have potential divergences. In the case of the smooth circular contour discussed above, the different divergent contributions exactly cancel each other and the Wilson loop is finite. However, if in these singular light-like points, we have a discontinuity in a higher derivative, the situation might change. As we will see in the following, for a discontinuity in the second derivative, divergences arise. In analogy to the cusp anomalous dimension for the case of a discontinuity in the first derivative, we can define a new anomalous dimension attributed to the divergences coming from the singular light-like points with discontinuity in \ddot{x} .

In order to compute these divergences, at one-loop order, we need to examine the vector contributions shown in figure 4.3 and the corresponding scalar diagrams. For this, we expand the coordinates around the singular point at $t_1 = t_2 = 0$ just as in the case of a cusp. The divergent one-loop contribution from the case of propagator endpoints on the same side of the singular point (fig. 4.3a), give:

$$\begin{aligned} & I_{(a),\pm}^{vec} + I_{(a),\pm}^{scal} \\ &= \int_0^{\dots} dt_1 \int_0^{\dots} dt_2 \frac{\dot{x}(t_1)\dot{x}(t_2) - \sqrt{\dot{x}^2(t_1)}\sqrt{\dot{x}^2(t_2)}}{(x(t_1) - x(t_2))^2 - i\epsilon} \\ &= \int_0^{\dots} dt_1 dt_2 \frac{\dot{x}_0^2 + t_2\dot{x}_0\ddot{x}_\pm + t_1\dot{x}_0\ddot{x}_\pm - \sqrt{\dot{x}_0^2 + 2t_1\dot{x}_0\ddot{x}_\pm}\sqrt{\dot{x}_0^2 + 2t_2\dot{x}_0\ddot{x}_\pm} + \mathcal{O}(t^2)}{(t_1 - t_2)^2\dot{x}_0^2 + (t_1 - t_2)t_1^2\dot{x}_0\ddot{x}_\pm - (t_1 - t_2)t_2^2\dot{x}_0\ddot{x}_\pm + \mathcal{O}(t^4)} - i\epsilon \\ &= \int_0^{\dots} dt_1 dt_2 \frac{t_2 + t_1 - \sqrt{2t_1}\sqrt{2t_2} + \mathcal{O}(t^2)}{(t_1 - t_2)(t_1^2 - t_2^2) + \mathcal{O}(t^4)} - i\epsilon. \end{aligned} \quad (4.25)$$

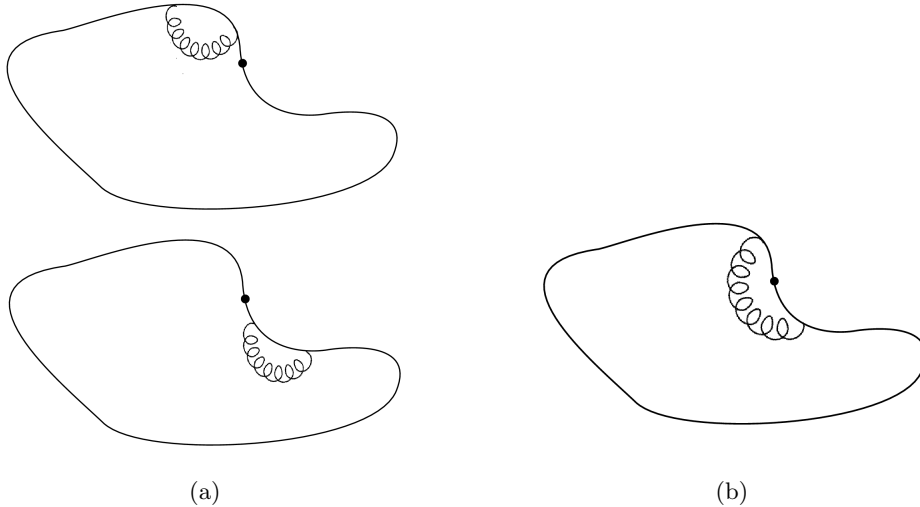


Figure 4.3: Divergent one-loop vector contributions to a Wilson loop with a contour point with light-like tangent and discontinuity in \ddot{x} . Additionally, one has to consider the corresponding scalar diagrams.

In the last line, we have used that the tangent in the point $x(t=0) \equiv x_0$ is light-like, i.e. $\dot{x}_0^2 = 0$. Note, that the contribution is independent of the left and right second derivatives \ddot{x}_\pm of $x(t)$. Changing to polar coordinates as in (3.33), we get

$$I_{(a)}^{vec} + I_{(a)}^{scal} = \int_0^{\pi/2} d\phi \frac{\cos \phi + \sin \phi - 2\sqrt{\cos \phi \sin \phi}}{(\cos \phi - \sin \phi)^2 (\cos \phi + \sin \phi) - i\epsilon} \int_0^1 \frac{dr}{r} + \text{finite}. \quad (4.26)$$

In the above expression, one can see the logarithmic divergence coming from the singular point at $r=0$, i.e. $t_1 = t_2 = 0$, and at first site, the ϕ -integral seems to have a pole in $\phi = \pi/4$ ($t_1 = t_2$), i.e. when the propagator ends coincide at some other point along the loop. As we have seen before, for smooth curves, there should not be any divergence from the latter situation, since the coupling to the scalars is such that the vector and scalar part exactly cancel each other in this case. Indeed, the pole is cancelled and the ϕ -integral turns out to be finite. Introducing a cutoff δ around the singular point, we finally obtain

$$\begin{aligned} I_{(a)}^{vec} + I_{(a)}^{scal} &= \left(1 - \frac{\pi}{2}\right) \ln \delta + \text{finite} \\ &=: \frac{1}{2} \Gamma_a^{(1)} \ln \delta + \text{finite} \end{aligned} \quad (4.27)$$

for the one-loop contribution to the ‘2nd order cusp anomalous dimension’ from diagrams 4.3a. Being independent of \ddot{x}_\pm , the result is the same for both sides; for the complete one-loop Wilson loop, we thus have to consider it twice.

Comparing (4.27) to (4.24), we see that we get the same result as for the circle contribution of fig. 4.2a. This makes sense, since the result is independent

of the second derivative of the curve and is completely determined through the fact that the tangent in the considered point is light-like.

Let us now examine the divergent one-loop contribution stemming from the vector and the scalar diagram of fig. 4.3b. For the sum of the scalar and the vector contribution we find:

$$I_{(b)}^{vec} + I_{(b)}^{scal} = \int_0^{\dots} dt_1 \int_0^{\dots} dt_2 \frac{\dot{x}(t_1)\dot{x}(-t_2) - \sqrt{\dot{x}^2(t_1)}\sqrt{\dot{x}^2(-t_2)}}{(x(t_1) - x(-t_2))^2} \quad (4.28)$$

$$= \int_0^{\dots} dt_1 dt_2 \frac{t_1 \dot{x}_0 \ddot{x}_+ - t_2 \dot{x}_0 \ddot{x}_- - \sqrt{2t_1 \dot{x}_0 \ddot{x}_+} \sqrt{-2t_2 \dot{x}_0 \ddot{x}_-} + \mathcal{O}(t^2)}{(t_1 + t_2)(t_1^2 \dot{x}_0 \ddot{x}_+ - t_2^2 \dot{x}_0 \ddot{x}_-) + \mathcal{O}(t^4) - i\epsilon} \quad (4.29)$$

With the following parameter choice

$$t_1 = ry \quad t_2 = r(1 - y) \quad (4.30)$$

we can split off the logarithmic divergence coming from the situation when the propagator endpoints come together in the singular point, i.e. $t_1 = t_2 = 0$ or equivalently $r = 0$ and obtain

$$I_{(b)}^{vec} + I_{(b)}^{scal} = \int_0^1 dy \frac{\dot{x}_0 \ddot{x}_+ y - \dot{x}_0 \ddot{x}_- (1 - y) - 2\sqrt{\dot{x}_0 \ddot{x}_+} \sqrt{-\dot{x}_0 \ddot{x}_-} \sqrt{y(1 - y)}}{(\dot{x}_0 \ddot{x}_+ y^2 - \dot{x}_0 \ddot{x}_- (1 - y)^2) - i\epsilon} \int_0^1 \frac{dr}{r} + \text{finite}. \quad (4.31)$$

The integral is a function of the quotient

$$c := \frac{\dot{x}_0 \ddot{x}_-}{\dot{x}_0 \ddot{x}_+} \quad (4.32)$$

which due to $\dot{x}_0^2 = 0$ is reparametrisation invariant and thus is a characteristic property of the curve in x_0 . With this definition we obtain

$$I_{(b)}^{vec} + I_{(b)}^{scal} = \int_0^1 dy \frac{(1 + c)y - c - 2\sqrt{-c} \sqrt{y(1 - y)}}{((1 - c)y^2 + 2cy - c) - i\epsilon} \int_{\delta}^1 \frac{dr}{r} + \text{finite}, \quad (4.33)$$

where we have introduced a cutoff δ as above. The integrand has singularities for the roots of the denominator:

$$\begin{aligned} X_1 &:= -\frac{c - \sqrt{c}}{1 - c}, \\ X_2 &:= -\frac{c + \sqrt{c}}{1 - c}. \end{aligned} \quad (4.34)$$

If $c < 0$, i.e. $\dot{x}_0\ddot{x}_-$ and $\dot{x}_0\ddot{x}_+$ have different signs, which means that the curve stays space-like or stays time-like on both sides of x_0 , the roots are complex and do not affect the integration and the vector integral becomes

$$I_{(b),c<0}^{vec} = \left(-\frac{1+c}{1-c} \ln \sqrt{-c} + \frac{\sqrt{-c}}{1-c} \pi \right) \ln \frac{1}{\delta} + \text{finite}. \quad (4.35)$$

Let us now examine the case of positive c , i.e. when $\dot{x}_0\ddot{x}_-$ and $\dot{x}_0\ddot{x}_+$ have the same sign, which means that the curve changes from space-like to time-like in x_0 . X_2 does not lie within the domain of integration $(0, 1)$ for any real value of c , whereas for $c > 0$, X_1 lies within the domain of integration. We then have to respect the $i\epsilon$ -prescription from the propagator when surrounding the pole and the vector integral becomes

$$I_{(b),c>0}^{vec} = \left(-\frac{1+c}{1-c} \ln \sqrt{c} + \left| \frac{1-\sqrt{c}}{1+\sqrt{c}} \right| i \frac{\pi}{2} \right) \ln \frac{1}{\delta} + \text{finite}. \quad (4.36)$$

The discussion of the poles is the same for the scalar part of the integral (4.33) and for $c < 0$, we obtain

$$I_{(b),c<0}^{scal} = \left(\frac{2\sqrt{-c} - \sqrt{2}(-c)^{\frac{1}{4}} - \sqrt{2}(-c)^{\frac{3}{4}}}{1-c} \pi \right) \ln \frac{1}{\delta} + \text{finite} \quad (4.37)$$

and for $c > 0$:

$$I_{(b),c>0}^{scal} = \left(-\sqrt{2} \frac{c^{\frac{1}{4}}}{1+\sqrt{c}} \pi + \sqrt{2} \left| \frac{c^{\frac{1}{4}}(1-c^{\frac{1}{4}})}{(1+\sqrt{c})(1+c^{\frac{1}{4}})} \right| i\pi \right) \ln \frac{1}{\delta} + \text{finite}. \quad (4.38)$$

The above results now define the one-loop contribution to our new ‘2nd order cusp anomalous dimension’ arising from this ‘cusp’ in the second derivative by

$$2(I_{(b)}^{vec} + I_{(b)}^{scal}) =: \Gamma_b^{(1)}(c) \ln \delta + \text{finite}. \quad (4.39)$$

For the whole ‘2nd order cusp anomalous dimension’, we need to sum up the above contributions: twice Γ_a from (4.27), for each side of the singular point, and twice $\Gamma_b(c)$ from (4.35) and (4.37), respectively (4.36) and (4.38), taking into account the case where t_1 and t_2 are exchanged. In the case where $c < 0$, we thus finally obtain

$$\begin{aligned} \Gamma_{(\text{cusp in } \ddot{x})}^{(1)}(c) &= 2\Gamma_a^{(1)} + 2\Gamma_b^{(1)}(c) \\ &= 4 - 2\pi + 4\frac{1+c}{1-c} \ln \sqrt{-c} - 4\frac{3\sqrt{-c} - \sqrt{2}((-c)^{1/4} + (-c)^{3/4})}{1-c} \pi \end{aligned} \quad (4.40)$$

for the anomalous dimension due to a jump in the second derivative in a point with light-like tangent. For $c > 0$, we get the analytic continuation:

$$\begin{aligned} \Gamma_{(\text{cusp in } \ddot{x})}^{(1)}(c) &= 4 - 2\pi + 4\frac{1+c}{1-c} \ln \sqrt{c} + 4\frac{\sqrt{2}(c^{1/4} - c^{3/4})}{1-c} \pi + \\ &\quad - 2 \left| \frac{1+c - 6\sqrt{c} + 2\sqrt{2}(c^{1/4} + c^{3/4})}{1-c} \right| i\pi. \end{aligned} \quad (4.41)$$

Note, that the expressions of course are symmetric under the exchange of c and $\frac{1}{c}$.

For $c \rightarrow \infty$, or equivalently $c \rightarrow 0$, which for instance corresponds to the case of a straight light-like segment at one side of the ‘2nd order cusp’, the ‘2nd order cusp anomalous dimension’ behaves as:

$$\Gamma_{\text{cusp in } \ddot{x}}^{(1)}(c) = 2 \ln(c) - 2\pi + 4. \quad (4.42)$$

Recall, that for the usual cusp anomalous dimension, in the limit of large Minkowskian cusp angles θ :

$$\cosh \theta := \frac{\dot{x}_+ \dot{x}_-}{|\dot{x}_+| |\dot{x}_-|} \approx \frac{e^\theta}{2}, \quad (4.43)$$

which corresponds to an angle between light-like sides, the cusp anomalous dimension was linear in the angle and the factor of the one-loop result was given by (3.8), i.e.:

$$\begin{aligned} \Gamma_{\text{cusp}}^{(1)}(\theta) &= \Gamma_{\text{cusp}}^{(1)} \cdot \theta = 2\theta \\ &= 2 \ln(\cosh \theta) + \text{const}. \end{aligned} \quad (4.44)$$

Comparing this to our result (4.42), we see that at one loop, the defined ‘2nd order cusp anomalous dimension’ behaves in the same way as the usual cusp anomalous dimension. This gives rise to the question, whether this relation is also true at higher loop order and whether perhaps, identifying c with $\cosh \theta$, for $c \rightarrow \infty$ or 0, the ‘2nd order cusp anomalous dimension’ defines the same universal function of the coupling then the usual cusp anomalous dimension for $\theta \rightarrow \infty$.

Let us finally have a look at the special case of a smooth curve with a light-like tangent in some point, but $\ddot{x}_- = \ddot{x}_+$ (i.e. $c = 1$), as for instance the circle of section 4.1, the above integral becomes

$$(I_{(b)}^{vec} + I_{(b)}^{scal})_{c=1} = \int_0^{\dots} dt_1 dt_2 \frac{t_1 - t_2 - 2i\sqrt{t_1 t_2} + \mathcal{O}(t^2)}{(t_1 + t_2)(t_1^2 - t_2^2) + \mathcal{O}(t^4) - i\epsilon}, \quad (4.45)$$

where we have fixed the sign indeterminacy of the coupling to the scalars as proposed in section 4.1. Performing the substitution (4.30) and taking into consideration the $i\epsilon$ -prescription from the propagator this can be solved to

$$\begin{aligned} (I_{(b)}^{vec} + I_{(b)}^{scal})_{c=1} &= \left(1 - 2i \int_0^1 dy \frac{\sqrt{y(1-y)}}{(2y-1) - i\epsilon} \right) \int_\delta^1 \frac{dr}{r} + \text{finite} \\ &= - \left(1 - \frac{\pi}{2} \right) \ln(\delta) + \text{finite}, \end{aligned} \quad (4.46)$$

where again a cut-off δ around the point with light-like tangent was introduced. The integral from the diagram with both propagator endpoints on the same

side of the singular point (4.25) does not depend on the second derivative \ddot{x}_\pm of the respective side and thus remains as in (4.27). This contribution has to be counted twice, once for every side, and the above contribution (4.46) also needs to be counted twice, considering the case where t_1 and t_2 are exchanged. We hence find that the divergent contributions exactly cancel each other and can reproduce our result found for the special case of the circle, that a smooth curve with isolated points with light-like tangent is finite. By generally fixing the sign indeterminacy in the coupling to the scalars in the way suggested in section 4.1, i.e. $\sqrt{\dot{x}^2} = +i\sqrt{|\dot{x}^2|}$ for space-like curves, we can thus achieve, that a generic smooth curve remains finite.

In the above computation, we have assumed a constant coupling to the scalars. Analogously to [29], one could have assumed an additional discontinuity in the coupling to the scalars $\Theta^I(t)$ in the supersymmetric Wilson loop of (2.10) and could have computed the corresponding anomalous dimension. In (4.40), we would then have an additional factor depending on the saltus in Θ^I in front of the scalar part of $\Gamma_b(c)$. Possibly, for a special choice of the coupling the anomalous dimension might vanish and the Wilson loop with discontinuity in the second derivative in a point with light-like tangent might become finite.

Now, the question remains whether a discontinuity in a higher than the second derivative in such a point also leads to divergences and thus to a corresponding ‘higher order cusp anomalous dimension’. Let us therefore have a look at a curve with a light-like tangent and a discontinuity in the third derivative in some point. For the diagrams where both propagator endpoints lie on the same side of the singular point, we get the same result as for a discontinuity in the second derivative in (4.27), since this contribution is independent of $\dot{x}_0\ddot{x}_\pm$. For the divergent part of the diagram where the propagator connects the two different sides of the higher order cusp, we obtain:

$$I_{(b),\ddot{x}}^{vec} + I_{(b),\ddot{x}}^{scal} = \int_0^{\ddot{\infty}} dt_1 \int_0^{\ddot{\infty}} dt_2 \frac{\dot{x}(t_1)\dot{x}(-t_2) - \sqrt{\dot{x}^2(t_1)}\sqrt{\dot{x}^2(-t_2)}}{(x(t_1) - x(-t_2))^2} \quad (4.47)$$

$$= \int_0^{\ddot{\infty}} dt_1 dt_2 \frac{t_1 - t_2 - 2i \frac{\dot{x}_0\ddot{x}_0}{|\dot{x}_0\ddot{x}_0|} \sqrt{t_1}\sqrt{t_2} + \mathcal{O}(t^2)}{(t_1 + t_2)(t_1^2 - t_2^2) + \mathcal{O}(t^4) - i\epsilon}. \quad (4.48)$$

This is the same as in (4.29) with $c = 1$, i.e. as for a smooth curve. As examined in (4.46) the sum of all contributions in this case are finite. The part depending on the saltus in \ddot{x} is of higher order in t and therefore is finite. Thus, no divergences arise from a discontinuity in a higher than second derivative of x in some point with light-like tangent and this situation does not define a new anomalous dimension.

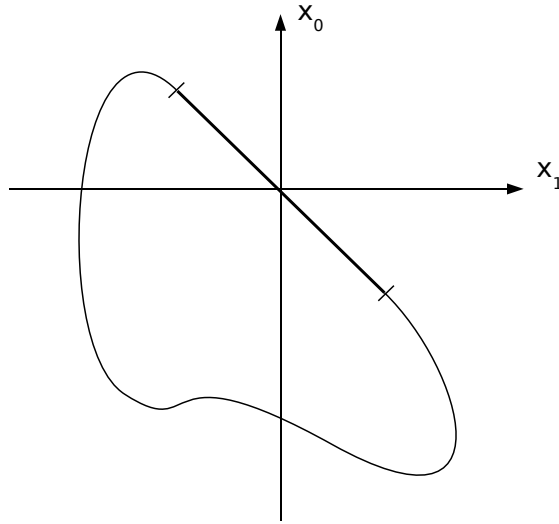


Figure 4.4: A Wilson loop with finite light-like segments is divergent.

4.3 Wilson Loops with Straight Finite Light-Like Segments

Instead of a curve with isolated points with light-like tangent, let us now have a look at a Wilson loop with finite light-like segments, as exemplarily shown in fig. 4.4. Such a Wilson loop will have divergences stemming from the point of transition between the light-like segment and the non-light-like continuation of the curve. As soon as one propagator endpoint approaches the transition point and the other endpoint lies somewhere along the light-like segment, the distance becomes light-like and the integral diverges. Such a divergence therefore is non-local. Thus, if we consider the supersymmetric Wilson loop with general parameter dependent coupling to the scalars

$$\langle W \rangle = 1 - \frac{a}{2} \int dt_1 dt_2 \frac{\dot{x}(t_1)\dot{x}(t_2) - \Theta^I(t_1)\Theta^I(t_2)|\dot{x}(t_1)||\dot{x}(t_2)|}{(x(t_1) - x(t_2))^2} + \mathcal{O}(a^2) \quad (4.49)$$

with the unit six-vector

$$\Theta^I(t)\Theta^I(t) = 1 \quad (4.50)$$

characterising the position of the loop on the S^5 , the question arises whether we can choose the coupling $\Theta(t)$ to the scalars such that the Wilson loop becomes finite, similar to the procedure used by [15, 17], as presented in section 2.2.1.

In order to examine the divergences coming from the light-like segment, we have to consider the diagrams represented in fig. 4.5 including the corresponding scalar diagrams. The first two diagrams are similar to diagrams considered

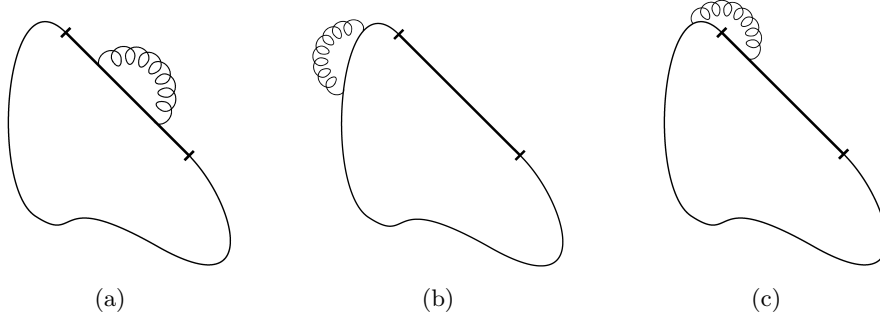


Figure 4.5: One-loop vector contributions to a Wilson loop with finite light-like segment.

before. Individually, the vector diagram 4.5a and the corresponding scalar diagram have linear divergences if the propagator endpoints come together somewhere along the light-like segment. As we have seen in section 3.2 in equation (3.23), these divergences exactly cancel each other for a constant coupling to the scalars. The same is true for the divergences from coincident propagator endpoints somewhere along the curve in diagram 4.5b, as long as the tangent to the curve is not light-like. This divergence is the same as for 4.3a and has already been computed for a constant coupling to the scalars in section 4.2. From (4.25), we see that for a general t -dependent coupling to the scalars we obtain

$$I_{(b)}^{(1)} = \int_0^{\dots} dt_1 dt_2 \frac{t_2 + t_1 - \Theta^I(t_1)\Theta^I(t_2)\sqrt{2t_1}\sqrt{2t_2} + \mathcal{O}(t^2)}{(t_1 - t_2)^2(t_1 + t_2) + \mathcal{O}(t^4)}. \quad (4.51)$$

The essentially new divergent contribution for a Wilson loop with finite light-like segment comes from diagram 4.5c. This contribution is divergent, as soon as the parameter t_2 on the non-light-like part of the curve approaches the transition point, independently of where on the light-like segment the other parameter t_1 is, since then the distance between the propagator endpoints becomes light-like. This is reflected in a divergence of the integrand for $t_2 = 0$, when expanding around the transition point $x(t_2 = 0) \equiv x_0$:

$$I_{(c)}^{(1)} = \int_0^{\dots} dt_1 dt_2 \frac{t_2 \dot{x}_0 \ddot{x}_2 - \Theta^I(-t_1)\Theta^I(t_2)\sqrt{\dot{x}_0^2}\sqrt{\dot{x}_0^2 + 2t_2 \dot{x}_0 \ddot{x}_2} + \mathcal{O}(t^2)}{(t_1 + t_2)t_2^2 \dot{x}_0 \ddot{x}_2 + \mathcal{O}(t^4)}, \quad (4.52)$$

where $\ddot{x}_2 \equiv \ddot{x}(t_2 \rightarrow 0)$ is the left second derivative in x_0 . The parametrisation was at first chosen to be negative on the light-like segment and we then performed the usual shift $t_1 \rightarrow -t_1$ in the integration. In the case of constant coupling to the scalars, the scalar term, being proportional to $|\dot{x}_0|^2$, vanishes and we find

$$I_{(c)}^{(1)} = \int_0^{\dots} dt_1 dt_2 \frac{1 + \mathcal{O}(t^2)}{(t_1 + t_2)t_2 + \mathcal{O}(t^3)}. \quad (4.53)$$

We can then explicitly see the logarithmic divergence for $t_2 = 0$ from the situation described above. The question now is, whether we can cure this non-local divergence by choosing an appropriate coupling to the scalars.

Zarembo's ansatz for the coupling to the scalars is, to only include the t -dependence into a unit vector in the direction of the tangent to the curve and thus letting the position of the loop on the S^5 follow the tangent of the space-time contour, as described in section 2.2.1. Having a look at the one-loop order of the resulting Wilson loop (2.18):

$$I^{(1)} = \int dt_1 dt_2 \frac{\dot{x}(t_1)\dot{x}(t_2) - M_\mu^I M_\nu^I \frac{\dot{x}^\mu(t_1)}{|\dot{x}(t_1)|} \frac{\dot{x}^\nu(t_2)}{|\dot{x}(t_2)|} |\dot{x}(t_1)| |\dot{x}(t_2)|}{(x(t_1) - x(t_2))^2} \quad (4.54)$$

$$= \int dt_1 dt_2 \frac{\dot{x}(t_1)\dot{x}(t_2) - \eta_{\mu\nu} \dot{x}^\mu(t_1) \dot{x}^\nu(t_2)}{(x(t_1) - x(t_2))^2} = 0, \quad (4.55)$$

we see that with this ansatz, it trivially becomes finite for an arbitrary curve. We now want to find a coupling to the scalars, that makes the above Wilson loop finite but non-trivial. For this our first attempt is, to generalise Zarembo's ansatz (2.15) by letting the matrices M_μ^I depend on the contour parameter t :

$$\Theta^I(t) = M_\mu^I(t) \frac{\dot{x}^\mu(t)}{|\dot{x}(t)|}. \quad (4.56)$$

Due to the condition (4.50) our ansatz for the matrices has to fulfil

$$M_\mu^I(t) M_\nu^I(t) = \eta_{\mu\nu} \quad (4.57)$$

for same parameters t .

Due to a $\dot{x}_0^2 = 0$ in the denominator, the integrand of the one-loop contribution from diagram 4.5a is ill-defined, unless we choose the simple Zarembo ansatz with constant matrices $M_{\mu,0}^I$, since then \dot{x}_0^2 cancels out. With this ansatz the vector and the scalar part cancel and the contribution vanishes identically:

$$I_{(a)}^{(1)} = \int_0^{\dots} dt_1 dt_2 \frac{1 - 1}{(t_1 - t_2)^2} = 0. \quad (4.58)$$

Along the light-like piece, we therefore need to choose the Zarembo coupling.

Let us now have a look at the contribution from fig. 4.5b. With the generalised Zarembo ansatz of (4.56), we obtain

$$I_{(b)}^{(1)} = \int_0^{\dots} dt_1 dt_2 \frac{\dot{x}(t_1)\dot{x}(t_2) - M_\mu^I(t_1) M_\nu^I(t_2) \dot{x}^\mu(t_1) \dot{x}^\nu(t_2)}{\dot{x}_0 \ddot{x}_2 (t_1 - t_2)^2 (t_1 + t_2) + \mathcal{O}(t^4)}. \quad (4.59)$$

In order to make this contribution finite, the $M_\mu^I(t)$ -matrices need to behave as

$$M_\mu^I(t_1) M_\nu^I(t_2) = \eta_{\mu\nu} (1 - (t_1 - t_2)^2 \tilde{g}(t_1, t_2)) \quad (4.60)$$

where $\tilde{g}(t_1, t_2)$ can be some function of the parameters which is finite or zero for $t_1 = t_2$.

Finally, with our generalised Zarembo ansatz the contribution from fig. 4.5c becomes

$$I_{(c)}^{(1)} = \int_0^{\dots} dt_1 dt_2 \frac{\dot{x}_0 \dot{x}(t_2) - M_{\mu,0}^I M_{\nu}^I(t_2) \dot{x}_0^\mu \dot{x}^\nu(t_2)}{\dot{x}_0 \ddot{x}_2(t_1 + t_2) t_2^2 + \mathcal{O}(t^4)}. \quad (4.61)$$

In order to make this contribution finite, we need a coupling

$$M_{\mu,0}^I M_{\nu}^I(t_2) = \eta_{\mu\nu} (1 + t_2^2 g(t_2)), \quad (4.62)$$

where $g(t_2)$ has to be finite for $t_2 = 0$. An obvious attempt would be to try the following ansatz for the coupling on the non-light-like piece of the curve: $M_{\mu}^I(t) = M_{\mu,0}^I (1 + f(t))$, entirely putting the t -dependence into a scalar function $f(t)$. This of course does not work since due to condition (4.57), the function would trivially have to be zero. Furthermore, it does not seem possible to find a coupling $M_{\mu}^I(t)$ on the non-light-like curve piece, that satisfies (4.60) and (4.62) at the same time. The generalised Zarembo ansatz of (4.56) therefore fails in making the considered Wilson loop finite.

As a second attempt, we therefore choose a more general ansatz for the coupling, allowing other directions for the position of the loop on the S^5 by additionally adding a term normal to the tangent vector. For the non-light-like curve piece, we can choose the curve length s as a parameter for a space-like curve, or equivalently the proper time for a time-like curve. Then $(\frac{dx}{ds})^2 \equiv x'^2 = \pm 1$ and we have $x'x'' = 0$, i.e. x'' is normal to the tangent vector. Taking the thus defined principal normal to the tangent vector, our coupling takes the form

$$\Theta^I(t) = M_{\mu,0}^I \frac{1}{N(t)} \left(a(t) \frac{\dot{x}^\mu(t)}{|\dot{x}(t)|} + b(t) \frac{x''^\mu(t)}{|x''(t)|} \right), \quad (4.63)$$

where $M_{\mu,0}^I$ are the constant matrices of the Zarembo ansatz, $N(t)$ is a normalisation factor in order to secure that Θ^I is a unit vector and $a(t)$ and $b(t)$ are functions of the contour parameter t , which should be chosen such that the singularities of the denominator are cancelled.

For diagram 4.5c, this can be achieved by choosing $a(t) = 1 - t^2 \tilde{a}(t)$ and $b(t) = t^2 \tilde{b}(t)$, where $\tilde{a}(t)$ and $\tilde{b}(t)$ should be finite or zero for $t = 0$. This ansatz determines the normalisation factor through (4.50) to be

$$N(t) = \sqrt{(1 - t^2 \tilde{a}(t))^2 \frac{\dot{x}^2}{|\dot{x}|^2} + t^4 \tilde{b}(t)^2 \frac{x''^2}{|x''|^2}} \quad (4.64)$$

$$= \sqrt{(\pm)(1 - 2t^2 \tilde{a}(t) + t^4 \tilde{a}(t)^2) + (\pm)'' t^4 \tilde{b}(t)^2}, \quad (4.65)$$

where (\pm) is determined by the sign of \dot{x}^2 and $(\pm)''$ by the sign of x''^2 . We then obtain the following coupling

$$\Theta^I(t) = M_{\mu,0}^I \frac{1}{N(t)} \left((1 - t^2 \tilde{a}(t)) \frac{\dot{x}^\mu(t)}{|\dot{x}(t)|} + t^2 \tilde{b}(t) \frac{x''^\mu(-t)}{|x''(-t)|} \right). \quad (4.66)$$

By choosing $\tilde{a}(t)$ and $\tilde{b}(t)$ in such a way, that they decline for large t , e.g.

$$\tilde{a}(t) = \tilde{b}(t) = e^{-t}, \quad (4.67)$$

we can make sure that our ansatz only is explicitly t -dependent near the critical transition point generating the divergence, and that we reobtain Zarembo's ansatz at large distances of it. Keeping in mind that along the light-like segment, we need to keep the simple Zarembo ansatz, diagram 4.5c becomes

$$I_{(c)}^{(1)} = \int_0^{\dots} d\tilde{t} dt \left(\frac{\dot{x}_0 \dot{x}(t)}{t^2 (\tilde{t} + t) \dot{x}_0 \ddot{x}_2 + \mathcal{O}(t^4)} - \frac{\frac{1}{N(t)} \eta_{\mu\nu} \frac{\dot{x}_0^\mu}{|\dot{x}_0|} \left((1 - t^2 e^{-t}) \frac{\dot{x}^\nu(t)}{|\dot{x}(t)|} + t^2 e^{-t} \frac{x''^\nu(t)}{|x''(t)|} \right) |\dot{x}_0| |\dot{x}(t)|}{t^2 (\tilde{t} + t) \dot{x}_0 \ddot{x}_2 + \mathcal{O}(t^4)} \right), \quad (4.68)$$

where the parameter \tilde{t} runs along the light-like segment and t along the non-light-like curve piece. For small t , i.e. if the propagator endpoint approaches the light-like segment, this behaves as

$$\begin{aligned} I_{(c)}^{(1)} &= \int_0^{\dots} d\tilde{t} dt \left(\frac{\dot{x}_0 \dot{x}(t)}{t^2 (\tilde{t} + t) \dot{x}_0 \ddot{x}_2 + \mathcal{O}(t^4)} - \frac{(1 + t^2) \eta_{\mu\nu} \frac{\dot{x}_0^\mu}{|\dot{x}_0|} \left(\frac{\dot{x}^\nu(t)}{|\dot{x}(t)|} + t^2 \left(\frac{\dot{x}^\nu(t)}{|\dot{x}(t)|} + \frac{x''^\nu(t)}{|x''(t)|} \right) \right) |\dot{x}_0| |\dot{x}(t)| + \mathcal{O}(t^3)}{t^2 (\tilde{t} + t) \dot{x}_0 \ddot{x}_2 + \mathcal{O}(t^4)} \right) \\ &= - \int_0^{\dots} d\tilde{t} dt \frac{t^2 \left(2\dot{x}_0 \dot{x}(t) + \dot{x}_0 x''(t) \frac{|\dot{x}(t)|}{|x''(t)|} \right) + \mathcal{O}(t^3)}{t^2 (\tilde{t} + t) \dot{x}_0 \ddot{x}_2 + \mathcal{O}(t^4)}. \end{aligned} \quad (4.70)$$

As intended, with our ansatz (4.66), the factor of t^2 in the denominator is cancelled and the contribution becomes finite.

It now remains to be checked whether our ansatz also cancels the divergences of diagram 4.5b when the propagator ends come together. For this we insert our ansatz for the coupling (4.66) into the contribution $I_{(b)}^{(1)}$ and expand $x(\tilde{t})$ around $t = \tilde{t}$ in the denominator:

$$I_{(b)}^{(1)} = \int_0^1 d\tilde{t} dt \frac{\dot{x}(t) \dot{x}(\tilde{t}) - \Theta^I(t) \Theta^I(\tilde{t}) |\dot{x}(t)| |\dot{x}(\tilde{t})|}{(t - \tilde{t})^2 \dot{x}^2(t) + \mathcal{O}((t - \tilde{t})^3)}. \quad (4.71)$$

Writing $\tilde{t} \equiv t + \epsilon$ the denominator then is of order ϵ^2 . To zeroth order in ϵ , the scalar part and the vector part in the numerator cancel due to the normalisation of the ansatz for equal parameters. It thus remains to be shown that the linear order of ϵ in the numerator vanishes. This can indeed be seen by explicitly calculating it (see appendix C).

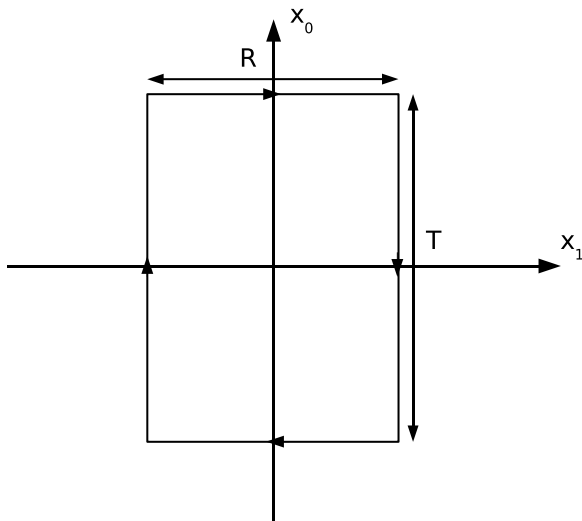


Figure 4.6: Rectangular Wilson loop in the (x_0, x_1) -plane of Minkowski space.

Generalising Zarembo's ansatz as in (4.63), we have thus found a coupling to the scalars, such that a Wilson loop with light-like segments becomes finite. Following the discussion of [15], one could now examine whether a Wilson loop with the proposed coupling globally preserves supersymmetry and if one can thus construct BPS operators for contours of special shape. However, an embedding of a curve with straight extended light-like segment in a simple submanifold as in [17], [18] seems difficult.

4.4 Rectangular Wilson Loop in Minkowskian Space

Various simple geometrical objects, such as the circle, whose divergences were examined in section 4.1 for the Minkowski case, and the rectangle have been calculated in Euclidean space. Having realised how different the behaviour of Wilson loops in a Minkowskian space-time structure can be, it therefore seems interesting to calculate these objects in Minkowski space and to compare the results to the Euclidean case. In this section, we will thus calculate the Wilson loop for a rectangle with two time-like and two space-like sides as represented in fig. 4.6 in the (x_0, x_1) -plane. For large time lengths, this Wilson loop has the physical significance of the static quark-antiquark-potential as was briefly explained in chapter 2.

The renormalised rectangular Wilson loop in Euclidean space with sides x and y to one-loop order, can for instance be found in [47]:

$$W(x, y) = 1 + 2a \left(2 + \ln \frac{x^2 y^2 \mu^2}{x^2 + y^2} + \frac{x}{y} \arctan \frac{x}{y} + \frac{y}{x} \arctan \frac{y}{x} \right), \quad (4.72)$$

where μ is the renormalisation group parameter. The 2-loop expression can

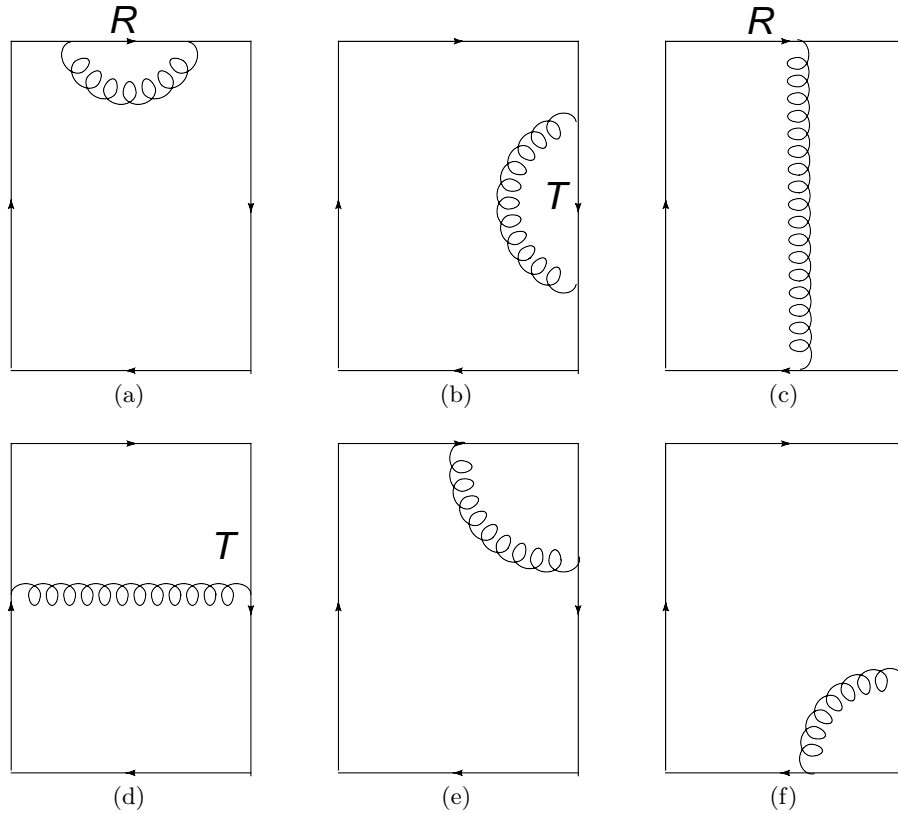


Figure 4.7: One-loop gauge field contributions to the rectangular Wilson loop.

for instance be found in [48]. This is the pure gauge field Wilson loop without scalars. In order to compare it to the Minkowski result, we therefore only need to consider the gauge field part.

In Minkowski space, the rectangular Wilson loop in the (x_0, x_1) -plane, as represented in figure 4.6, can be parametrised as follows: For the parameter running along the upper space-like edge (R), we get

$$x(t_1) = \begin{pmatrix} \frac{T}{2} \\ -\frac{R}{2} + Rt_1 \end{pmatrix} \quad \Rightarrow \quad \dot{x}(t_1) = \begin{pmatrix} 0 \\ R \end{pmatrix} \quad (4.73)$$

If the parameter runs along the right time-like edge (T), we get

$$x(t_2) = \begin{pmatrix} \frac{T}{2} - Tt_2 \\ \frac{R}{2} \end{pmatrix} \quad \Rightarrow \quad \dot{x}(t_2) = \begin{pmatrix} -T \\ 0 \end{pmatrix} \quad (4.74)$$

and analogously for the other two sides of the rectangle.

In order to calculate the pure gauge field Wilson loop to one-loop order, we need to take into account the graphs shown in figure 4.7. The diagrams with a propagator which has both ends on one and the same edge of the rectangle, 4.7a and 4.7b are divergent due to the situation when the propagator ends come

together, somewhere along the edge of the rectangle. For 4.7a we get

$$I_{(a)} = \int_0^1 dt_2 \int_0^1 dt_1 \frac{\dot{x}(t_1)\dot{x}(t_2)}{(x(t_1) - x(t_2))^2} \quad (4.75)$$

$$= \int_0^1 dt_2 \int_0^1 dt_1 \frac{-R^2}{-R^2(t_1 - t_2)^2}. \quad (4.76)$$

The integral is divergent due to the singularity of the integrand at $t_1 = t_2$. We can regularise it by introducing a cutoff, preventing the propagator endpoints from coming closer than some Δ , or equivalently, we can add Δ to the denominator:

$$I_{(a)} = \int_0^1 dt_2 \int_0^1 dt_1 \frac{1}{(t_1 - t_2)^2 + \frac{\Delta^2}{R^2}} \quad (4.77)$$

$$= 2 \ln \left(\frac{\Delta}{R} \right) - 2. \quad (4.78)$$

This is divergent as we send Δ to zero. We can therefore introduce a scale μ , drop infinite terms and obtain

$$I_{(a)} = -2 \ln(R\mu) - 2. \quad (4.79)$$

μ then is the renormalisation group parameter.

If the propagator endpoints both run along one of the time-like edges T (fig. 4.7b), we obtain the same contribution but substituting R by T .

We then have the contributions from the diagrams where the propagator connects the opposite sides of the rectangle, shown in fig. 4.7c and 4.7d. For the case where the propagator connects the two space-like edges (R) we get

$$I_{(c)} = \int_0^1 dt_1 \int_0^1 dt_2 \frac{\dot{x}(t_1)\dot{x}(t_2)}{(x(t_1) - x(t_2))^2} \quad (4.80)$$

$$= \int_0^1 dt_1 \int_0^1 dt_2 \frac{R^2}{T^2 - R^2(1 - t_1 - t_2)^2} \quad (4.81)$$

$$= \frac{R^2}{T^2} \int_0^1 dt_1 \int_0^1 dt_2 \frac{1}{1 - \frac{R^2}{T^2}(t_1 - t_2)^2}, \quad (4.82)$$

where we have substituted $1 - t_1$ by t_1 . If we now assume that T be larger than R , we see that the integrand has no singularity within the integration limits

$t_1, t_2 \in [0, 1]$ and we can directly solve the integral:

$$I_{(c)}^{T>R} = \frac{R^2}{2T^2} \int_0^1 dt_1 \int_0^1 dt_2 \left(\frac{1}{1 - \frac{R}{T}(t_1 - t_2)} + \frac{1}{1 + \frac{R}{T}(t_1 - t_2)} \right) \quad (4.83)$$

$$= \frac{1}{2} \frac{R}{T} \int_0^1 dt_1 \left(\ln \left(1 - \frac{R}{T}(t_1 - t_2) \right) - \ln \left(1 + \frac{R}{T}(t_1 - t_2) \right) \right) \Bigg|_{t_2=0}^{t_2=1} \quad (4.84)$$

$$= \frac{R}{T} \ln \left(\frac{1 + \frac{R}{T}}{1 - \frac{R}{T}} \right) + \ln \left(1 - \frac{R^2}{T^2} \right). \quad (4.85)$$

The diagram with the propagator that connects the two opposite time-like edges (T) of the rectangle is the same but with exchanged R and T :

$$I_{(d)} = \frac{T^2}{R^2} \int_0^1 dt_1 \int_0^1 dt_2 \frac{1}{1 - \frac{T^2}{R^2}(t_1 - t_2)^2 - i\epsilon}. \quad (4.86)$$

However, still assuming T to be larger than R , we now have to be more careful about the integration, since we now have a singularity at $(t_1 - t_2) = \pm \frac{R}{T}$ which is the case where the distance between the propagator endpoints becomes light-like. However, for the singularities that lie somewhere along the side of the rectangle, the result is finite and real due to the $i\epsilon$ -prescription of the propagator, since treating the integral as a principal value yields a finite result and the additional terms from compassing the poles cancel each other. This holds as long as the singularity is not exactly at the boundary of the integration. When one of the parameters lies on the integration boundary at the corner of the rectangle, the $i\epsilon$ -prescription does not help making the result finite. However, since the divergence is a logarithmic one, as can be seen in (4.84), and the logarithm is integrable, this does not lead to any additional divergences. With these considerations we get the following contribution from diagram 4.7d for $T > R$:

$$I_{(d)}^{T>R} = \frac{T}{R} \ln \left(-\frac{1 + \frac{T}{R}}{1 - \frac{T}{R}} \right) + \ln \left(\frac{T^2}{R^2} - 1 \right). \quad (4.87)$$

The case where R is larger than T is analogous. The singularities now appear in diagram 4.7c, but again they do not lead to additional divergences and in total, we get the same result as before, but with exchanged R and T . For both cases, the total result for the sum of fig. 4.7c and 4.7d can hence be formulated as follows:

$$I_{(c)} + I_{(d)} = \frac{R}{T} \ln \left(\frac{1 + \frac{R}{T}}{|1 - \frac{R}{T}|} \right) + \frac{T}{R} \ln \left(\frac{1 + \frac{T}{R}}{|1 - \frac{T}{R}|} \right) - \ln \left(\frac{R^2 T^2}{(R^2 - T^2)^2} \right). \quad (4.88)$$

The discussion of the singularities however, only holds as long as $R \neq T$. The case of the square would have to be considered apart.

Finally, the diagrams 4.7e and 4.7f remain. Here, $\hat{x}(t_1)$ and $\hat{x}(t_2)$ are orthogonal and the contribution vanishes.

For the complete gauge field Wilson loop to one-loop order, we now need to sum over the above contributions: Diagrams 4.7a and 4.7b have to be considered twice each, for every side of the rectangle. The contributions with propagators connecting opposite sides, (4.88), also need to be counted twice each, since one has to take into account the case where t_1 and t_2 are exchanged. In total, we get

$$\begin{aligned}
 W(R, T) &= 1 - \frac{a}{2} \left(2I_{(a)} + 2I_{(b)} + 2(I_{(c)} + I_{(d)}) \right) + \mathcal{O}(a^2) \\
 W &= 1 + a \left(-\frac{R}{T} \ln \left(\frac{1 + \frac{R}{T}}{|1 - \frac{R}{T}|} \right) - \frac{T}{R} \ln \left(\frac{1 + \frac{T}{R}}{|1 - \frac{T}{R}|} \right) + \right. \\
 &\quad \left. + \ln \left(\frac{R^4 T^4 \mu^4}{(R^2 - T^2)^2} \right) + 4 \right) + \mathcal{O}(a^2) \quad (4.89)
 \end{aligned}$$

for the rectangular gauge field Wilson loop in Minkowski space to one loop order.

We can now compare our result to the Euclidean result (4.72), which we can rewrite as follows

$$\begin{aligned}
 W &= 1 + a \left(i\frac{x}{y} \ln \left(\frac{1 + i\frac{x}{y}}{1 - i\frac{x}{y}} \right) + i\frac{y}{x} \ln \left(\frac{1 + i\frac{y}{x}}{1 - i\frac{y}{x}} \right) + \right. \\
 &\quad \left. + \ln \left(\frac{x^4 y^4 \mu^4}{(x^2 + y^2)^2} \right) + 4 \right) + \mathcal{O}(a^2). \quad (4.90)
 \end{aligned}$$

Comparing the two expressions, we see that we have exact correspondence if we identify the sides (x, y) with (R, T) and perform a Wick rotation $T \rightarrow iT$. This is the result one might already have expected, for a rectangle that has clearly distinct time-like and space-like sides, which are orthogonal to each other. We can thus directly see that we only get T^2 -terms and no mixed term RT in the integrand, which would become imaginary after Wick rotation.

This is not so obvious in the case of the circle though, where a Wick rotation of the radius $R \rightarrow iR$ transforms the circle into a hyperboloid rather than again into a circle. It thus seems worth computing the one-loop Wilson loop for the Minkowski circle with points with light-like tangents, which was shown to be finite in section 4.1, and to compare it with the Euclidean result, which was for instance calculated in [16]. There, an anomaly for the conformal inversion, that maps the Euclidean circle to the Wilson line, which simply equals one, was stated, which determines the circular Wilson loop to all orders in the coupling. It would thus be interesting to examine, whether this also holds for the Minkowski case.

Comparing the results for the Euclidean circular Wilson loop to the string worldsheet associated to it through the AdS/CFT correspondence as described in 2.2, in [16] the full supersymmetric Wilson loop including the scalars was

calculated. For a similar check of the correspondence for the Minkowski rectangular Wilson loop, we would of course also need the supersymmetric rectangular Wilson loop, including the scalars.

Supersymmetric Rectangular Wilson Loop

In order to compute the supersymmetric rectangular Wilson loop including the scalars, additionally to the diagrams considered above, we need to compute the corresponding scalar diagrams.

As for a generic smooth curve, the vector and the scalar contributions from the propagators that have both ends on one and the same edge of the rectangle (fig. 4.7a and 4.7b) cancel each other

$$I_{(a)}^{\text{vector}} + I_{(a)}^{\text{scalar}} = \int_0^1 dt_1 \int_0^1 dt_2 \frac{\dot{x}(t_1)\dot{x}(t_2) - \sqrt{\dot{x}^2(t_1)}\sqrt{\dot{x}^2(t_2)}}{(x(t_1) - x(t_2))^2} \quad (4.91)$$

$$= \int_0^1 dt_1 \int_0^1 dt_2 \frac{-R^2 - \sqrt{-R^2}\sqrt{-R^2}}{-R^2(t_2 - t_1)^2} = 0 \quad (4.92)$$

and the divergences from the vector part (4.79) fall away.

We then have the contributions from the diagrams where the propagator connects the opposite sides of the rectangle. Here, the scalar part equals the vector part and for the supersymmetric Wilson loop, we simply need to consider the above contributions (4.88) twice.

Since the vector-diagrams of 4.7e and 4.7f vanish as seen above, finally, only its scalar version remains to be computed:

$$I_{(e)}^{\text{scalar}} = - \int_0^1 dt_1 \int_0^1 dt_2 \frac{\sqrt{\dot{x}^2(t_1)}\sqrt{\dot{x}^2(t_2)}}{(x(t_1) - x(t_2))^2} \quad (4.93)$$

$$= -\sqrt{-R^2}\sqrt{T^2} \int_0^1 dt_1 \int_0^1 dt_2 \frac{1}{(T^2 t_2^2 - R^2 t_1^2)} \quad (4.94)$$

where in the integration, we have shifted $(1 - t_1)$ to t_1 . Here, we again fix the sign indeterminacy as proposed in section 4.1: $\sqrt{-R^2} = +i\sqrt{R^2}$. Changing to

polar coordinates as in (3.33), this becomes

$$I_{(e)}^{\text{scalar}} = -i\sqrt{R^2}\sqrt{T^2} \left(\int_0^{\frac{\pi}{4}} d\phi \int_0^{\frac{1}{\cos\phi}} dr r \frac{1}{r^2(T^2 \sin^2 \phi - R^2 \cos^2 \phi)} + \right. \quad (4.95)$$

$$\left. + \int_{\frac{\pi}{4}}^{\frac{\pi}{2}} d\phi \int_0^{\frac{1}{\sin\phi}} dr r \frac{1}{r^2(T^2 \sin^2 \phi - R^2 \cos^2 \phi)} \right)$$

$$= -i\sqrt{R^2}\sqrt{T^2} \left(\int_0^{\frac{\pi}{2}} d\phi \frac{1}{(T^2 \sin^2 \phi - R^2 \cos^2 \phi)} \int_0^1 \frac{dr}{r} - F(T, R) \right), \quad (4.96)$$

where we expect the integrals defined by

$$F(T, R) := \int_0^{\frac{\pi}{4}} d\phi \frac{\ln(\cos \phi)}{(T^2 \sin^2 \phi - R^2 \cos^2 \phi)} + \int_{\frac{\pi}{4}}^{\frac{\pi}{2}} d\phi \frac{\ln(\sin \phi)}{(T^2 \sin^2 \phi - R^2 \cos^2 \phi)} \quad (4.97)$$

to be finite as we do not expect any divergences coming from the boundary at $t_1 = t_2 = 1$.

In polar coordinates, the logarithmic divergence at $r = 0$, corresponding to $t_1 = t_2 = 0$, i.e. to the case where the propagator ends come together at the corner, becomes manifest. The factor in front of this logarithmic divergence is determined by the ϕ -integral:

$$\begin{aligned} \int_0^{\frac{\pi}{2}} d\phi \frac{1}{(T^2 \sin^2 \phi - R^2 \cos^2 \phi) - i\epsilon} &= \int_0^{\frac{\pi}{2}} \frac{d\phi}{\cos^2 \phi} \frac{1}{T^2 \tan^2 \phi - R^2 - i\epsilon} \\ &= \frac{1}{2} \int_{-\infty}^{\infty} \frac{dz}{T^2 z^2 - R^2 - i\epsilon} \\ &= \frac{1}{2TR} \int_{-\infty}^{\infty} \frac{dy}{y^2 - 1 - i\epsilon} \\ &= \frac{i\pi}{2TR}. \end{aligned} \quad (4.98)$$

Introducing a cutoff δ for the r -integral in (4.96), the first term simplifies to

$$-i\sqrt{R^2}\sqrt{T^2} \frac{i\pi}{2TR} \int_{\delta}^1 \frac{dr}{r} = \frac{\pi}{2} \ln \frac{1}{\delta}. \quad (4.99)$$

For the boundary terms (4.97), we obtain:

$$\begin{aligned}
 F(T, R) &= -i\sqrt{R^2}\sqrt{T^2} \int_0^{\frac{\pi}{2}} d\phi \frac{\ln\left(\frac{1}{2}(1 + |\cos(2\phi)|)\right)}{T^2 \cos^2 \phi - R^2 \sin^2 \phi - i\epsilon} \\
 &= -i\sqrt{R^2}\sqrt{T^2} \frac{1}{2T^2} \int_0^{\frac{\pi}{2}} \frac{d\phi}{\cos^2 \phi} \frac{\ln\left(\frac{1}{2}\left(1 + \left|\frac{1-\tan^2 \phi}{1+\tan^2 \phi}\right|\right)\right)}{1 - \frac{R^2}{T^2} \tan^2 \phi - i\epsilon} \\
 &= -\frac{i}{4} \int_{-\infty}^{\infty} dy \underbrace{\frac{\ln\left(\frac{1}{2}\left(1 + \left|\frac{1-\frac{R^2}{T^2}y^2}{1+\frac{R^2}{T^2}y^2}\right|\right)\right)}{y^2 - 1 - i\epsilon}}_{=:f(y)} \\
 &= -\frac{i}{4} 2\pi i \operatorname{Res}(f(y), 1) \\
 &= \frac{\pi}{4} \ln\left(\frac{1}{2}\left(1 + \left|\frac{1 - \frac{R^2}{T^2}}{1 + \frac{R^2}{T^2}}\right|\right)\right). \tag{4.100}
 \end{aligned}$$

In total, for the contribution from the scalar propagator ending on adjacent sides as in fig 4.7e, we thus find

$$I_{(e)}^{\text{scalar}} = \frac{\pi}{2} \left(\ln \frac{1}{\delta} + \frac{1}{2} \ln \left(1 + \left| \frac{1 - \frac{R^2}{T^2}}{1 + \frac{R^2}{T^2}} \right| \right) - \ln 2 \right). \tag{4.101}$$

If we again assume that $T > R$, this becomes

$$I_{(e)}^{\text{scalar}} = -\frac{\pi}{4} \left(2 \ln \delta + \ln \left(1 + \frac{R^2}{T^2} \right) + \ln 2 \right). \tag{4.102}$$

In the case where $R > T$, we get the same result but with exchanged T and R . The contribution from the opposite corner is the same and the one from the two other corners, 4.7f, has the same form but with T and R exchanged:

$$I_{(f)}^{\text{scalar}} = -\frac{\pi}{4} \left(2 \ln \delta + \ln \left(1 + \frac{T^2}{R^2} \right) + \ln 2 \right). \tag{4.103}$$

The total result is symmetric in R and T and therefore is the same independently of which side of the rectangle is larger. In total, for the one-loop supersymmetric rectangular Wilson loop in Minkowski space, we thus have to consider twice the contribution from every corner (4.102) and (4.103) and four times the contributions from the opposite sides (4.88), twice for the scalar and the vector part and twice for exchanged t_1 and t_2 :

$$\begin{aligned}
 W(R, T) &= 1 - \frac{a}{2} \left(4 (I_{(c)} + I_{(d)}) + 4 I_{(e)}^{\text{scalar}} + 4 I_{(f)}^{\text{scalar}} \right) + \mathcal{O}(a^2) \\
 &= 1 - 2a \left(\frac{R}{T} \ln \left(\frac{1 + \frac{R}{T}}{|1 - \frac{R}{T}|} \right) + \frac{T}{R} \ln \left(\frac{1 + \frac{T}{R}}{|1 - \frac{T}{R}|} \right) - \ln \left(\frac{R^2 T^2}{(R^2 - T^2)^2} \right) - \right. \\
 &\quad \left. - \pi \ln \delta - \frac{\pi}{2} \ln 2 + \frac{\pi}{4} \ln \left(\frac{R^2 T^2}{(R^2 + T^2)^2} \right) \right) + \mathcal{O}(a^2), \tag{4.104}
 \end{aligned}$$

where the first line is the contribution from the diagrams where the propagator connects the opposite sides of the rectangle and the second line comes from the diagrams where the propagator connects adjacent sides.

A comparison of this result to the area of the string worldsheet associated to the rectangular Wilson loop through the AdS/CFT correspondence, would yield a non-trivial test of the correspondence.

V

Conclusion and Outlook

We reviewed the basics of the AdS/CFT correspondence in chapter 1 and put a special emphasis on the role of the Wilson loop operator, its construction in the supersymmetric gauge theory and the recently proposed duality between light-like polygonal Wilson loops and gluon scattering amplitudes in $\mathcal{N} = 4$ SYM in chapter 2.

Scattering amplitudes, as well as light-like Wilson loops with cusps are divergent. Hence, a full comparison of the two objects requires regularisation on both sides of the duality. This has been done for dimensional regularisation up to 2-loop order in perturbation theory, for different numbers of gluons, as is briefly reviewed in section 3.1 of chapter 3.

In section 3.2, we proposed an alternative regularisation of the Wilson loop, matching off-shell gluon scattering amplitudes with momenta $p^2 = -m^2$. The regularisation, performed for the supersymmetric Wilson loop, consists in introducing a position dependent cutoff near the cusps of the non-light-like polygon. The thus regularised Wilson loop was explicitly shown to match the off-shell 4-gluon scattering amplitudes to one-loop order, up to a finite term independent of the kinematics and up to terms vanishing for $m^2 \rightarrow 0$. While the full off-shell gluon scattering amplitudes and cut Wilson loop are gauge dependent, we have shown that the leading divergent squared logarithmic term, which is related to the cusp anomalous dimension, is gauge invariant.

An obvious continuation would be to check, whether the regularised Wilson loop still matches the gluon scattering amplitudes to higher loop order in perturbation theory and to generalise to arbitrary number of gluons. Moreover, it also seems interesting to consider finite off-shellness of the amplitudes and to compare, whether the terms that appear in the space-like Wilson loop for finite m coincide.

On the string theory side of the AdS/CFT correspondence, one could construct a regularisation of the string worldsheets ending on the off-light-cone polygonal contour on the boundary of AdS in the limit of classical string theory, yielding a strong coupling result for the Wilson loop. For the light-like case, an alternative to dimensional regularisation, likewise introducing a position dependent cutoff in the radial direction of AdS, has already been discussed in [31].

Furthermore, our regularisation could be of interest in the discussion of the dual conformal symmetry of Wilson loops and scattering amplitudes [7, 8, 13], briefly reviewed in section 2.3.4. However, the construction of a conformal Ward identity, as found for the light-like polygonal Wilson loop in [13], seems difficult for the non-light-like Wilson loop with cut contour in question.

In chapter 4, we have examined special properties of Wilson loops in Minkowski space with light-like tangents and straight extended light-like segments.

From the claim that the Wilson loop for a smooth curve be finite, we fixed an indeterminacy in the sign of the coupling of the locally supersymmetric Wilson loop to the scalars, specific to the Minkowski case. We showed, that a contour point with light-like tangent and a discontinuity in the second derivative leads to a divergence, which defines an anomalous dimension, similarly to the cusp anomalous dimension for a discontinuity in the first derivative. We have computed this ‘second order cusp anomalous dimension’ to one loop in section 4.2. Identifying the quotient characterising the jump in the second derivative $c := \dot{x}_0 \ddot{x}_- / \dot{x}_0 \ddot{x}_+$ with the cusp angle $\cosh \theta$ of a usual cusp, we showed that for large c the defined ‘second order cusp anomalous dimension’ behaves in the same way as the usual cusp anomalous dimension at large angles. This gives rise to the question, whether this relationship also holds at higher loop order and whether the ‘second order cusp anomalous dimension’ perhaps even defines the same universal function of the coupling constant.

In 4.3, we pointed out that a Wilson loop with a straight extended light-like segment is divergent. We constructed a coupling of the supersymmetric Wilson loop to the scalars such that this non-local divergence cancels and the Wilson loop becomes finite. It would be interesting to examine, whether Wilson loops with the proposed coupling to the scalars preserve a certain amount of supersymmetry for special contour shapes, following the discussion in [15, 17, 18]. An embedding of a curve with straight light-like segments in a simple submanifold as in [17, 18] seems difficult, though.

It seems natural to assume an additional jump in the coupling to the scalars, also in the case of the curve with light-like tangent and a discontinuity in the second derivative discussed above, as was done for the common cusp anomalous dimension in [29]. We would then obtain the corresponding anomalous dimension, as a function of the saltus in \ddot{x} of the usual loop-variables and of the saltus in the coupling. It would then again be interesting to examine whether the discontinuity in the coupling can be chosen such that the anomalous dimension vanishes and the Wilson loop becomes finite, similar to the discussion for extended light-like segments in section 4.3.

Having investigated special local features of Wilson loops in Minkowski space related to their embedding in space-time, we then examined the Wilson loops for simple geometrical contours in Minkowski space, such as the circle and the rectangle, in order to compare the results to their Euclidean versions. In 4.4, we computed the full rectangular Wilson loop in Minkowski space and explicitly showed that the Minkowskian result arises from the Euclidean one by Wick rotation of the time-like side $T \rightarrow iT$. This result corresponds to our expectations for the case of the rectangle with neatly separated and orthogonal time-like and space-like edges.

This is not so obvious in the case of the circle, however, since there, a Wick rotation of the radius $R \rightarrow iR$ transforms a circle into a hyperboloid. It thus seems interesting to compute the Wilson loop for a circle in Minkowski space and to compare it to the Euclidean result. In the Euclidean case, the circle

is the conformal inversion of a straight line, whose Wilson loop simply equals one. Though $\mathcal{N} = 4$ SYM is conformal, the circular Wilson loop acquires an anomalous contribution and is a non-trivial function of the coupling constant, which may be calculated exactly to all orders in the coupling [16]. Hence, it would be interesting to compute the Wilson loop for such a circle and its conformal inversion in Minkowski space in order to check whether the situation is analogous.

Appendix A

Aspects of SU(N) Gauge Theory

A.1 Generators of SU(N)

Throughout this thesis, T^a denote the generators of the SU(N) Lie algebra:

$$[T^a, T^b] = i f^{abc} T^c$$

where f^{abc} are the structure constants of the gauge group. In the fundamental representation of SU(N), we can choose

$$\begin{aligned} \text{Tr}(T^a T^b) &= \frac{1}{2} \delta^{ab} \\ \Rightarrow \text{Tr}(T^a T^a) &= \frac{1}{2} (N^2 - 1). \end{aligned} \quad (\text{A.1})$$

With

$$\text{Tr}(T^a T^a) = C_F N \quad (\text{A.2})$$

the Casimir C_F then is

$$C_F = \frac{N^2 - 1}{2N} \xrightarrow{N \rightarrow \infty} \frac{N}{2} \quad (\text{A.3})$$

for large N.

A.2 Propagators

In SU(N) gauge theory, the gauge field propagator in four space-time dimensions in generalised Feynman gauge takes the form

$$\left\langle A_\mu^a(x) A_\nu^b(y) \right\rangle_\alpha = \frac{\eta_{\mu\nu}}{4\pi^2((x-y)^2 - i\varepsilon)} + \frac{\alpha - 1}{16\pi^2} \partial_\mu \partial_\nu \log(\Lambda^2(x-y)^2 - i\varepsilon) \quad (\text{A.4})$$

as for instance can be found in [47].

In Feynman gauge $\alpha = 1$ and the four dimensional gauge field propagator becomes

$$\left\langle A_\mu^a(x) A_\nu^b(y) \right\rangle = \frac{1}{4\pi^2} \frac{\delta^{ab} \eta_{\mu\nu}}{(x-y)^2}. \quad (\text{A.5})$$

The scalar propagator is gauge independent:

$$\left\langle \phi_I^a(x) \phi_J^b(y) \right\rangle = -\frac{1}{4\pi^2} \frac{\delta^{ab} \delta_{IJ}}{(x-y)^2}. \quad (\text{A.6})$$

A.3 Propagators in Dimensional Regularisation

For dimensional regularisation, we need the propagator in $D = 4 - 2\epsilon$ dimensions. In Feynman Gauge, the gauge field propagator then takes the form

$$\langle A_\mu^a(x) A_\nu^b(y) \rangle = -\frac{\pi^\epsilon}{4\pi^2} \Gamma(1 - \epsilon) \frac{\delta^{ab} \eta_{\mu\nu}}{(-(x - y)^2)^{1-\epsilon}} \quad (\text{A.7})$$

and the scalar propagator becomes

$$\langle \phi_I^a(x) \phi_J^b(y) \rangle = \frac{\pi^\epsilon}{4\pi^2} \Gamma(1 - \epsilon) \frac{\delta^{ab} \delta_{IJ}}{(-(x - y)^2)^{1-\epsilon}}, \quad (\text{A.8})$$

where $\Gamma(z)$ is the Euler gamma function (see also [47]).

If we have a UV divergence, regularisation demands lowering the dimension, i.e. $\epsilon > 0$. We can extract a dimensional factor of $m^{2\epsilon}$ from the fraction in the propagator and multiply with the coupling, while extracting its dimension into a UV scale μ_{UV} , as in (3.3), and obtain the prefactor of the one-loop order of the Wilson loop (3.31). It can then be expanded in orders of the regularisation parameter ϵ :

$$\begin{aligned} \frac{(g \cdot \mu_{\text{UV}}^\epsilon)^2 N}{4} \frac{\pi^\epsilon}{4\pi^2} \Gamma(1 - \epsilon) m^{2\epsilon} &= \frac{g^2 N}{16\pi^2} (\mu_{\text{UV}}^2 \pi m^2)^\epsilon \Gamma(1 - \epsilon) \\ &= \frac{a}{2} (1 + \epsilon \ln(\mu_{\text{UV}}^2 \pi m^2)) (1 + \epsilon \Gamma'(1)) + \mathcal{O}(\epsilon^2) \\ &= \frac{a}{2} (1 + \epsilon \ln(m^2 \mu_{\text{UV}}^2 \pi e^\gamma)) + \mathcal{O}(\epsilon^2) \\ &= \frac{a}{2} (1 + \epsilon \ln(\frac{m^2}{\mu^2})) + \mathcal{O}(\epsilon^2) \end{aligned} \quad (\text{A.9})$$

where γ is the Euler constant and μ was defined in (3.11).

Appendix B

Integrals

B.1 Wilson Loops and Scattering Amplitudes in Off-Shell Regularisation

Integral $I_{ij}^{(2)}$:

Remembering that B_{ij} , as defined in (3.35), is negative and its absolute value gets large for $m^2 \rightarrow 0$, the integral $I_{ij}^{(2)}$, defined in (3.40) can be evaluated as follows:

$$\begin{aligned}
\frac{1}{2} I_{ij}^{(2)} &:= \int_0^{\frac{\pi}{2}} d\phi \frac{\ln(1 + |B_{ij}| \sin \phi)}{1 + |B_{ij}| \sin \phi} & (B.1) \\
&= \int_0^{\frac{1}{\sqrt{|B_{ij}|}}} d\phi \frac{\ln(1 + |B_{ij}| \sin \phi)}{1 + |B_{ij}| \sin \phi} + \int_{\frac{1}{\sqrt{|B_{ij}|}}}^{\frac{\pi}{2}} d\phi \frac{\ln(|B_{ij}| \sin \phi)}{|B_{ij}| \sin \phi} + \mathcal{O}\left(\frac{1}{|B_{ij}|^2}\right) \\
&= \frac{1}{|B_{ij}|} \int_1^{1+\sqrt{|B_{ij}|}} dy \frac{\ln y}{y} + \frac{\ln |B_{ij}|}{|B_{ij}|} \int_{\frac{1}{\sqrt{|B_{ij}|}}}^{\frac{\pi}{2}} d\phi \frac{1}{\sin \phi} + \\
&\quad + \frac{1}{|B_{ij}|} \int_{\frac{1}{\sqrt{|B_{ij}|}}}^{\frac{\pi}{2}} d\phi \frac{\ln(\sin \phi)}{\sin \phi} + \mathcal{O}\left(\frac{1}{|B_{ij}|^2}\right) \\
&= \frac{1}{|B_{ij}|} \left(\frac{1}{2} \ln^2(1 + \sqrt{|B_{ij}|}) - \ln |B_{ij}| \ln \left(\tan \frac{1}{2\sqrt{|B_{ij}|}} \right) + \right. \\
&\quad \left. + \int_{\frac{1}{\sqrt{|B_{ij}|}}}^{\frac{\pi}{2}} d\phi \frac{\ln(\sin \phi)}{\sin \phi} \right) + \mathcal{O}\left(\frac{1}{|B_{ij}|^2}\right)
\end{aligned}$$

Expanded in orders of $\frac{1}{|B_{ij}|}$, the integral in the last line becomes

$$\int_{\frac{1}{\sqrt{|B_{ij}|}}}^{\frac{\pi}{2}} d\phi \frac{\ln(\sin \phi)}{\sin \phi} = -\frac{\pi^2}{24} + \frac{1}{2}(\ln 2)^2 - \frac{1}{8}(\ln |B_{ij}|)^2 + \mathcal{O}\left(\frac{1}{|B_{ij}|}\right). \quad (B.2)$$

Additionally approximating

$$\ln^2(1 + \sqrt{|B_{ij}|}) = \frac{1}{4} \ln^2(|B_{ij}|) + \mathcal{O}\left(\frac{1}{|B_{ij}|}\right) \quad (\text{B.3})$$

and

$$\begin{aligned} \ln\left(\tan \frac{1}{2\sqrt{|B_{ij}|}}\right) &= -\ln\left(2\sqrt{|B_{ij}|}\right) + \mathcal{O}\left(\frac{1}{|B_{ij}|}\right) \\ &= -\ln(2) - \frac{1}{2} \ln(|B_{ij}|) + \mathcal{O}\left(\frac{1}{|B_{ij}|}\right), \end{aligned} \quad (\text{B.4})$$

we finally find:

$$\begin{aligned} I_{ij}^{(2)} &= 2 \ln(2) \frac{\ln |B_{ij}|}{|B_{ij}|} + \frac{\ln^2(|B_{ij}|)}{|B_{ij}|} + \frac{1}{|B_{ij}|} \left(-\frac{\pi^2}{12} + \ln^2(2)\right) + \mathcal{O}\left(\frac{1}{|B_{ij}|^2}\right) \\ &= -\frac{1}{B_{ij}} \left(\ln(-B_{ij}) + \ln(2)\right)^2 + \frac{1}{B_{ij}} \frac{\pi^2}{12} + \mathcal{O}\left(\frac{1}{B_{ij}^2}\right). \end{aligned} \quad (\text{B.5})$$

Integral A_{ij} :

The integral A_{ij} defined in (3.42) can be evaluated for large $-B_{ij}$ by expanding in orders of $\frac{1}{B_{ij}}$:

$$\begin{aligned} A_{ij} &:= B_{ij} \int_0^{\frac{\pi}{2}} d\phi \frac{\ln(\cos^2 \frac{\phi}{2})}{1 - B_{ij} \sin \phi} = \int_0^{\frac{\pi}{2}} d\phi \frac{\ln(\cos^2 \frac{\phi}{2})}{\frac{1}{B_{ij}} - \sin \phi} \\ &= -\int_0^{\frac{\pi}{2}} d\phi \frac{\ln(\cos^2 \frac{\phi}{2})}{\sin \phi} + \mathcal{O}\left(\frac{1}{B_{ij}}\right) \\ &= -\int_0^{\frac{\pi}{2}} d\phi \frac{\ln\left(\frac{1}{2} + \frac{1}{2} \cos \phi\right)}{\sin \phi} + \mathcal{O}\left(\frac{1}{B_{ij}}\right) \\ &= -\int_0^1 dx \frac{\ln(1+x) - \ln 2}{1-x^2} + \mathcal{O}\left(\frac{1}{B_{ij}}\right) \\ &= \frac{\pi^2}{24} + \mathcal{O}\left(\frac{1}{B_{ij}}\right). \end{aligned} \quad (\text{B.6})$$

B.2 Circular Wilson Loop

The scalar part (4.15) of the ϕ -integral, of the diagram of fig. 4.2b can be solved with the help of the Sokhatsky-Weierstrass theorem for an integral with a simple pole. Be $a < 0 < b$, then:

$$\int_a^b d\alpha \frac{f(\alpha)}{\alpha \pm i\epsilon} = \mathcal{P} \int_a^b d\alpha \frac{f(\alpha)}{\alpha} \mp i\pi f(0) \quad (\text{B.7})$$

where \mathcal{P} denotes the principal value. The integral (4.15) has a pole at $\phi = \frac{\pi}{4}$. We thus substitute $\phi = \frac{\pi}{4} + \alpha$:

$$\begin{aligned} & \int_0^{\frac{\pi}{2}} d\phi \frac{\mp 2i \sqrt{\cos \phi \sin \phi}}{(\sin \phi + \cos \phi)^2 (\sin \phi - \cos \phi) - i\epsilon} \\ &= \mp \frac{i}{2} \int_{-\frac{\pi}{4}}^{\frac{\pi}{4}} d\alpha \frac{\sqrt{\cos^2 \alpha - \sin^2 \alpha}}{\cos^2 \alpha \sin \alpha - i\epsilon} \\ &= \mp \frac{i}{2} \int_{-\frac{\pi}{4}}^{\frac{\pi}{4}} d\alpha \underbrace{\frac{\sqrt{\cos^2 \alpha - \sin^2 \alpha}}{\cos^2 \alpha}}_{=:f(\alpha)} \frac{\alpha}{\sin \alpha} \frac{1}{\alpha - i\epsilon} \\ &= \mp \frac{i}{2} \mathcal{P} \int_{-\frac{\pi}{4}}^{\frac{\pi}{4}} d\alpha \frac{f(\alpha)}{\alpha} \pm \frac{\pi}{2} f(0) = \pm \frac{\pi}{2} \end{aligned}$$

where in the last step, we have used that the principal value vanishes due to the symmetry of $f(\alpha)$.

Appendix C

Coupling to the Scalars for Wilson Loop with Straight Light-Like Segment

For the contribution of diagram 4.5b to a Wilson loop with light-like segment as considered in 4.3, with the ansatz for the coupling proposed in (4.66) with $\tilde{a}(t)$ and $\tilde{b}(t)$ as in (4.67), we get:

$$\begin{aligned}
 I_{(b)} &= \int_0^1 d\tilde{t} dt \frac{\dot{x}(t)\dot{x}(\tilde{t}) - \Theta^I(t)\Theta^I(\tilde{t}) |\dot{x}(t)||\dot{x}(\tilde{t})|}{(x(t) - x(\tilde{t}))^2} \tag{C.1} \\
 &= \int_0^1 d\tilde{t} dt \frac{\dot{x}(t)\dot{x}(\tilde{t})}{(t - \tilde{t})^2 \dot{x}^2(t) + \mathcal{O}((t - \tilde{t})^3)} - \frac{1}{N(\tilde{t})N(t)} |\dot{x}(t)||\dot{x}(\tilde{t})| \eta_{\mu\nu} \times \\
 &\quad \times \frac{\left((1 - t^2 e^{-t}) \frac{\dot{x}^\mu(t)}{|\dot{x}(t)|} + t^2 e^{-t} \frac{x''^\mu(t)}{|x''(t)|} \right) \left((1 - \tilde{t}^2 e^{-\tilde{t}}) \frac{\dot{x}^\nu(\tilde{t})}{|\dot{x}(\tilde{t})|} + \tilde{t}^2 e^{-\tilde{t}} \frac{x''^\nu(\tilde{t})}{|x''(\tilde{t})|} \right)}{(t - \tilde{t})^2 \dot{x}^2(t) + \mathcal{O}((t - \tilde{t})^3)} \tag{C.2}
 \end{aligned}$$

where we have chosen the parameters to run from 0 to 1 along the non-light-like curve piece. In (C.2), we have expanded $x(\tilde{t})$ around $\tilde{t} = t$ in the denominator. The denominator of the integrand has a second order root for coinciding propagator endpoints, $t = \tilde{t}$. In order to examine, whether this leads to a divergence, we choose $\tilde{t} = t + \epsilon$ and expand the coupling for small deviations ϵ of the two parameters. The denominator then is of order ϵ^2 . Due to the unit-vector condition of the coupling, the zeroth order in ϵ exactly cancels the vector part of the integral. It thus remains to be shown, that the linear order in ϵ vanishes. For this, we compute the scalar part of the numerator of (C.2) to first order in ϵ .

The normalisation factor was

$$N(t) = \sqrt{\pm 1 \mp 2t^2 e^{-t} \pm t^4 e^{-2t} \pm'' t^4 e^{-2t}}, \tag{C.3}$$

where \pm is determined by the sign of \dot{x}^2 and \pm'' by the sign of the principal normal to the tangent x''^2 . Assuming that \dot{x}^2 and x''^2 have opposite signs, which for instance is true if we assume that the continuation of the light-like segment can be approximated as a circle, the expansion of the product of the normalisation factor becomes

$$\frac{1}{N(t)} \frac{1}{N(t + \epsilon)} = \frac{1}{N(t)^2} \left(1 + \epsilon \frac{\pm 2t e^{-t} \mp t^2 e^{-t}}{N(t)^2} \right). \tag{C.4}$$

For the term proportional to $\dot{x}(t)\dot{x}(\tilde{t})$, we obtain

$$(1 - t^2 e^{-t})(1 - \tilde{t}^2 e^{-\tilde{t}})\eta_{\mu\nu} \frac{\dot{x}^\mu(t) \dot{x}^\nu(\tilde{t})}{|\dot{x}(t)| |\dot{x}(\tilde{t})|} = (1 - t^2 e^{-t})^2 \left(1 + \epsilon \frac{-2te^{-t} + t^2 e^{-t}}{1 - t^2 e^{-t}} \right) \frac{\dot{x}^2(t)}{|\dot{x}(t)|^2} + \mathcal{O}(\epsilon^2) \quad (\text{C.5})$$

and for the term proportional to $x''(t)x''(\tilde{t})$, we get

$$t^2 e^{-t} \tilde{t}^2 e^{-\tilde{t}} \eta_{\mu\nu} \frac{x''^\mu(t) x''^\nu(\tilde{t})}{|x''(t)| |x''(\tilde{t})|} = (t^2 e^{-t})^2 \left(1 + \epsilon \left(\frac{2}{t} - 1 \right) \right) \frac{x''^2(t)}{|x''(t)|^2} + \mathcal{O}(\epsilon^2). \quad (\text{C.6})$$

For the mixed terms proportional to $\dot{x}(t)x''(\tilde{t})$ and $x''(t)\dot{x}(\tilde{t})$, the order zero terms in ϵ vanish due to the orthogonality of \dot{x} and x'' and for the linear contributions, we get

$$(1 - t^2 e^{-t}) \tilde{t}^2 e^{-\tilde{t}} \eta_{\mu\nu} \frac{\dot{x}^\mu(t) x''^\nu(\tilde{t})}{|\dot{x}(t)| |x''(\tilde{t})|} + t^2 e^{-t} (1 - \tilde{t}^2 e^{-\tilde{t}}) \eta_{\mu\nu} \frac{x''^\mu(t) \dot{x}^\nu(\tilde{t})}{|x''(t)| |\dot{x}(\tilde{t})|} = \epsilon (1 - t^2 e^{-t}) t^2 e^{-t} \frac{\dot{x}(t)\dot{x}''(t) + \ddot{x}(t)x''(t)}{|\dot{x}(t)||x''(t)|} + \mathcal{O}(\epsilon^2). \quad (\text{C.7})$$

Due to the orthogonality of \dot{x} and x'' :

$$\frac{d}{dt}(\dot{x} x'') = \dot{x} \dot{x}'' + \ddot{x} x'' = 0 \quad (\text{C.8})$$

and the linear contribution from the mixed terms vanishes.

Summing up the above terms, the zeroth order in ϵ of course is one due to the unit-vector condition of Θ and one sees that the linear order of the coupling vanishes:

$$\begin{aligned} \Theta^I(t)\Theta^I(t+\epsilon) &= 1 \pm \epsilon \frac{1}{N(t)^2} \left(2te^{-t} - t^2 e^{-t} - 2te^{-t} + t^2 e^{-t} + 2t^3 e^{-2t} - \right. \\ &\quad \left. - t^4 e^{-2t} + t^4 e^{-2t} - 2t^3 e^{-2t} \right) + \mathcal{O}(\epsilon^2) \\ &= 1 + \mathcal{O}(\epsilon^2). \end{aligned} \quad (\text{C.9})$$

Inserting this result into the considered Wilson loop contribution (4.71), the order zero of the coupling cancels the vector part by construction and we are left with a part quadratic in $(t - \tilde{t})$ in the scalar numerator, which exactly cancels the singularity. We have thus shown, that coupling to the scalars as in our ansatz (4.66) makes a Wilson loop with light-like segments finite.

Note, that the cancellation of the linear terms in ϵ works anyway, even for the case where \dot{x} and x'' have same signs. In this case, for the expansion of the coupling, we find

$$\frac{1}{N(t)} \frac{1}{N(t+\epsilon)} = \frac{1}{N(t)^2} \left(1 \pm \epsilon \frac{2te^{-t} - 4t^3 e^{-2t} - t^2 e^{-t} + 2t^4 e^{-2t}}{N(t)^2} \right). \quad (\text{C.10})$$

The expansion of one of the terms (C.5) and (C.6) takes opposite sign and the mixed term in (C.7) remains the same. Thus, in total we obtain

$$\begin{aligned}
\Theta^I(t)\Theta^I(t+\epsilon) &= 1 \pm \epsilon \frac{1}{N(t)^2} \left(2te^{-t} - 4t^3e^{-2t} - t^2e^{-t} + 2t^4e^{-2t} - \right. \\
&\quad \left. - 2te^{-t} + 2t^3e^{-2t} + t^2e^{-t} - t^4e^{-2t} + \right. \\
&\quad \left. + 2t^3e^{-2t} - t^4e^{-2t} \right) + \mathcal{O}(\epsilon^2) \\
&= 1 + \mathcal{O}(\epsilon^2). \tag{C.11}
\end{aligned}$$

We therefore do not need to assume any relative signs of the tangent vector and its principal normal such that our ansatz makes the considered Wilson loop with light-like contour piece finite.

Bibliography

- [1] G. Hooft, “A planar diagram theory for strong interactions”, *Nuclear Physics B*, vol. 72, no. 3, pp. 461–473, 1974.
- [2] J. Maldacena, “The Large-N Limit of Superconformal Field Theories and Supergravity”, *International Journal of Theoretical Physics*, vol. 38, no. 4, pp. 1113–1133, 1999.
- [3] K. Wilson, “Confinement of quarks”, *Physical Review D*, vol. 10, no. 8, pp. 2445–2459, 1974.
- [4] J. Maldacena, “Wilson Loops in Large N Field Theories”, *Physical Review Letters*, vol. 80, no. 22, pp. 4859–4862, 1998.
- [5] L. Alday and J. Maldacena, “Gluon scattering amplitudes at strong coupling”, *JHEP*, vol. 706, no. 064, pp. 0705–0303, 2007.
- [6] L. Alday and J. Maldacena, “Comments on gluon scattering amplitudes via AdS/CFT”, *arXiv*, vol. 710.
- [7] J. Drummond, G. Korchemsky and E. Sokatchev, “Conformal properties of four-gluon planar amplitudes and Wilson loops”, *Nuclear Physics, Section B*, vol. 795, no. 1-2, pp. 385–408, 2008.
- [8] J. Drummond, J. Henn, G. Korchemsky and E. Sokatchev, “On planar gluon amplitudes/Wilson loops duality”, *Nuclear Physics, Section B*, vol. 795, no. 1-2, pp. 52–68, 2008.
- [9] A. Polyakov, “Gauge fields as rings of glue”, *Nuclear Physics B*, vol. 164, 1980.
- [10] G. Korchemsky and A. Radyushkin, “Loop-space formalism and renormalization group for the infrared asymptotics of QCD”, *Physics Letters B*, vol. 171, no. 4, pp. 459–467, 1986.
- [11] G. Korchemsky and A. Radyushkin, “Renormalization of the Wilson loops beyond the leading order”, *Nuclear Physics B*, vol. 283, 1987.
- [12] J. Drummond, J. Henn, V. Smirnov and E. Sokatchev, “Magic identities for conformal four-point integrals”, *JHEP*, vol. 701, p. 064, 2007.
- [13] J. Drummond, J. Henn, G. Korchemsky and E. Sokatchev, “Conformal Ward identities for Wilson loops and a test of the duality with gluon amplitudes”, *arXiv*, vol. 712.
- [14] J. Drummond and J. Henn, “All tree-level amplitudes in N= 4 SYM”, *Arxiv preprint arXiv:0808.2475*, 2008.

- [15] K. Zarembo, “Supersymmetric Wilson loops”, *Nuclear Physics, Section B*, vol. 643, no. 1-3, pp. 157–171, 2002.
- [16] N. Drukker and D. Gross, “An Exact Prediction of $N=4$ SUSYM Theory for String Theory”, *Arxiv preprint hep-th/0010274*, 2000.
- [17] N. Drukker, S. Giombi, R. Ricci and D. Trancanelli, “More supersymmetric Wilson loops”, *Physical Review D*, vol. 76, no. 10, p. 107703, 2007.
- [18] N. Drukker, S. Giombi, R. Ricci and D. Trancanelli, “Supersymmetric Wilson loops on S^3 ”, *JHEP*, vol. 5, p. 017, 2008.
- [19] E. D’Hoker and D. Freedman, “Supersymmetric gauge theories and the AdS/CFT correspondence”, *Strings, Branes And Extra Dimensions: TASI 2001, Boulder, Colorado, USA, 4-29 June 2001*, 2004.
- [20] O. Aharony, S. Gubser, J. Maldacena, H. Ooguri and Y. Oz, *Large N Field Theories, String Theory and Gravity*. North-Holland, 2000.
- [21] H. Nastase, “Introduction to AdS-CFT”, *Arxiv preprint arXiv:0712.0689*, 2007.
- [22] M. Lüscher and G. Mack, “Global conformal invariance in quantum field theory”, *Communications in Mathematical Physics*, vol. 41, no. 3, pp. 203–234, 1975.
- [23] L. Brink, J. Schwarz and J. Scherk, “Supersymmetric Yang-Mills theories”, *Nuclear Physics B*, vol. 121, no. 1, pp. 77–92, 1977.
- [24] M. Sohnius, “Introducing supersymmetry”, *Physics Reports*, vol. 128, no. 2-3, 1985.
- [25] J. Maldacena, “TASI 2003 Lectures on AdS/CFT”, *Arxiv preprint hep-th/0309246*, 2003.
- [26] E. Witten, “Anti De Sitter Space And Holography”, *Arxiv preprint hep-th/9802150*, 1998.
- [27] M. Peskin and D. Schroeder, *An Introduction to Quantum Field Theory*. Basic Books, 1993.
- [28] I. Montvay and G. Münster, *Quantum fields on a lattice*. Cambridge University Press New York, 1994.
- [29] N. Drukker, D. Gross and H. Ooguri, “Wilson loops and minimal surfaces”, *Physical Review D*, vol. 60, no. 12, p. 125006, 1999.
- [30] Z. Bern, L. Dixon and V. Smirnov, “Iteration of planar amplitudes in maximally supersymmetric Yang-Mills theory at three loops and beyond”, *Physical Review D*, vol. 72, no. 8, p. 85001, 2005.
- [31] L. Alday, “Lectures on Scattering Amplitudes via AdS/CFT”, *arXiv*, vol. 804.

-
- [32] D. Gross and P. Mende, “The high-energy behavior of string scattering amplitudes”, *Physics Letters B*, vol. 197, no. 1-2, pp. 129–134, 1987.
- [33] N. Beisert, B. Eden and M. Staudacher, “Transcendentality and crossing”, *J. Stat. Mech*, vol. 1021, 2007.
- [34] C. Anastasiou, L. Dixon, Z. Bern and D. Kosower, “Planar Amplitudes in Maximally Supersymmetric Yang-Mills Theory”, *Physical Review Letters*, vol. 91, no. 25, p. 251602, 2003.
- [35] Z. Bern, M. Czakon, L. Dixon, D. Kosower and V. Smirnov, “Four-loop planar amplitude and cusp anomalous dimension in maximally supersymmetric Yang-Mills theory”, *Physical Review D*, vol. 75, no. 8, p. 85010, 2007.
- [36] Z. Bern, L. Dixon, D. Kosower, R. Roiban, M. Spradlin, C. Vergu and A. Volovich, “The Two-Loop Six-Gluon MHV Amplitude in Maximally Supersymmetric Yang-Mills Theory”, *arXiv*, vol. 803.
- [37] J. Drummond, J. Henn, G. Korchemsky and E. Sokatchev, “The hexagon Wilson loop and the BDS ansatz for the six-gluon amplitude”, *Physics Letters B*, vol. 662, no. 5, pp. 456–460, 2008.
- [38] J. Drummond, J. Henn, G. Korchemsky and E. Sokatchev, “Hexagon Wilson loop= six-gluon MHV amplitude”, *eprint arXiv: 0803.1466*, 2008.
- [39] J. Drummond, J. Henn, G. Korchemsky and E. Sokatchev, “Dual superconformal symmetry of scattering amplitudes in $N=4$ super-Yang-Mills theory”, *Arxiv preprint arXiv:0807.1095*, 2008.
- [40] N. Berkovits and J. Maldacena, “Fermionic T-Duality, Dual Superconformal Symmetry, and the Amplitude/Wilson Loop Connection”, *eprint arXiv: 0807.3196*, 2008.
- [41] J. Henn, “Duality between Wilson Loops and Scattering Amplitudes”, *eprint arXiv: 0810.3849*, 2008.
- [42] J. Henn, *Duality between Wilson Loops and Scattering Amplitudes*. PhD thesis, Université Claude Bernard - Lyon 1, 2008.
- [43] H. Dorn and C. Grosse Wiesmann, “Matching gluon scattering amplitudes and Wilson loops in off-shell regularization”, *Phys. Lett.*, vol. B668, pp. 429–431, 2008, 0807.2999.
- [44] G. Korchemsky, “Double logarithmic asymptotics in QCD”, *Physics Letters B*, vol. 217, no. 3, pp. 330–334, 1989.
- [45] A. Brandhuber, P. Heslop and G. Travaglini, “MHV amplitudes in $N=4$ super-Yang-Mills and Wilson Loops”, *Nuclear Physics, Section B*, 2007.
- [46] S. Gates Jr, M. Grisaru, M. Rocek and W. Siegel, “Superspace, or One thousand and one lessons in supersymmetry”, *Arxiv preprint hep-th/0108200*, 2001.
-

- [47] H. Dorn, “Renormalization of Path Ordered Phase Factors and Related Hadron Operators in Gauge Field Theories”, *Fortschritte der Physik/Progress of Physics*, vol. 34, no. 1, pp. 11–56, 1986.
- [48] R. Kirschner, J. Kripfganz, J. Ranft and A. Schiller, “Short distance expansion of wilson loops, gluon condensation and monte carlo lattice results”, *Nuclear Physics B*, vol. 210, no. 4, 1982.

Hilfsmittel

Diese Diplomarbeit wurde mit $\text{\LaTeX} 2_{\epsilon}$ gesetzt. Die Grafiken wurden mit Hilfe von JAXODRAW, OPENOFFICE.ORG 2.0 und MATHEMATICA 6 (Wolfram Research) erstellt. Die in dieser Arbeit enthaltenen Rechnungen wurden unter Einbeziehung von MATHEMATICA 6 erstellt.

Selbständigkeitserklärung

Hiermit erkläre ich, die vorliegende Diplomarbeit selbständig sowie ohne unerlaubte fremde Hilfe verfasst und nur die angegebenen Quellen und Hilfsmittel verwendet zu haben.

Mit der Auslage meiner Diplomarbeit in den Bibliotheken der Humboldt-Universität zu Berlin bin ich einverstanden.

Berlin, den 1. Dezember 2008

Charlotte Grosse Wiesmann
